INVESTIGATION ON MECHANICAL AND MODAL PROPERTIES OF ALUMINIUM BASED FIBRE METAL LAMINATES

MOHAMAD NAZIRUL MUBIN BIN MERZUKI

MASTER OF SCIENCE

UNIVERSITI MALAYSIA PAHANG

UNIVERSITI MALAYSIA PAHANG

DECLARATION OF THESIS AND COPYRIGHT

Author's Full Name : <u>MOHAMAD NAZIRUL MUBIN BIN MERZUKI</u>

Date of Birth : <u>15 JULY 1993</u>

Title : <u>INVESTIGATION ON MECHANICAL AND MODAL</u>

<u>PROPERTIES OF ALUMINIUM BASED FIBRE METAL</u>

<u>LAMINATES</u>

Academic Session : <u>SEMESTER 2 2019/2020</u>

I declare that this thesis is classified as:

☐ CONFIDENTIAL (Contains confidential information under the Official Secret Act 1997)*

☐ RESTRICTED (Contains restricted information as specified by the organization where research was done)*

☑ OPEN ACCESS I agree that my thesis to be published as online open access (Full Text)

I acknowledge that Universiti Malaysia Pahang reserves the following rights:

1. The Thesis is the Property of Universiti Malaysia Pahang
2. The Library of Universiti Malaysia Pahang has the right to make copies of the thesis for the purpose of research only.
3. The Library has the right to make copies of the thesis for academic exchange.

Certified by:

_____ _____
(Student's Signature)   (Supervisor's Signature)

_____ _____
New IC/Passport Number   Name of Supervisor
Date: Date:

NOTE : * If the thesis is CONFIDENTIAL or RESTRICTED, please attach a thesis declaration letter.

SUPERVISOR'S DECLARATION

We hereby declare that we have checked this thesis and in our opinion, this thesis is adequate in terms of scope and quality for the award of the degree of Master of Science.

_____

(Supervisor's Signature)

Full Name :

Position :

Date :

_____

(Co-supervisor's Signature)

Full Name :

Position :

Date :

STUDENT'S DECLARATION

I chain-like declare that the work in this thesis is based on my original work except for quotations and citations which have been duly acknowledged. I also declare that it has not been previously or concurrently submitted for any other degree at Universiti Malaysia Pahang or any other institutions.

_____
(Student's Signature)
Full Name : MOHAMAD NAZIRUL MUBIN BIN MERZUKI
ID Number : MMM17020
Date :

INVESTIGATION ON MECHANICAL AND MODAL PROPERTIES OF ALUMINIUM BASED FIBRE METAL LAMINATES

MOHAMAD NAZIRUL MUBIN BIN MERZUKI

Thesis submitted in fulfillment of the requirements
for the award of the degree of
Master of Science

Faculty of Mechanical and Automotive Engineering Technology

UNIVERSITI MALAYSIA PAHANG

JUNE 2020

ACKNOWLEDGEMENTS

ABSTRAK

Kombinasi bahan antara aloi dan bahan komposit telah lama digunakan sebelum mencapai tahap prestasi yang diperlukan ketika ini. Untuk mencapai kombinasi sifat-sifat bahan dan prestasi yang terbaik, adalah penting untuk mengkaji tingkah laku dinamiknya. Selain itu, bagi mengelak timbulnya masalah yang berkait dengan getaran, adalah penting untuk mendapatkan frekuansi tabii dan bentuk ragam semasa pemilihan bahan. Projek ilmiah ini dijalankan untuk mengkaji sifat mekanik aluminium aloi dan bahan komposit. Projek ini juga menilai tingkah laku dinamik kombinasi antara aluminium aloi (Al-2024-T0) dan tiga bahan komposit yang berbeza (CFRP, GFRP, UD-CFP) dengan menggunaka ujian getaran bebas. Plat fiber metal laminates (FML) yang digunakan sebagai specimen dibuat dengan menggunakan kaedah pengacuan mampatan. Manakala, kaedah fabrikasi mengikut piawaian ASTM D3039 dan sifat mekanik plat digunakan untuk kaedah ujian tegangan. Penilaian frekuansi tabii dan bentuk ragam FML dengan aluminium aloi (Al-2024-T0) dan tiga bahan komposit yang berbeza, dinilai melalui konfigurasi yang berbeza susunan iaitu 2/1 dan 3/2, dalam pelbagai jenis keadaan sempadan., Ujian ragaman menggunakan hentaman tukul dengan pergerakan sensor yang berubah dilaksanakan berdasarkan piawaian E756. Pada masa yang sama, model kaedah unsur terhingga yang menggunakan perisian komersial ABAQUS juga digunakan untuk menentukan frekuansi tabii dan bentuk ragam. Keputusan daridada eksperimen ragaman telah dibandingkan dengan keputusan simulasi unsur terhingga (FEA). Keputusan menunjukkan frekuansi tabii plat FML meningkat apabila banyak lapisan Al terbenam dalam lapisan komposit. Ia menunjukkan peningkatan peratusan frekuansi tabii dari 29.41 % sehingga 71.89 %. Keputusan kajian juga menunjukkan, frekuansi tabii pada plat FML bergantung pada keadaan sempadan dengan peratusan peningkatan 54.36 % hingga 88.53 %. Bentuk ragam telah diplotkan untuk plat berlapis yang berlainan dengan bantuan ABAQUS and ME'scopeVES dalam mendapatkan ketepatan bentuk ragam. Keputusan kajian ini disahkan dengan hasil dapatan untuk ralat antara analisis berangka (simulasi) dan eskperimen ujian ragaman adalah 0.08% sehingga 16.17%. Kesimpulannya, dengan kehadiran plat aluminium aloi dalam lapisan komposit, nilai frekuansi tabii akan meningkat. Keadaan sempadan sangat mempengaruhi nilai frekuansi tabii kerana kesan halangan di tepi.

ABSTRACT

The combination of materials between metal alloys and composite materials has been used for thousands of years to reach better performance requirement. To achieve the best combination of material properties and service performance, a study on the dynamic behaviour is one of the main points to be considered. Besides, it is important to investigate the natural frequency and the possible mode shape of the selected of the materials to avoid problems related to vibrations. This master project was aimed to investigate the mechanical properties of aluminium alloys and composite materials. At the same time, the dynamic behaviour of combination between aluminium alloys (Al 2024-T0) and three different composite materials (CFRP, GFRP, UD-CFP) by free vibration test also evaluated. Compression moulding technique was used to fabricate the fibre metal laminate (FML) plates. The fabrication method was according to ASTM D3039 standard and mechanical properties of the plate were determined from the tensile test method. Variation of natural frequency and mode shape of FML based on the aluminium alloys (Al 2024-T0) and three different composite materials were evaluated through different configuration lay-up of 2/1 and 3/2 stacking sequences with multiple boundary conditions. Based on E756 standard, modal testing using impact hammer with roving accelerometer method was carried on to the specimens. Finite element analysis (FEA) models by using commercial ABAQUS software was used to determine natural frequency and mode shape. The experimental results from modal testing were then compared with the FEA values. It was found that, the natural frequency of the FMLs plates increased when more Al layers were embedded in the composite layers. The results reveal that a percentage increase in natural frequency from 29.41 % to 71.98 %. Meanwhile, the percentage increment in natural frequency was from 54.36 % to 88.53 % between fixed-free and fixed-fixed boundary conditions. The vibration analysis of FML plates were validated, where the percentage error between numerical analysis and experimental results are observed to be 0.08 % to 16.17 %. In conclusion, with the presence of aluminium alloy plates in the composite layers, the natural frequency will increase as the value of stiffness increase. The boundary conditions significantly affected the natural frequency of FML plates because of the restraint effect at the edges.

TABLE OF CONTENT

LIST OF TABLES

LIST OF FIGURES

LIST OF ABBREVIATIONS

FMLs	Fibre metal laminates
Al	Aluminium
GFRP	Glass fibre reinforced polymer
CFRP	Carbon fibre reinforced polymer
UD-CFP	Unidirectional carbon fibre prepreg
EMA	Experimental modal analysis
FEA	Finite element analysis
DOF	Degree of freedom
FRF	Frequency response function
ARALL	Aramid reinforced aluminium laminates
GF	Glass fibre
GE	Glass epoxy
CF	Carbon fibre
CE	Carbon epoxy
SRPP	Self-reinforced polypropylene
GLARE	Glass fibre reinforced aluminium laminates
L/R	Length/Radius
L/H	Length/Height
UD	Uni-Directional
^{o}F	Fahrenheit
E	Modulus Elasticity
S4R	4-node, quadrilateral, stress/displacement shell element
C3D8R	Eight-node brick element with reduced integration
3D	Three-dimensional
MCST	Modified couple stress theory
a/b	Width/Length
NI	National Instrument
ARALL	Aramid fibre reinforcement aluminium laminates
CARALL	Carbon fibre reinforcement aluminium laminates

CHAPTER 1

INTRODUCTION

1.1   Introduction

This chapter contains a general introduction of the research that was carried out the framework of this thesis. The research content is described in Section 1.2, 1.3 and 1,4. The focus of the thesis, as well as the main objectives, are discussed in Section 1.5 and 1.6.

1.2   Overview of Composite Materials

A fibre reinforced laminates are made of multi-layers of the fibre reinforced polymer (fibres and matrix) by stacking the unidirectional fibre or woven. Fibre-reinforced polymer (FRP) is a composite material made of a polymer matrix reinforced with fibres. Figure 1.1 shows the fibre layers in various forms can be incorporated into a matrix either in continuous length and random discontinuous lengths.

The most common fibres in commercial application are various type of carbon, glass, as well as aramid. A limited usage of other fibres includes polyester, polyethylene, boron, basalt and aluminium oxide. The various type of matrix could be classified based on chemical compositions and microstructural arrangements. The matrix materials could be polymer, a ceramic or a metal. A polymer is most commonly used as the matrix, which can be epoxy, vinylester and thermosetting plastic.
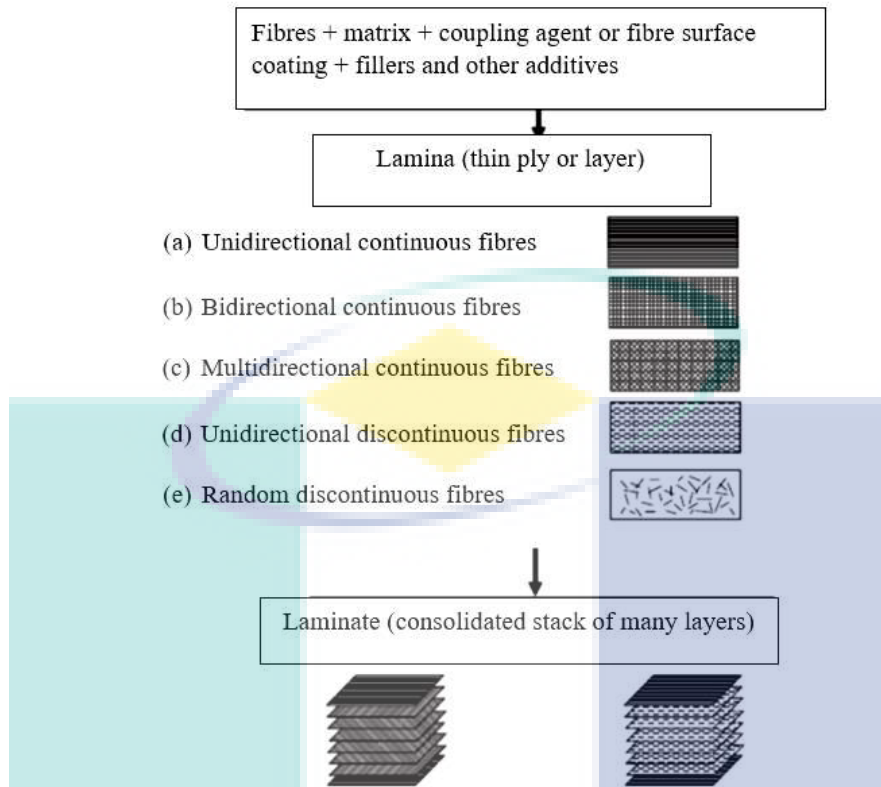
Figure 1.1   Various stacking construction of fibre reinforced laminates

Source: Mallick (2007)

1.2.1   Fibre Type

The role of the reinforcement in a composite is to increase the mechanical properties of the matrix system. The properties of the composite are affected in different ways by different fibres used in composites. Figure 1.2 shows the tensile properties and characteristics of common fibres.

Glass is the most common fibre applied in polymer matrix composites. Liquid glass is formed by blending quarry products heating the mixture in a furnace at temperature 1200 to 1600 °C to produce glass fibre filaments with 10 - 20 microns in diameter. The advantages of glass fibres are low cost, relatively high strength and electrical insulator. There are several types of glass fibre used for structural reinforcement include, C-glass, E-glass, D, S and R-glass, shown in Table 1.1.

Table 1.1   Several type of common glass fibre

Materials	Applications
C-glass (corrosion)	Resistance to corrosion in a chemical environment, such as storage tanks
E-glass (electric)	High resistivity and high strength, electrical and structural application
D-glass (dielectric)	Applied for low constant application
S-glass (silica)	Corrosive environment, fatigue, high strength, modulus and stability under extreme temperature
R-glass (reinforcement)	Enhance mechanical properties, usually used in structural application such as construction

Carbon fibre is produced by controlled carbonisation, graphitisation and oxidation of carbon-rich organic precursors in fibre form. The advantages are high strength and stiffness, creep and fatigue resistance. Cost, poor impact resistance and electric conductor are several disadvantages of carbon fibre.

Aramid fibre is an artificial organic polymer, formed by spinning a solid fibre from a liquid chemical blend called an aromatic polyamide (PPTA). The advantages are high specific tensile strength, impact and abrasion resistance and fatigue resistance. The advantages are poor in compression and low-temperature resistance.
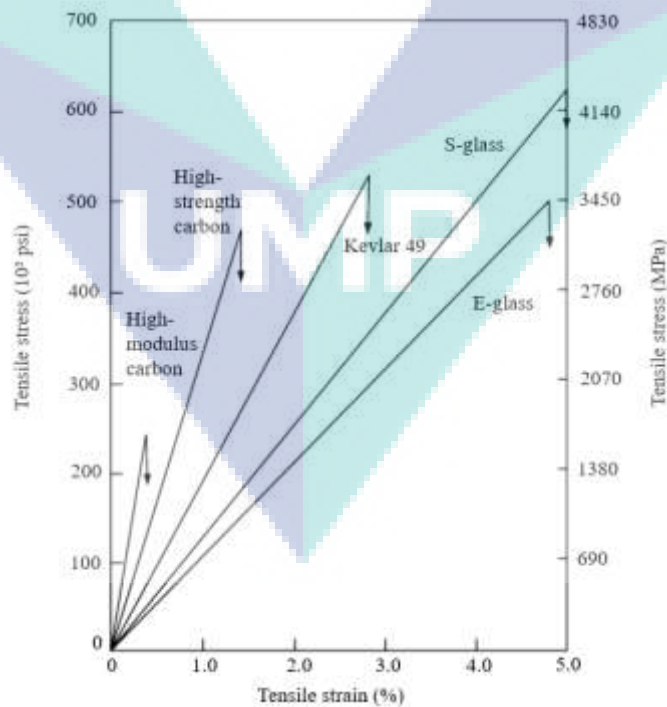
Figure 1.2   Tensile stress-strain diagrams for various reinforcing fibres
Source: Mallick (2007)

3

1.2.2   Resin system for composites

Polymers are classified into two types, 'thermosetting' and 'thermoplastic', according to the effect of heat on their properties. Thermosetting materials, known as thermoset are formed from a chemical reaction in-situ, where the hardener and resin or catalyst and resin are mixed and then undergo a nonreversible chemical reaction to form an infusible, hard product. Once cured, thermosets will not turn to liquid again even heated.

Thermoplastic, such as metal, soften with heating and eventually melt, hardening again with cooling. The resin used in fibre reinforced composite is referred to as the polymer in sometimes. An important common property of all polymers is that they are composed of a long chain-like molecule consisting of many simple repeating units. The comparison of properties between thermosetting and thermoplastic are shown in Table 1.2.

Table 1.2   The properties comparison between thermoset and thermoplastic

Thermosetting	Thermoplastic
Decompose on heating	Soften on heating and pressure, easy to repair
Lower fabrication temperature	Higher fabrication temperature and viscosities
Cannot be reprocessed	Can be reprocessed
Low strain to failure	High strains to failure
cLong cure cycle	Short cure cycles

Source: Kaw (2006)

1.3   History and Development of Fibre Metal Laminates

Nowadays, due to developing technology cause the development and use of materials for structural and other design are changing rapidly. Several important aspects in structural studies are reducing the weight without any changes the strength and dynamic behaviour of the structure. Consequently, this engineering challenge has led a number of researchers to design and manufacture materials that offer properties such as lightweight, high strength and withstand typical problem caused by vibration.

Traditionally, metal alloys such as steel and stainless steel mainly used in any structural application. Replacing metals to composites are the best way to achieve minimizing weight. Composite materials consist of two or more different constituents.

Each material is having different properties, resulting in altogether different properties for composite materials produced. Composite is ideal for structural applications where a high strength to weight ratios are needed (Adediran, 2007). As technology progresses, the cost involved in manufacturing and designing composite materials will reduce, bringing added cost benefits also. Fibre metal laminates (FMLs) are hybrid composites by the combination of thin metals (usually alloy) and fibre reinforced polymers (FRP) to optimise the mechanical properties, shown in Figure 1.3, as these composites offer better damage tolerance to fatigue crack growth, and foreign body impact-damage, corrosion resistance, fault detection, techniques with advantages in repairing, recycling and joining (Liaw, 2001; Marissen, 1981; Sun, 1993; Vlot, 1993). The combination of both materials has been used for thousands of years to reach better performance requirement (Bellini, 2019). A large variety of metals are available as reinforced for fibre metal laminates (FMLs). Among the desirable characteristics of most metals are high strength, high stiffness and resistance to corrosion, shown in Figure 1.4. Aluminium is most commonly used in car manufacturing and aerospace industries due to its good fatigue resistance and high strength to weight ratio. Composite materials, such as glass fibre and carbon fibre are winnings popularity due to offers good mechanical properties such as high strength, low weight, resistant to corrosion, impact-resistant, and high fatigue strength. Other benefits from composite materials include ease of fabrication, flexibility in design, and variable material properties that meet almost any application. Basically, composite materials have a different orientation of fibres and each layer is generally orthotropic.
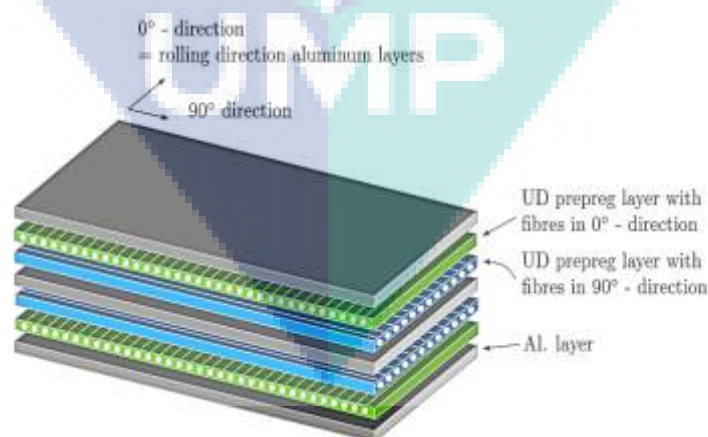
Figure 1.3   Typical layout of a fibre metal laminate
Source: Mohamed (2012); Sun (1993); Vlot (1993)
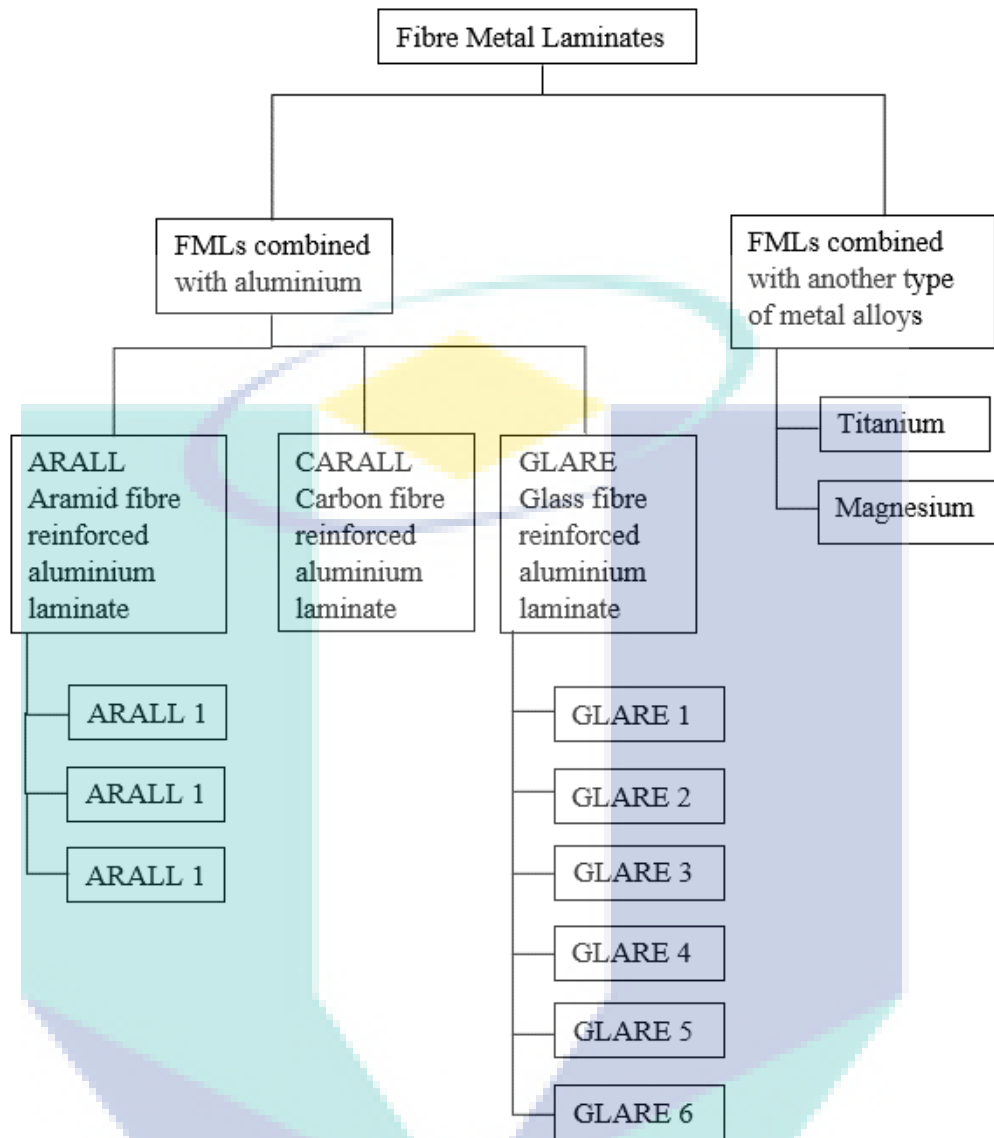
Figure 1.4   Classification of fibre metal laminates

Source: Sinmazçelik et al. (2011)

1.3.1   Aramid Fibre Reinforced Aluminium Laminates

The first advancement in fibre metal laminate technology called ARALL was developed by (Vogelesang & Gunnink, 1983) and colleagues in 1978 at Delft University. It was a structural material suitable for aerospace application because of possessing high strength, low weight characteristics and fatigue insensitive. The laminate with alternating thin aluminium alloy layers and uniaxial aramid fibre prepreg shown in Figure 1.5.
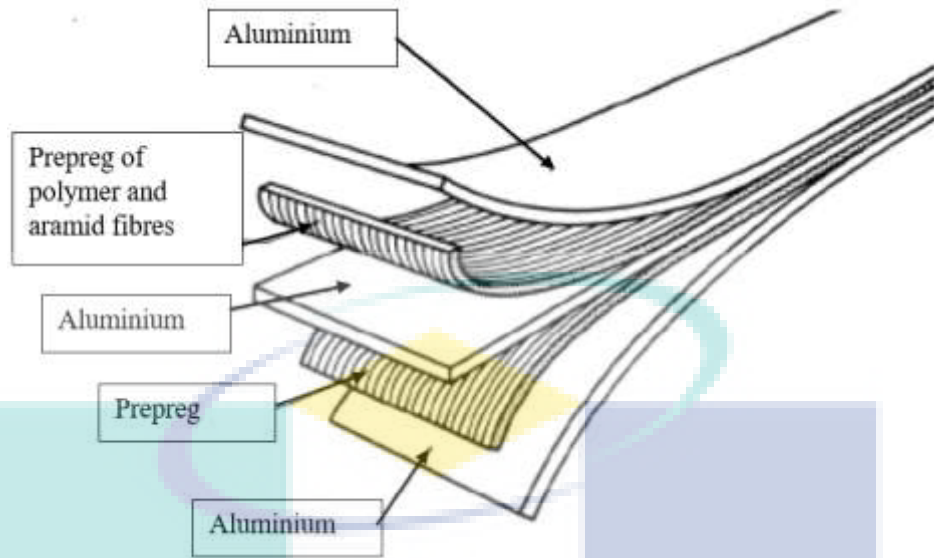
Figure 1.5   Schematic representation of ARALL layup

Source: Alderliesten (2005)

ARALL laminated are developed with the utilization of high strength aramid fibres encapsulated in structural epoxy adhesive intervened between many layers of thin aluminium alloys. ARALL has a built-in characteristic of high strength-to-weight ratio because of its constituent materials. By using various type of aluminium alloys, four different types of ARALL were manufactured. With the acceptance of two international patents in the year 1984, Alcoa Company started to the production of four different types of standardized ARALL materials. A list of commercially produced ARALL is given in Table 1.3.

Table 1.3   Commercially available ARALL

	Metal type	Metal thickness (mm)	Fibre layer (mm)	Fibre direction (º)	Characteristic
ARALL 1	7075-T6	0.3	0.22	0/0	Fatigue, strength
ARALL 2	2024-T3	0.3	0.22	0/0	Fatigue, formability
ARALL 3	7475-T6	0.3	0.22	0/0	Fatigue, strength
ARALL 4	2024-T8	0.3	0.22	0/0	Fatigue, elevated temperature

Source: Khan, Alderliesten, and Benedictus (2009)

1.3.2 Glass Fibre Reinforced Aluminium Laminates

The next generation of fibre metal laminates, GLARE also developed at Delft University for aeronautical application with an aim to improve the ARALL by using advanced glass fibre. Figure 1.6 shows a schematic representation of GLARE fibre metal laminates having 3/2 configuration. GLARE has much more loading flexibility than ARALL because of enhanced compressive properties of glass fibres over aramid fibres. Due to which glass fibre failure in GLARE under fatigue loading occurs very rarely. GLARE has higher tensile and compressive strength, better impact behaviour and higher residual strength as compared to ARALL fibre metal laminates. Cross-ply fibre build-up is possible in GLARE laminates due to better adhesion between the glass fibre and resin.

Aluminium 2024-T3

Unidirectional glass fibres layer
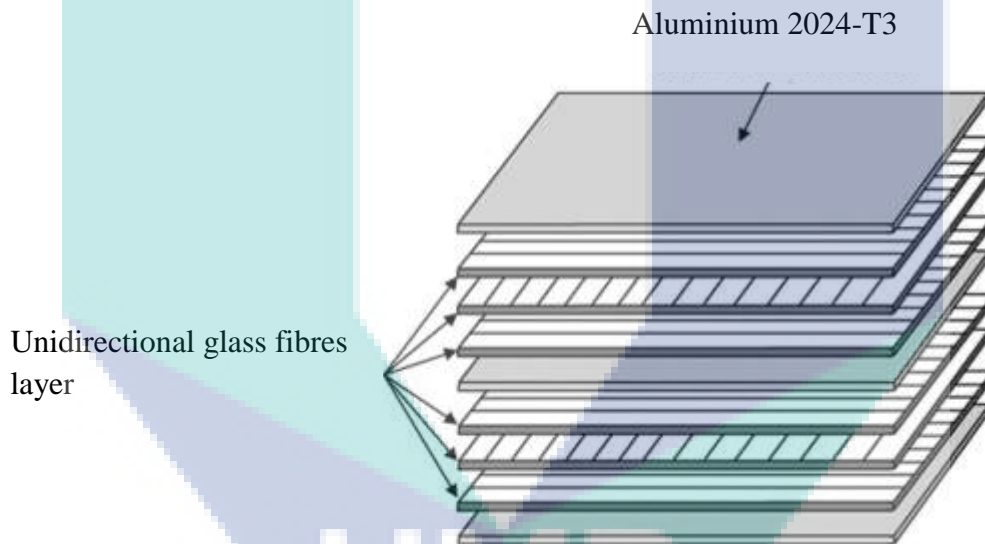
Figure 1.6   Schematic illustration of GLARE laminate
Source: Seo (2010)

GLARE laminates nowadays are produced in six different standard grades as shown in Table 1.4. Unidirectional S2 glass fibres embedded in the epoxy adhesive are used in all six standard grade of GLARE materials. GLARE materials prepreg is commercialised with a nominal fibre volume fraction of 60 % in all six standard classes. Currently, GLARE is being utilised in the main fuselage skin and the leading edges of the horizontal and vertical tailplane of Airbus A380 aircraft (Sinmazçelik, Tamer, Avcu Egemen, Bora Mustafa Özgür, Çoban Onur, 2011).

Table 1.4   Commercially available GLARE grade

GRADE	SUB	Metal Type	Metal Thickness (mm)	Fibre Direction	Fibre Layer (mm)	Characteristics
1	-	7475-T761	0.3-0.4	0/0	0.266	Fatigue, strength, yield stress
2	GLARE 2A	2024-T3	0.2-0.5	0/0	0.266	Fatigue, strength
	GLARE 2A	2024-T3	0.2-0.5	90/90	0.266	Strength, fatigue
3	-	2024-T3	0.2-0.5	0/90	0.266	Impact, fatigue
4	GLARE 4A	2024-T3	0.2-0.5	0/90/0	0.266	Strength in 0º, fatigue
	GLARE 4B	2024-T3	0.2-0.5	90/0/90	0.266	Strength in 90º, fatigue
5	-	2024-T3	0.2-0.5	0/90/90/0	0.266	Impact
6	GLARE 6A	2024-T3	0.2-0.5	45/+45	0.266	Off-axis properties, shear
	GLARE 6B	2024-T3	0.2-0.5	-45/+45	0.266	Off-axis properties, shear

Source: Sinmazçelik et al. (2011)

1.3.3   Carbon Fibre Reinforced Aluminium Laminates

The development of carbon-reinforced aluminium laminates is to improve the poor compressive strength of ARALL laminates. Carbon fibre/epoxy prepregs layers are utilized in CARALL laminates instead of aramid/epoxy prepregs. Carbon fibre/epoxy composite have higher specific modulus but lower specific strength, impact resistance and failure strain as compared to aramid fibre/epoxy composites. Under the fatigue loading, aramid fibre composites showed better low cycle fatigue performance but worse cycle fatigue performance as compared to carbon fibre composites. The production process of CARALL laminates is similar to ARALL and GLARE laminates. Surfaces of aluminium sheets are chemically pretreated for good adhesive between aluminium alloys and carbon fibre/epoxy layers before the curing process. After, laminates process, the whole laminated system is cured under temperature and pressurized conditions in an autoclave. Figure 1.7 shows a representation of a carbon-reinforced aluminium laminate.

CARALL laminate is most suitable for aerospace application because of their high stiffness and good impact properties. Other requests for this laminates is impact-absorbers for helicopter struts and aircraft seats (Lin, Kao, & Yang, 1991). Nowadays, woven carbon fibre/epoxy prepregs are becoming more dominant over the unidirectional

prepreg layers in CARALL laminates due to their bi-directional balance properties in fabric plane. Figure 1.8 shows different carbon fibre weave patterns used in CARALL laminates.
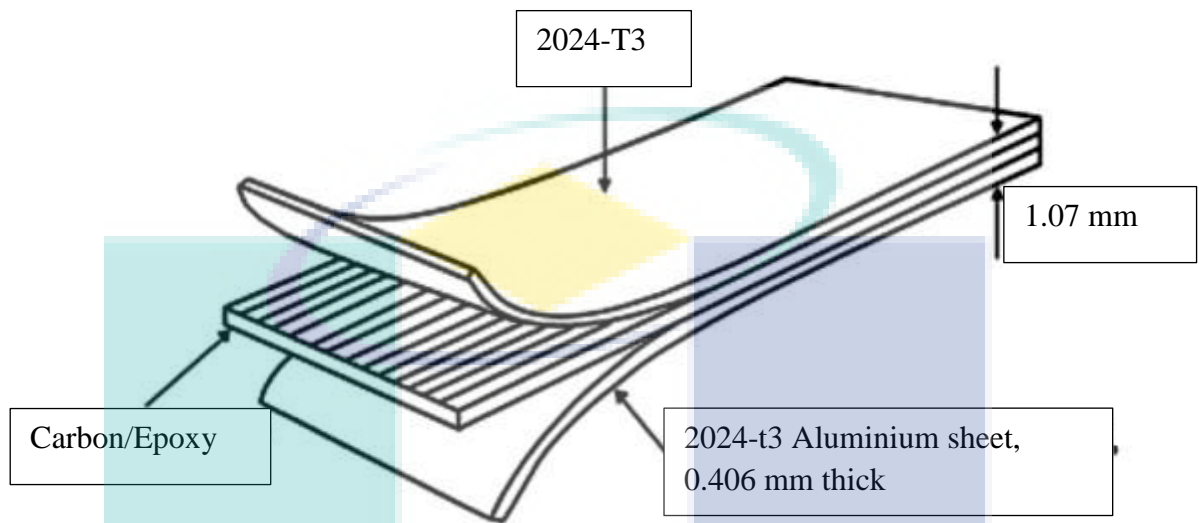
Figure 1.7   Schematic illustration of a 2/1 CARALL laminates
Source: Lawcock (1998)

Plain weave   Twill weave   Satin weave
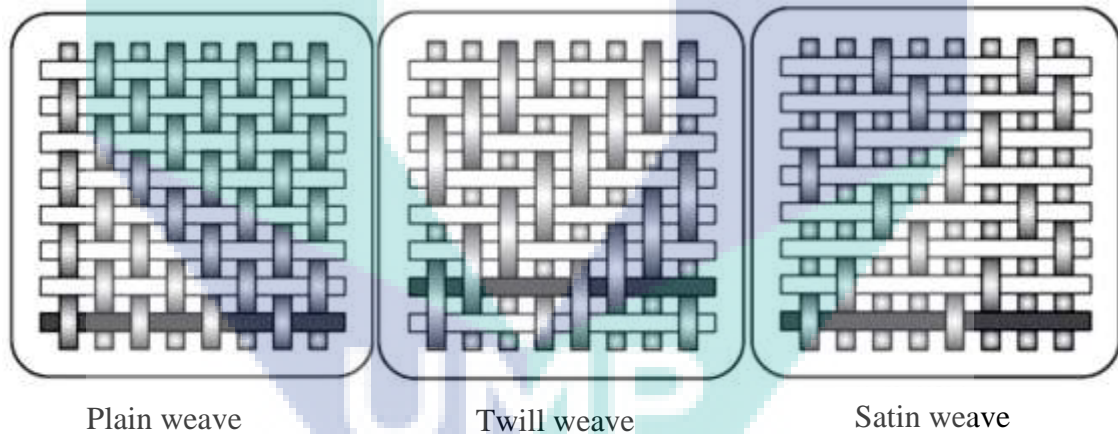
Figure 1.8   Different woven carbon fibre weave patterns
Source: Rattan and Bijwe (2006)

1.4   Applications

Fibre metal laminates are mainly used in the aerospace industry due to their increased stiffness and strength in comparison to aluminium. ARALL was originally used by US Air Force as a material for highly fatigue rear cargo door of the C-17 cargo aircraft to reduce overall weight shown in Figure 1.9 (Hammond, 2005). Besides, ARALL 3 fibre metal laminates were used to build wing panels by Fokker for F-27 aircraft to achieve 25

% weight reduction as compared to aluminium materials (Vlot & Gunnink, 2001). ARALL find its usage in secondary structures, mainly impact susceptible area as lower flap skins (Laliberte, 2000).

A special variant of ARALL was used as armor plating in the year 1986. This ARALL type consists of ceramic tiles on the outside to break up a bullet that hit the materials while ARRALL backing layer would absorb the remaining kinetic energy and would stop the bullet in this way. The tubes made of ARALL fibre metal laminates can be used in the application for chemical and nuclear industry because they remain leak proof even if damages. Fokker also used ARALL as materials to develop crack stoppers for early F-100 aircraft.

Figure 1.9   Cargo door using ARALL materials on C-17
Source: Vlot (2001)

GLARE laminates are not susceptible to low-frequency fibre failure like ARALL which make it well suited to fuselage application. Airbus A380 currently uses FMLs for its panels in the upper fuselage as shown in Figure 1.11 and is an indication of the future applications of GLARE with modern airplane (Krimbalis, 2009). GLARE fibre metal laminates are used for various structural application including a full-scale rear pressure bulkhead and fuselage barrel tests by several aircraft manufacturers like Bombardier and Deutsche Aerospace. GLARE was used for maintenance of the corroded aluminium stiffness in the cargo bay are of an airplane used to transport seafood by replacing them with the GLARE stiffness, shown in Figure 1.10. The prepreg layer works as the

corrosion barrier, and the corrosion of the stiffeners stopped after the outer aluminium layer was corroded.
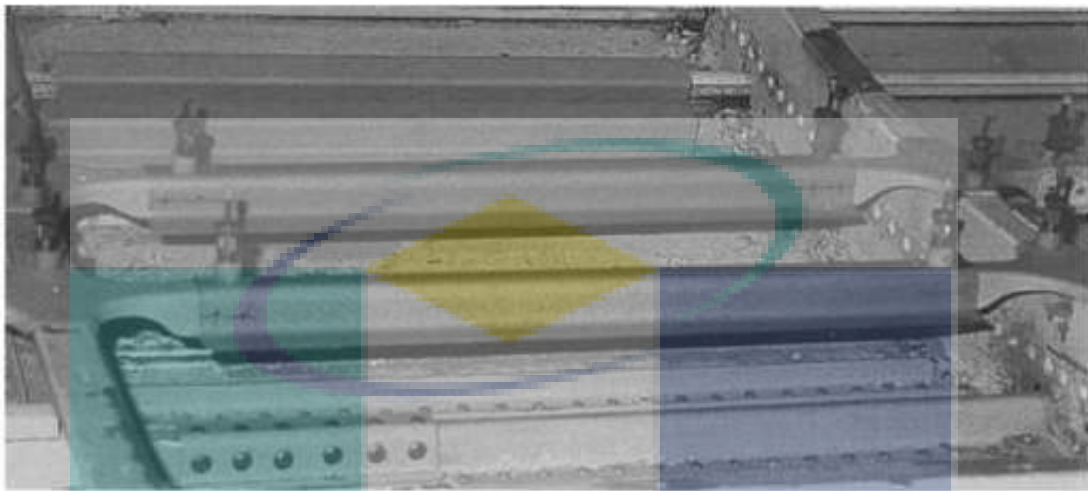
Figure 1.10   A part of area GLARE stiffeners in cargo bay area in F28
Source: Vlot and Gunnink (2001)

GLARE is used in the production of forward radar bulkhead for the Learjet LEAR 45 business aircraft because of its offer combination of high stiffness and excellent bird-strike impact resistance. Another application is GLARE laminates also used in the production A330/A340 cockpit crown, explosion hardened containers, aircraft electronic cabinets and bulk bay floors on Boeing 777 jetliners. The area of aircraft which is most susceptible to impacts is Bulk cargo floors. Glare laminates are used as a floor materials because of their superior impact resistance for Airbus 320/A321, A330/A340 families of aircraft as well as on MD-11 retrofits. The ideal area for application of FMLs on aircraft is summarized in Figure 1.12.
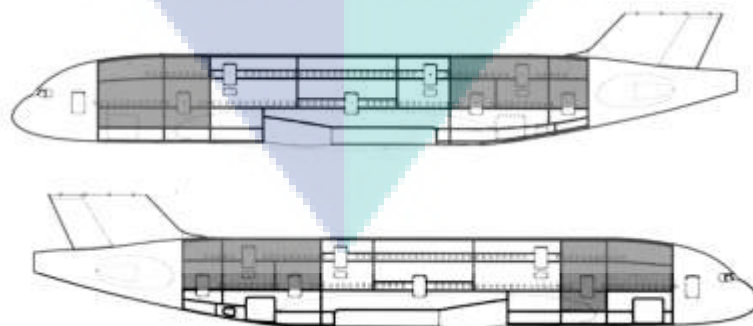
Figure 1.11   The application of GLARE as the upper fuselage panel for A380
Source: Vlot (2001)
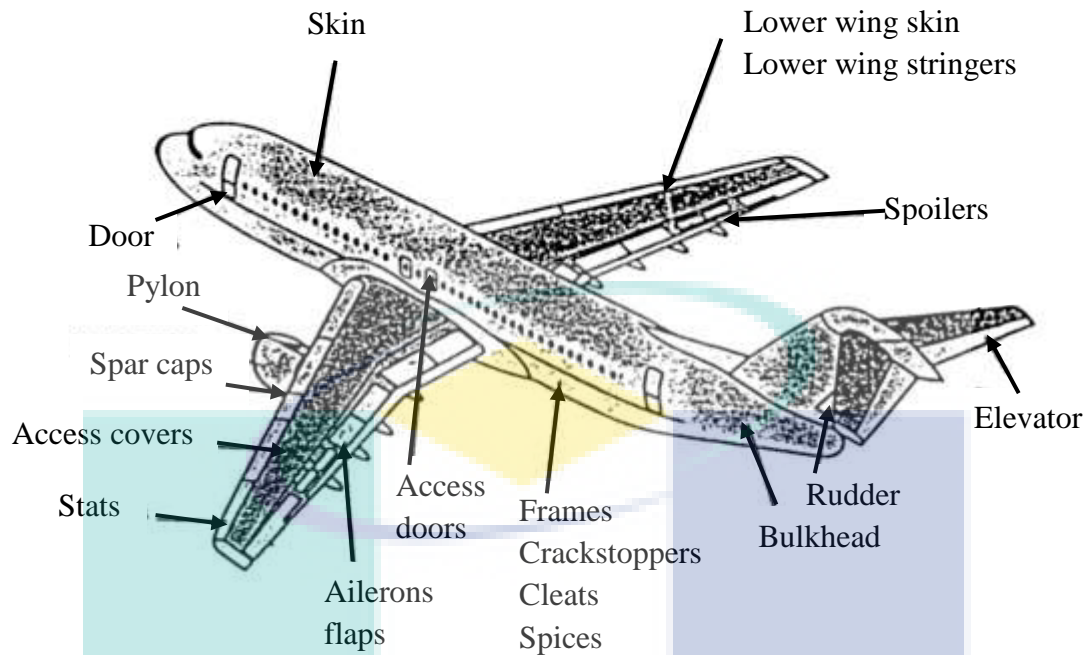
Figure 1.12   Another parts in aerospace used ARALL and GLARE

Source: Pho (1992)

FMLs panels are ultimately thinner than aluminium alone because high fatigue resistance and the weight is at least 15 ~25% less than aluminium alone. Almost more than 1000 kg are saved after using the GLARE materials on the upper fuselage of the Airbus A380 as compared to aluminium (Sara, 2017). In addition to the advantages of FMLs such as better damage tolerance to fatigue crack growth and corrosion resistance, another advantage of the laminated composite-metal alloy is the controllability of the structural properties by changing the fibre orientation angles, the number of plies, configuration and location of the metal alloy layers. These two materials have been combined to form a hybrid structure that is called fibre metal laminates (FMLs) (Sinmazçelik et al., 2011).

To achieve the best combination of material properties and performance, studying the dynamic behaviour is the main point for consideration. To avoid the typical problem caused by vibrations, it is important to obtain the natural frequency and the mode shape of the selection of the materials. However, there are several studies on composites and FMLs materials in open literature. The determination of mechanical and dynamic properties of structures made of composite materials is of great importance (Kahya & Turan, 2017; Ozsoy, 2016).

1.5 Problem Statements

Weight saving is critical issue in almost area of engineering design and analysis. Although lightweight structure are desirable for cost reduction and efficiency enhancement, the use of light weight materials often results in increased flexibility and poor stability. The fibre metal laminates are a mixture of high performance and low-performance materials which provides a distinctive performance on the final product. FMLs materials show potentials for structural applications where a high strength to weight and stiffness to weight ratios are needed. As technology progresses, the cost involved in manufacturing and designing composite materials will reduce, thus bringing added cost benefits also.

The increased use of composite in aerospace, automobile and railroad sector revealed a now state of problem regarding their application compatibility with other materials, particularly for vibration issue. For example, in general aircraft or some spacecraft, vibrations may have several causes such as airflow over the surface, engine normal operation and aerodynamic brakes. Besides, most of these effects are mainly predominant during the takeoff and landing phases. In the automotive industry, the car body may have several causes by the effect of engine operation and the power transmission system (Burdzik, 2013). This effect will be caused the structure vibrate since a frequency close to the first natural frequency of the materials. Notwithstanding their inevitability, these vibrations must be minimized by appropriate design feature through the selection of materials in order to improve performance and reliability levels of structures. This is done by using modal analysis which allows one to determine the natural frequency of the selecting proper composite materials, associated mode shapes. Modal parameters of a structure are natural frequency and mode shape. Frequency is directly proportional to stiffness and inverse of mass. However, the modal parameter is a function of the physical properties of the materials. Thus, changes in physical properties such as used different type of materials and combined with metal layers will cause detectable changes in the modal properties.

Although many researchers have explored FML and its application, majority of them were using aluminium type 2024-T3. Only few studies of FMLs have used metal layer aluminium type 2024-T0. Therefore, this research aims to investigate the combination of aluminium alloys type 2024-T0 and several different type of composite

materials in modal analysis. The reason for considering the use of different composite materials as every composite material has different physical properties and aluminium one of the lightweight materials alloys. Different configuration and boundary conditions are investigated in this research. Finite element models are constructed using a commercial finite element software package ABAQUS to support and verify the modal analysis experiment.

1.6 Objectives

The main objectives of this present project are as explained below:

(a) To obtain the mechanical properties of aluminium alloys and composite materials

(b) To determine of modal properties of the combination between aluminium alloys and three different composite materials by using free vibration test.

(c) To verify the results of dynamic behaviour between free vibration test results and finite element analysis.

1.7 Research Scopes

The study focused on the mechanical and modal properties of aluminium based on fibre metal laminates. The tensile test is used to obtain the mechanical properties values such as Young's modulus and Poisson' ratio of each materials. Alloy sheet metal 2024-T0 (Al) and three types of composite materials, which are carbon fibre (CF), glass fibre (GF) and unidirectional prepreg carbon fibre (UD-CFP) used in this experimental. The experimental modal analysis by using an impact hammer based on parameters such as different configuration and boundary conditions. The modal analysis are limited only on natural frequency and mode shape. The all result from experimental can be verified with finite element analysis by using ABAQUS/CAE. The results will be used to carry out a comparative study between numerical and experimental results.

CHAPTER 2

LITERATURE REVIEW

2.1 Introduction

This chapter presents a literature review of the manufacture on fibre metal laminates and the previous and recent research work on free vibration of fibre metal laminates by using impact hammer. Besides, review also include other important aspects such as the types of fibre metal laminates and the dynamical behaviour of fibre-metal laminates.

2.2 Manufacturing of Fibre Metal Laminates

Fibre metal laminates (FMLs) are one of the popular materials revolution in the composite area that have allowed significant weight reduction in structural design and also provided excellent fatigue properties and corrosion resistance in applications. During the past decades, fibre metal laminates were mostly used in the aerospace industry as the material offers many advantages. Fibre-metal laminates consist of two materials which are combination of metal alloy with fibre epoxy. Several processes can be used to combine these two materials, such as by autoclave processing, resin transfer moulding (RTM), using vacuum bag system and compression mould.

2.2.1 Autoclave Processing

Autoclave processing is the most common process used to manufacture FMLs materials (Upadhya et al., 2011), as shown in Figure 2.1. There are several steps to produce FMLs by using autoclave (Sinmazçelik et al., 2011). The first step involves the metal alloy surface layer to be pre-treated chemical treatment such as chromic acid and phosphoric acid to provide good bonding between the adhesive system and the metal

alloy surface. Then, resin is uniformly applied over the metal plates and fibre reinforced materials by using a hand lay-up process.
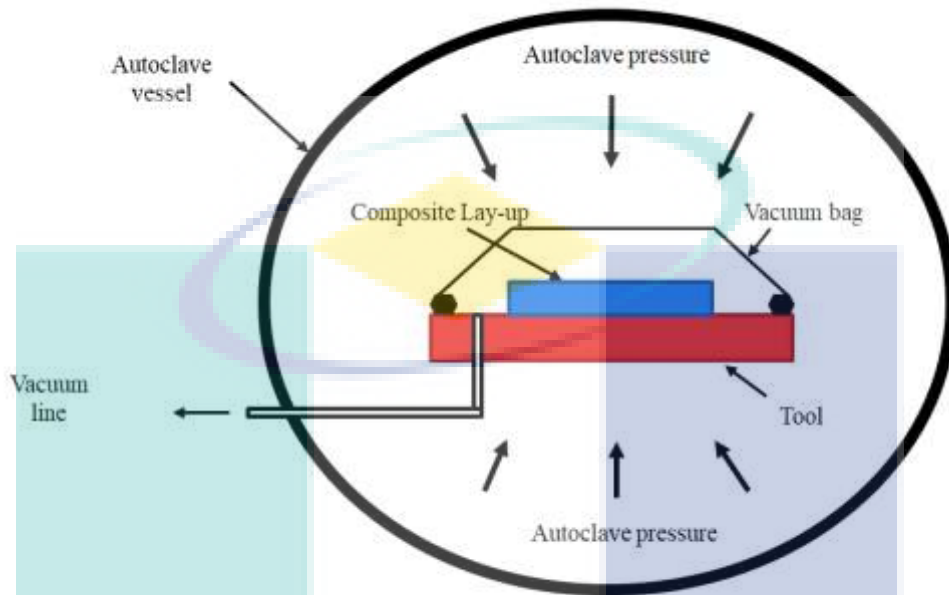
Figure 2.1   Schematic diagram of autoclave processing

For curing preparation, uniform pressure is applied through the vacuum bag technique. While curing, several other processes take place, which, the flow-consolidation process, chemical reactions, as well as bonding between fibre with the metal layer. In autoclave processing only the temperature and pressure are required to ensure composite layer consolidation and cure. Basically, FMLs need to cure at a temperature of up to 120°C in order to avoid damages on the aluminium alloys (Müller, 2017). During this time, the temperature of the resin viscosity is reduced and flows. The pressure was needed to press and to consolidate the plies and suppress voids. Chang et al. (2008) used the autoclave curing process to consolidated hybrid FMLs to investigate fatigue crack initiation in hybrid FMLs.

2.2.2   Vacuum Assisted Resin Transfer Moulding

Vacuum-assisted resin transfer moulding (VARTM) is capable of manufacturing FMLs, as shown in Figure 2.2. The VARTM process is a family of closed-mould low-pressure processes. The flow of resin materials through unwetted fibre is one of the common features of resin transfer processes. Usually, low viscosity fast-curing resins such as polyester and epoxy with continuous mat reinforcement and low fibre-volume

content will be used in the process. The quality of FMLs depends on the fluidity of the resin VARTM FMLs cure in 5 hours at temperature of 125 ºF, followed by another 6 hours at temperature of 165 ºF (Baumert et al., 2009). Abraham et al. (1998) used VARTM to manufacture glass fibre epoxy composites and compared the physical properties of the material with that manufactured by using autoclave consolidation process.
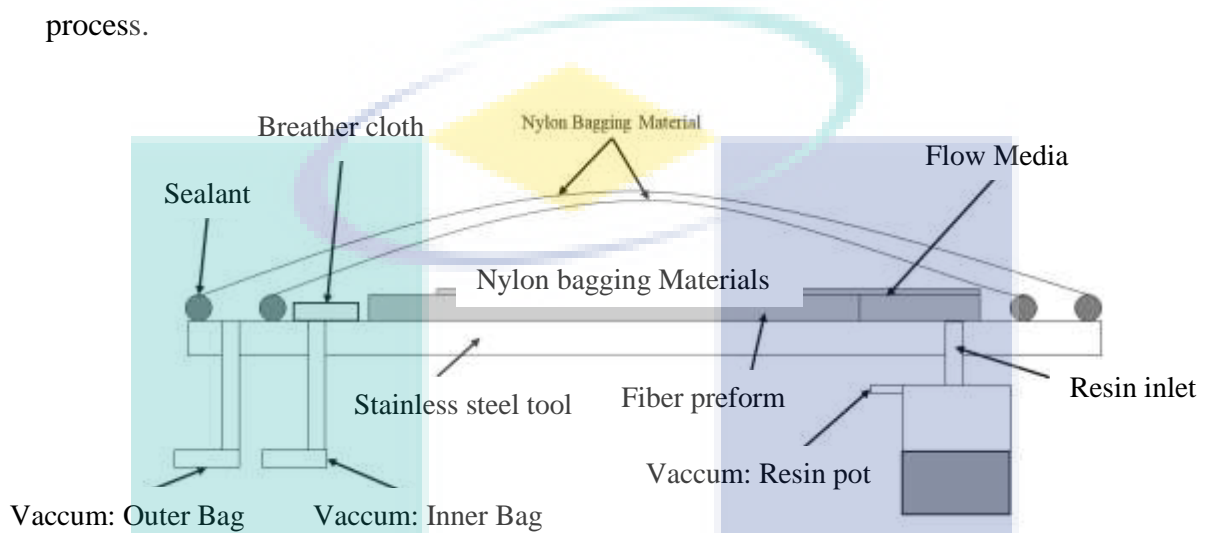
Figure 2.2   Schematic diagram of the VARTM process

2.2.3   Vacuum Bagging

Vacuum bagging is another famous manufacturing process for FMLs, which is shown in Figure 2.3. Vacuum bagging was often performed to repair aircraft composite components. The process is an extension of the wet lay-up process where pressure is applied to the laminate once it is laid-up in order to attain better consolidation. It can be accomplished by sealing a plastic film over the wet laid-up laminate and onto the product. A vacuum pump is used to extract all the air under the bag, and thus up to one atmosphere of pressure can be applied to the laminate to consolidate it. Based on research by Benedict (2012), the researcher used the vacuum bagging method to fabricate GLARE that took 6 hours to cure and to ensure a good bond. The pressure of the vacuum was approximately 1 atm. There are many advantages of using vacuum bagging such as higher fibre content laminates can be fabricated than with normal wet lay-up techniques, besides offering low void contents and better fibre wet-out due to pressure and resin flow throughout the structural fibre with excess resin flowing into the bag.
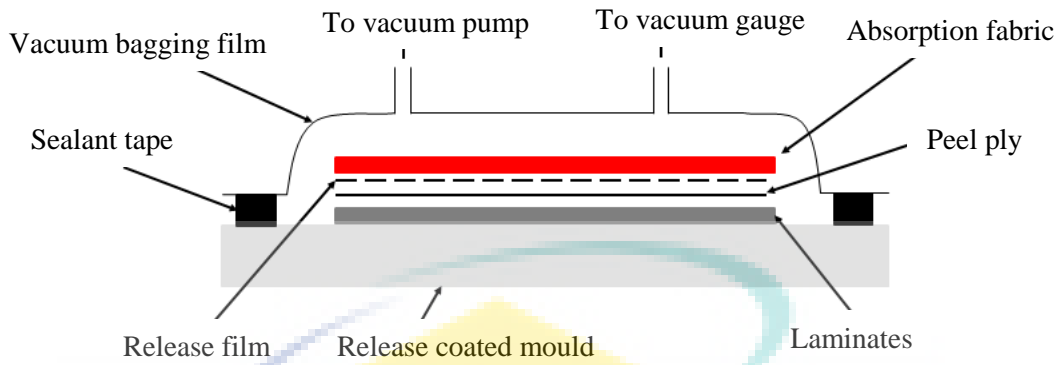
Figure 2.3   Process of vacuum bagging

2.2.4   Compression Moulding

The compression moulding process is also widely used in manufactured FMLs. The principal benefit of compression moulding is that it can produce parts of complex geometry in short periods of time (Mallick, 2007), as shown in Figure 2.4. There are several steps involved, in which the specimens need to be fabricated by conventional hand lay-up. Make sure the specimen does not exceed the mould dimension. Generally, the specimen is placed on a mould and then a pressure value is set to press the specimen.
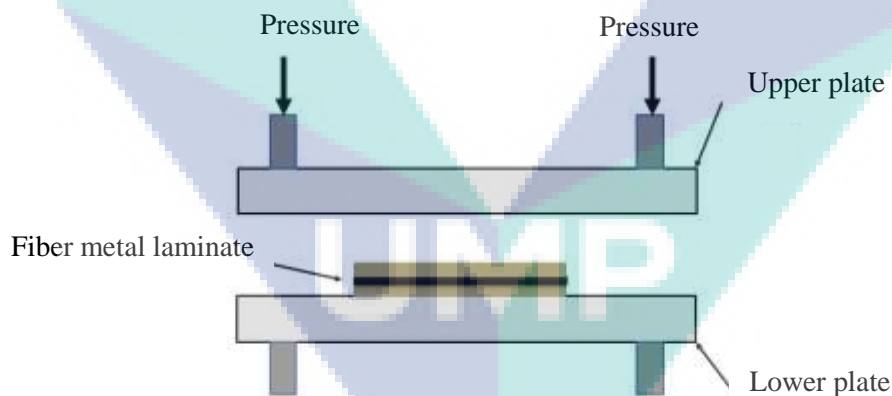
Figure 2.4   Schematic diagram of the compression moulding process

The advantages of this process include ease of handling, inexpensive and lower tooling costs. In a previous study, researchers used cold press compression moulding process to fabricate thermoplastic fibre-metal laminates, which combined two composite materials with aluminium alloy 2024-T3 (Reyes & Kang, 2007). In another study on the mechanical properties of a novel fibre-metal laminate based on polypropylene

composites, researchers used the compression moulding process to fabricate aluminium alloy combined with self-reinforced polypropylene (SRPP) (Carrillo & Cantwell, 2009). There have been reports on the fabrication of flax, hemp and jute plain-woven natural fibre reinforced polypropylene composite panels by using compression process to study the response of natural fibre composites to ballistic impact via fragment-simulating projectiles (Wambua et al., 2007). The compression moulding process was also used to manufacture polypropylene fibre reinforced metal laminates in investigating the impact (M. R. Abdullah & Cantwell, 2006). Table 2.1 shows a summary of the manufacturing process of FMLs from the year 2013 until 2018.

Table 2.1   A summary of manufacturing fibre metal laminates

Fibre materials and metal	Manufacturing techniques	References
Aluminium 1100-H14 with aramid fabric/PP matrix composite	Aluminium sheet, PP film and aramid woven fabric are fabricated using hot press compression at 175°C with the pressure of 2 MPa for 20 min.	Gonzalez et al. (2017)
Aluminium 2024-T3 alloy with self-reinforced polypropylene (SRPP)	Aluminium sheets and SRPP prepared by the pneumatic press and heated to 135°C at a rate of 10°C/min	Santiago et al. (2017)
Aluminium 2024-T3, glass fibre reinforced polymer and carbon fibre reinforced polymer	The hybrid materials prepared by autoclave method, cure cycle at a heating 2°C/min up to 135°C and held at this temperature for 2 hours	Bieniaś (2017)
Aluminium 6061 alloy with carbon and glass fibre.	Aluminium alloy with carbon and glass fibre are manufactured using compression moulding at room temperature.	Hariharan and Santhana (2016)
Stainless steel (AISI 316L) with glass fibre reinforced polymer	The prepreg layers were positioned between two plates, then packed into the vacuum bag, thus simultaneously and synchronously cured in the autoclave	Poodts et al. (2015)
Aluminium 2024-T3 with glass fibre reinforced polymer (Glare 2B)	The hybrid fibre metal laminate was prepared using an autoclave and consisted of four-layer aluminium and two layers Glare 2B, and the curing temperature was 120°C for 1 hour.	Sugiman and Crocombe (2012)
Aluminium 5005-0 with a self-reinforced polypropylene (SRPP)	Aluminium alloy with SRPP was manufactured by placed in a hydraulic press and heated 120°C	Sexton et al. (2012)

2.3   Advantages and Disadvantages of Fibre Metal Laminates

Fibre-metal laminates (FMLs) are a combination between of plies of fibre reinforced polymer and a thin sheet of metal alloys. ARALL (Aramid fibre reinforced aluminium laminate), CARALL (Carbon fibre reinforced aluminium laminate), and GLARE (Glass fibre reinforced aluminium laminate) are a classification of FML based on metal plies (Sinmazçelik et al., 2011; Vermeeren, 2003). FMLs reveal superior mechanical properties like high corrosion resistance, outstanding strength to weight ratio compared to the conventional lamina consisting only fibre-reinforced lamina or monolithic aluminium metal alloys (Chang et al. (2008). It also provides excellent mechanical properties and damages tolerance capabilities that meet the strict requirements of aerospace applications such as cargo interior or fuselage (Morinière et al., 2014). Table 2.2 shows a summary of the advantages of FMLs based on previous studies. Conversely, the FMLs long cure cycle to cure the polymer matrix in the composite plies is one of the disadvantages associated with epoxy-based fibre metal laminates (Cortes 2006; Morinière et al., 2014). This prolonged cure cycle, will significantly multiply the cycle of the entire production, reduce productivity, increase labour costs and essentially the overall production cost of FMLs (Aniket et al., 2016).

Table 2.2   Advantages of FMLs

Characteristics	Details	References
Strength	FMLs consists of a combination between plies of fibre-reinforced polymeric and thin layers of metals which have high strength and stiffness	Alderliesten and Benedictus (2007); Beumler (2006)
Fatigue resistance	High fatigue resistance of FMLs achieved by the intact bridging fibres in the wake of the crack, which can hold the crack opening	Alderliesten and Benedictus (2007); Vlot (1996)
Energy absorption capacity	Significant energy can absorb by FMLs through localized fibre fracture and shear failure in the metal pies	Cortes (2006); Cortes and Cantwell (2004)
Impact resistance	The advantages of FMLs are about impact deformation, especially when compared to composites.	Vogelesang and Vlot (2000)
Corrosion resistance	Due to polymer-based in FMLs, it gives excellent moisture resistance and high corrosion	Alderliesten (2009); Gutowski (1997); Vlot (1996)

2.4   Theory and Formulation of Mechanical Vibration

Vibrations are mechanical oscillations of physical objects, such as a plate, particles or bodies that are displaced from a position of equilibrium. It happens as the physical object experiences change from kinetic energy to potential energy. Vibrations are divided into two cases, which are free and force vibrations. The free vibrations when the body oscillates do not require external force acts on the body further to keep in motion. Meanwhile, force vibration is force keeps the body in vibration throughout its entire period of motion. Every object consists of distinct response based on materials properties, geometry, and boundary condition. It is convenient to explain the vibrational response with few main parameters such as amplitude, mode shape and frequency.

Amplitude describes the amount of maximum displacement in a vibration structure shows in Figure 2.5. It can also be explained in terms of gain, which is the ratio of dynamic amplitude to the static amplitude. The mode shape is the deflection pattern that corresponds to a particular vibration solution and also displacement that the physical object experiences as a function of initial structural position. The mode shape depends on the boundary condition of the structure. Figure 2.6 and Figure 2.7 illustrate mode shape on different boundary conditions. Frequency refers to a number of oscillations per time period. It is directly related to a system's eigenvalue.
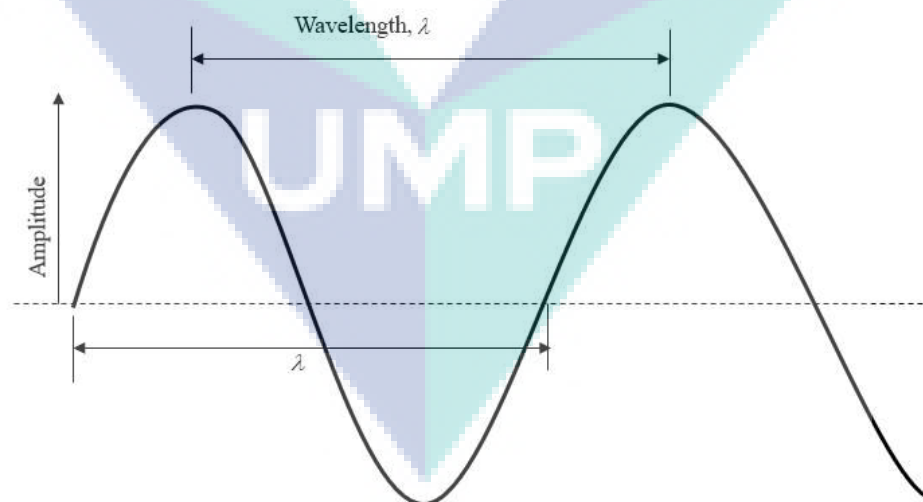
Figure 2.5   The amplitude illustration in a vibration structure
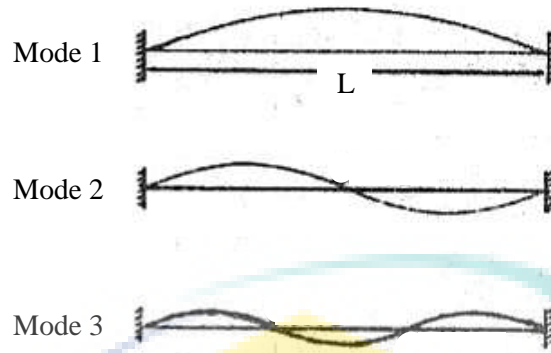
Figure 2.6   Mode shape for fixed-fixed boundary condition
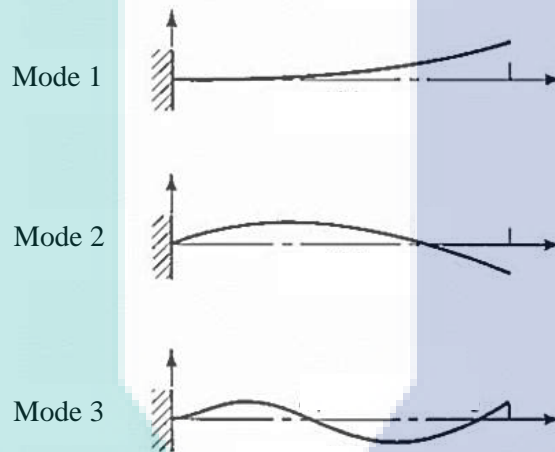
Figure 2.7   Mode shape for fixed-free boundary condition

2.4.1   Fundamental Equation of Free Vibration

Free vibration means the motion of a structure does not require dynamic equation external forces. The equation of motion of linear single degree of freedom (SDF) system,

$$m\frac{d^2u}{dt^2} + kx = 0$$

2.1

Free vibration is initiated by giving a disturbance to the system from its static equilibrium position. Thus, by imparting the mass some displacement u and velocity $\dot{u}$ at time zero.

$$u = u(0), \ \dot{u} = \dot{u}(0)$$

23

By standard methods, the solution to the equation is obtained,

$$u(t) = u(0)\cos\omega_n t + \frac{\dot{u}(0)}{\omega_n}\sin\omega_n t \qquad\qquad 2.2$$

By defining the circular frequency ω_n by equation

$$\omega_n = \sqrt{\frac{k}{m}}, \text{ rad/sec} \qquad\qquad 2.3$$

The natural period of the oscillation for the undamped system to complete one cycle of free vibration is

$$T_n = \frac{2\pi}{\omega_n}, \qquad\qquad 2.4$$

Natural cyclic frequency of vibration is donated by

$$f_n = \frac{1}{T_n}, \text{Hz} \qquad\qquad 2.5$$

2.4.2 Formulation of Free Vibration on Composite Laminates

Here, an FMLs plate is considered of length 'a', width 'b', and thickness 'h' consisting of n number of thin layers, is represented for oriented at an angle with lamina system. The displacement function in shear deformation theory is

$$
\begin{aligned}
u(x, y, z) &= u_0(x, y) + z\theta_x(xy), \\
v(x, y, z) &= v_0(x, y) + z\theta_y(xy), \\
w(x, y, z) &= w_0(x, y),
\end{aligned} \qquad\qquad 2.6
$$

Where u, v and w are the displacements in x, y and z directions, $u_0, v_0,$ and w_0 are initial θ_x and θ_y are the rotations of the cross-section perpendicular to X and Y axes. The Green-Lagrange strain relations is where $\varepsilon_{xx}, \varepsilon_{yy},$ and γ_{xy} are the bending strains and $\gamma_{xz}, \gamma_{yz},$ are the transverse shear strains.

24

$$\begin{Bmatrix} \varepsilon_{xx} \\ \varepsilon_{yy} \\ \gamma_{xy} \\ \gamma_{xz} \\ \gamma_{yz} \end{Bmatrix} = \begin{Bmatrix} \dfrac{\partial u}{\partial x} \\ \dfrac{\partial v}{\partial y} \\ \dfrac{\partial u}{\partial y} + \dfrac{\partial v}{\partial x} \\ \dfrac{\partial u}{\partial z} + \dfrac{\partial w}{\partial x} \\ \dfrac{\partial v}{\partial z} + \dfrac{\partial w}{\partial y} \end{Bmatrix}, \qquad\qquad 2.7$$

From the (Rath, 2012) studied, the constitution equation for plate are

$$\{F\} = [D]\{\varepsilon\},$$
$$\{F\} = \{N_x, N_y, N_{xy}, M_x, M_y, M_{xy}, Q_x, Q_y\}^T,$$
$$\{\varepsilon\} = \{\varepsilon_x, \varepsilon_y, \gamma_{xy}, \kappa_x, \kappa_y, \kappa_{xy}, \varphi_x, \varphi_y\}^T, \qquad\qquad 2.8$$
$$[D] = \begin{bmatrix} A_{ij} & B_{ij} & 0 \\ B_{ij} & D_{ij} & 0 \\ 0 & 0 & S_{ij} \end{bmatrix},$$

where $N_x, N_y,$ and N_{xy} are in-plane stress resultants, M_x, M_y and M_{xy} are moment resultants, Q_x, Q_y are transverse shear stress resultants. A_{ij}, B_{ij}, D_{ij} are extensional, bending-stretching coupling, bending and S_{ij} are transverse shear stiffness.

$$(A_{ij}, B_{ij}, D_{ij}) = \sum_{k=1}^{n} \int_{z_{k-1}}^{k} \left[\bar{Q}_{ij} \right]_k (1, z, z^2) dz \quad (i, j = 1, 2, 6), \qquad\qquad 2.9$$

$$(S_{ij}) = \alpha \sum_{k=1}^{n} \int_{z_{k-1}}^{k} \left[\bar{Q}_{ij} \right]_k (1, z, z^2) dz \quad (i, j = 4, 5),$$

where $\left[\bar{Q}_{ij} \right]$ is the off-axis elastic constant matrix and 'α' is the shear correction factor where (5/6) is adopted. $\left[\bar{Q}_{ij} \right]$ in Eq. (2.8) is defined as

$$\left(\bar{Q}_{ij} \right)_k = [T_1]^T [Q_{ij}]_k [T_1] \quad (i, j = 1, 2, 6), \qquad\qquad 2.10$$

$$\left(\bar{Q}_{ij}\right)_k = [T_2]^T [Q_{ij}]_k [T_2] \quad (i, j = 4, 5),$$

$$[T_1] = \begin{bmatrix} \cos^2\theta & \sin^2\theta & \sin\theta\cos\theta \\ \sin^2\theta & \cos^2\theta & -\sin\theta\cos\theta \\ -2\sin\theta\cos\theta & 2\sin\theta\cos\theta & \sin^2\theta - \cos^2\theta \end{bmatrix}, \quad [T_2] = \begin{bmatrix} \cos\theta & \sin\theta \\ -\sin\theta & \cos\theta \end{bmatrix}, \qquad 2.11$$

where the $[T_1]$ and $[T_2]$ are transformation matrices, $[\bar{Q}_{ij}]$ is on axis elastic constant matrix and defined as

$$[\bar{Q}_{ij}]_k = \begin{bmatrix} Q_{11} & Q_{12} & 0 \\ Q_{12} & Q_{22} & 0 \\ 0 & 0 & Q_{66} \end{bmatrix} \quad (i, j = 1, 2, 6), \qquad 2.12$$

$$[Q_{ik}]_k = \begin{bmatrix} Q_{44} & 0 \\ 0 & Q_{55} \end{bmatrix} \quad (i, j = 4, 5),$$

in which

$$Q_{11} = E_{11} / (1 - v_{12}v_{21}), \quad Q_{12} = v_{12}E_{22} / (1 - v_{12}v_{21}),$$

$$Q_{22} = E_{22} / (1 - v_{12}v_{21}), \quad Q_{44} = G_{13}, \quad Q_{55} = G_{23},$$

where E_{11}, E_{22} are Young's moduli of lamina along and cross the fibres, G_{12}, G_{13} and G_{23} are shear moduli of lamina, v_{12}, v_{21} are Poisson rations along and across the fibres. The element mass matrix $[M_e]$ as

$$[M_e] = \int_{-1}^{+1} [N]^T [P][N][J]d\xi d\eta, \qquad 2.13$$

where $[N]$ is shape function matrix an $[P]$ is the inertia matrix and can expressed as

$$[N] = \sum_{i=1}^{4} \begin{bmatrix} N_i & 0 & 0 & 0 & 0 \\ 0 & N_i & 0 & 0 & 0 \\ 0 & 0 & N_i & 0 & 0 \\ 0 & 0 & 0 & N_i & 0 \\ 0 & 0 & 0 & 0 & Ni \end{bmatrix} \text{ and } [P] = \begin{bmatrix} P_1 & 0 & 0 & 0 & 0 \\ 0 & P_1 & 0 & 0 & 0 \\ 0 & 0 & P_1 & 0 & 0 \\ 0 & 0 & 0 & I & 0 \\ 0 & 0 & 0 & 0 & I \end{bmatrix}$$

in which

$$P_1 = \sum_{K=1}^{n} \int_{z_{k-1}}^{z_k} (\rho)_k \, dz \text{ and } I_1 = \sum_{K=1}^{n} \int_{z_{k-1}}^{z_k} (\rho)_k \, z^2 dz, \qquad \qquad 2.14$$

where $(\rho)_k$ is the mass density of kth layer from the bottom surface. The element stiffness matrix is

$$[K_e] = \int_{-1}^{+1} \int_{-1}^{+1} [B]^T [D][B][J] d\xi d\eta, \qquad \qquad 2.15$$

where $[B]$ is the strain displacement matrix, stress strain $[D]$ and Jacobian determinant $[J]$. The natural frequency of FML plates are determined by

$$\left| [K] - \omega^2 [M] \right| = 0 \qquad \qquad 2.16$$

where $[K]$ is the global stiffness matrix, $[M]$ is the global mass matrix and ω is the natural frequency.

2.5   Composite Materials with Different Boundary Conditions

Composite materials structures are becoming increasingly important in many application. Vibration analysis of composite plates were investigated with different boundary conditions (Patil et al., 2014). The findings showed that for all tested boundary conditions, natural frequency of composite plates is the highest for clamped plates. Extensive experimental work has also been conducted to investigate the free vibration of glass fibre epoxy composite plates with different boundary conditions (Dhanduvari et al., 2015). The author found that the natural frequency of the fixed-fixed boundary condition was the highest, followed by those of cantilever and simply supported boundary conditions. Another study via free vibration analysis was conducted on composites reinforced with natural fibre with respect to several parameters like laminate stacking sequences, support conditions, materials hybridisation and number of layer (Thomas et al., 2018). The results showed that clamped-clamped boundary conditions have the highest frequency.

Several researchers have attempted to model free vibration on composite plates using finite element method. The Ritz method was once incorporated with algebraic

polynomial displacement function to investigate vibration problems for laminated composites with different boundary conditions (Mohamad, 1991) and it was noted that two adjacent clamped edges increase the natural frequency value as compared to other boundary conditions.

Dimensional elasticity theory was also used to perform free vibration analysis on variable stiffness laminated composite rectangular plates (Houmat, 2018). The author investigated various combinations of free, simply supported and clamped boundary conditions and showed that each boundary condition gave different values of natural frequency.

In another study, the higher-order structural theory was used to investigate the free vibration characteristic of variable stiffness laminated composite shells with the systematic parametric study on the influence of various boundary conditions and geometric parameters (Anand et al., 2018). Their results showed the influence of the boundary conditions, whereby boundary conditions have a significant impact on the fundamental frequency irrespective of the shell geometry and that clamped boundary condition results in higher frequency.

Arafa (2016) investigated the effects of stiffness configuration, the number of layers and boundary conditions on free vibration response of stiffened laminated composite plates. The author stated that various boundary conditions have significant effects, whereby the natural frequency for clamped supports were higher than that of the simple supports. Free vibration and sound radiation characteristics of rectangular thin plates with classical boundary conditions like clamped, simply-supported were evaluated in a study (Yuan et al., 2019). From the results, the author stated that clamped boundary conditions increased the natural frequency of thin plates.

Deepesh (2015) used ANSYS to conduct free vibration analysis of composite laminates. The researcher focused on different simply supported boundary conditions, lamination parameters and effect of side-to-side thickness ratio, aspect ratio and modulus ratio. The author argued that clamped boundary conditions showed higher natural frequency value as compared to simply supported boundary conditions. Table 2.3 shows the several types of boundary conditions that already done study by previous researchers.

Table 2.3   Several types of boundary conditions that already done study by previous researchers.

Type of Boundary Conditions	References
Clamped	Yuan et al. (2019)
Clamped-clamped	Thomas et al. (2018)
Clamped	Anand et al. (2018)
Clamped	Arafa (2016)
Fixed-fixed	Dhanduvari et al. (2015)
Clamped	Deepesh (2015)
Clamped plate	Patil et al. (2014)

2.6   Vibration Analysis on FML Materials

This subtopic discussed macromechanical and micromechanical approach of composite materials in vibration studied.

2.6.1   Macromechanical Approach

Many researchers have been studied the vibration on fibre metal laminates by applying different macromechanical approach. Ghasemi et al. (2013) presented the free vibration analysis of fibre metal laminated plate on different fibre orientation effects. The layup was chosen by author where $\theta = 0°, 15°, 30°, 45°, 60°, 75°, 90°$. It has been observed that by increasing the θ (from $0°\sim45°$) the non-dimensional natural frequency of plate increased and the θ (from $60°\sim90°$) showed that the non-dimensional natural frequency of the plate decreased. It is worth to note that as θ of the fibre approaches $45°$, lateral stiffness and shear of the plate would increase. Incidentally, the natural frequency would also increase. Similar, Khalili et al. (2010) observed that the maximum values of ω_n were in the range of $\theta = 20°\sim25°$ and with the minimum values at $\theta = 90°$.

Abdullah et al. (2009) investigated the effects of different orientation of composite layers in FMLs on natural frequency response parameters. Five different stacking sequences of FML composite plates were discussed, of which each stacking constituent were of different fibre angles: $S1 = 0°$, $S2 = 15°\& - 15°$, $S3 = 30°\& - 30°$, $S4 = 45°\& - 45°$, $S5 = 0°\&90$. The author concluded that having small orientation angles would provide higher natural frequency. Yang et al. (2017) has shown that FMLs become more rigid when the ply $\theta = 0°$and the deflection is minimum when stacking sequences of FML beam is (Al-0°/0°-Al-0°/0°-Al).

Ghashochi and Sadr (2013) investigated the effects of ply angle and number of layers for PSO algorithm in attaining fundamental frequency optimisation of fibre-metal laminated panels. Their results showed that maximum natural frequency and optimum fibre orientation were not substantially influenced and approached a limiting value with the addition of layer number. Based on Liu and Liaw (2002) pertaining to dynamical Young's moduli and damping ratios of FML (GLARE 5) with different lay-up configurations: different thickness and content of aluminium alloy 2024-T3 resulted in almost constant moduli within a frequency range up to 5000 Hz. The author mentioned that less aluminium content would lower the dynamic Young's modulus.

Furthermore, Ghasemi et al. (2013) investigated the effect of layer sequence of the metal layer in FMLs on the first non-dimensional natural frequency, whereby the Al layer was placed instead of the carbon-epoxy layer of the structure separately. Results on layer sequences of the FMLs indicated that the values of non-dimensional natural frequency increased. Based on materials properties, Al layers had greater lateral elastic modulus than that of carbon-epoxy layers, which could increase the value of natural frequency. Table 2.4 shows the several effect factors in macromechanical approach available in literature.

Table 2.4   Summarisation of macromechanical approach

Laminate configuration	Effect factors	Remark	References
10 layers	Layer sequences of FML, $\theta = 0°, 15°, 30°, 45°, 60°, 75°, 90°,$	Natural frequency increase when $\theta = 0°\sim45°$ and decrease $\theta = 45°\sim90°$, natural frequency increase when the Al layer increase	Ghasemi et al. (2013)
10 plies	Layer sequences, $\theta = 0°, 30°, -30°, 45°, -45°, 90°,$	FML panels, natural frequency	Ghashochi and Sadr (2013)
8 plies	$\theta = 0°, 15°, -15°, 30°, -30°, 45°, -45°, 90°$	Aluminium/glass-epoxy, aluminium/kevlar-epoxy, aluminium/carbon-epoxy plates, frequency	Abdullah et al. (2009)

2.6.2   Micromechanical Approach

Micromechanical approach has been applied in the studies on fibre-metal laminates. The effects of volume fraction, metal thickness and L/R ratios of rotating fibre-metal laminate circular cylinder shells by free vibration analysis have been previously studied (Ghasemi & Mohandes, 2017). The effects of boundary conditions on the frequencies of the rotating cylindrical shells were remarkable. The author stated that by raising height-to-width ratio, the natural frequency would increase.

Another study Ghasemi et al. (2013) considered the geometrical parameters and embedding aluminium plies in different layers of the structure on natural frequency of truncated conical FML shell with various boundary conditions. The effect of increasing the number of embedding aluminium in the structures could be seen from the increase in frequency parameters. In fact, regardless of the quantity of aluminium layers embedded in the structure, there will be a significant increase in the frequency parameter of the system. The highest frequency of the system was detected when a couple of aluminium layers is embedded in the 1st (first layer) and 10th layers (last layer). The cone length also affected the frequency such that an increase in cone length of the FML shell resulted in a drop in the in the frequency parameter of the system

The effects of aspect ratio (*L/H*) and different metal alloys: aluminium, titanium, magnesium, composite fibre (glass, carbon and aramid) on free vibration analysis of rotating and non-rotating FML have been investigated (Harshan et al., 2016). The results from the vibration analysis of a flapwise bending non-rotating FML indicated that there were no significant differences in mode shape for the different metal alloys, but the natural frequency was highest for GLARE followed by titanium and magnesium based FMLs. The flapwise bending vibration analysis of rotating FMLs did not show any significant differences in mode shape for the different metals and GLARE had again led with higher natural frequency when compared to the other FMLs. However, the fundamental natural frequency decreased with the increase in aspect ratio due to the softening effect resulting from the increase in rotational speed and decrease in cross sectional area.

Researcher has studied the effect of the length-to-width and length-to-thickness ratio on linear and nonlinear free vibrations of fibre-metal laminates by a closed form

solution (Shooshtari & Razavi, 2010). The result showed an increase in the nonlinear frequency ratio for higher aspect ratios. Higher moduli ratio (E1/E2) indicated higher nonlinear frequency ratio. The natural frequency was also found to increase as the length-to-thickness ratio increases.

By using continuous wavelet transform (CWT), Yang et al. (2017) dynamic analysis was performed on cracked FML beams carrying moving loads. With a single open side crack, the fundamental frequency gradually increases from the crack location at the clamped end, near the free end of the beam. The minimum and maximum fundamental frequencies were found at the clamped end and free end of the beam, respectively.

The stability of parametric vibration of laminated hybrid composite plates was investigated by (Chun, Wei, & Rean, 2009). Based on Bolotin's method, dynamic instability was determined by solving the eigenvalue problem. The effects of various parameters such as layer thickness ratio, layer number and core materials were all investigated. The thickness ratio caused excitation of the frequency by which dynamic stability indices were significantly affected. The excited frequency diminishes with the increase in layer thickness ratio and decrease in stacked-layer number.

Ghasemi and Mohandes (2018) investigated the free vibration of micro and nano-FML circular cylindrical shells based on modified couple stress theory (MCST) using Love's first approximation shell theory and beam modal function Moreover, the effects of volume fractions on composite section, material properties, length-to-radius ratio of FML circular cylindrical shells were also discussed. Higher values of elastic modulus also affected the frequency values.

In addition, by increasing the value of material length scale parameter caused a decline in the frequencies of micro-FML cylindrical shells. Ghasemi and Mohandes (2017) investigated free vibration on beam modal function model of FML cylindrical shells subjected to different boundary conditions. The distinction of frequencies for specimens of different material properties of composite fibre and volume fraction of the composites were also studied. Table 2.5 shows the summary of micromechanical approach available in literature.

Table 2.5   Micromechanical approach in dynamic behaviour study of fibre metal laminates

Approach	Remarks	References
Effect of different magnitudes of volume fraction of metal, metal thicknesses, axial and circumferential wave numbers and L/R ratios	Variations of frequencies with different rotational speeds	Ghasemi and Mohandes (2017)
Effect of different metal alloys, different angular velocities, aspect ratio (L/H)	Natural frequency, rotating and non-rotating FML	Harshan et al. (2016)
Geometrical parameter, embedding aluminium plies, boundary condition	Conical FML shells	Ghasemi et al. (2013)
Effect of the length-to-width, length-to-thickness ratio	Dimensionless frequencies of some mode of rectangular Glare 3 (3/2)	Shooshtari and Razavi (2010)
Layer thickness ratio, layer number, core materials	(Al/GFRP/Al, Al/CFRP/Al), Excitation frequency, instability region, dynamic instability index	Yang et al. (2017)
Volume fraction, lay-ups, materials properties, materials length scale parameters, boundary conditions	ARALL & GLARE micro cylinder, frequency	Ghasemi and Mohandes (2018)

2.6.3   Different Configuration of FMLs

Botelho et al. (2005) manufactured carbon fibre/epoxy, glass fibre/epoxy and their hybrids aluminium 2024-T3 alloy/carbon fibre/epoxy and aluminium 2024-T3 alloy/glass fibre/epoxy composites. The researcher studied about damping behaviour of continuous fibre/metal composites materials using free vibration method, as shown in Figure 2.8. The study revealed that FMLs based on carbon fibre/epoxy showed higher frequency value than of FMLs based on glass fibre/epoxy. The researcher also stated that the individual damping mechanism of the composite laminae and the thin metal alloys, of the FMLs and the interface between the different materials also have effects on vibration damping.
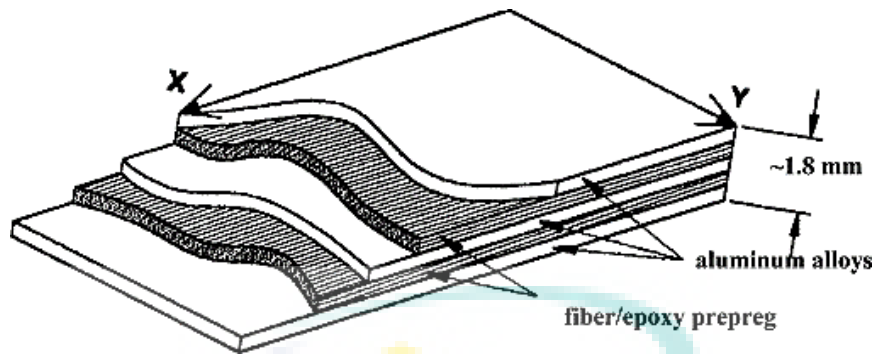
Figure 2.8   The configuration of continuous fibre/metal/epoxy hybrid composite (3/2 lay-up)

Pardini et al. (2005) prepared GLARE laminates with a lay-up of 3/2. The GLARE laminates were then investigated for a comparison of elastic properties measured by tensile testing and free vibration-damping experiments. Furthermore, the authors mentioned that the results were also compared with the findings of conventional polymer composite materials. The authors reported similar results for elastic modulus, obtained by tensile testing and storage modulus, obtained by free vibration experiments, either with dry specimens or even specimens submitted to hydrothermal conditioning (specimens exposed at $80^o C$ and 90% RH, for 60 days).

Malekzadeh et al. (2010) fabricated hybrid (FML) cylindrical shells based on aluminium alloy/carbon fibre/epoxy (CARE), aluminium alloy/glass fibre/epoxy (GLARE) and aluminium alloy/Kevlar fibre/epoxy (ARALL). The author studied the transient dynamic response of clamped free hybrid composite circular cylindrical shells. The authors also investigated the effect of lay-up, material properties, fibre orientation and volume fraction of metal layers on the dynamic responses of the shell.

Ghasemi et al. (2013) administered an experiment to discover the effects of geometrical and material parameters on free vibration analysis of FML plates. The FMLs were prepared by combining T300/934 carbon-epoxy layer and 2024-T3 aluminium layer. The researcher applied first order shear deformation theory (FSDT) as well as the Fourier series method to analytically solve the Rayleigh-Ritz analytical method. Moreover, the results showed important parameters such as the sequence of metal layers, aspect ratio (a/b) of the plate and fibre orientation of the composites play important factors in affecting free vibration of the FMLs.

Fu et al. (2014) explored the analysis of nonlinear dynamic response for delaminated fibre-metal laminate (FML) beams under unsteady temperature field. The FMLs were fabricated consisting of three layers of aluminium 2024-T3 and two layers of glass fibre reinforcement. Additionally, the results showed temperature increasing the vibration amplitude of the delaminated beams. Moreover, the deflection of the delaminated FML beams under the unsteady temperature field increases to a maximum as the time increases and then remain constant.

Sessner et al. (2017) studied the damping characteristics of fibre-metal elastomer laminates using piezo-indicated-loss-factor experiments. In the study, two distinct materials were used; metal sheets and two types of elastomers. Besides this, the lay-up of the constituents was varied. The authors pointed out that the different laminate lay-ups were compared with each other in order to determine the influences of individual constituents. Vibrations were induced with a frequency ranging from 100 Hz to 20 kHz whereby the laminates were mounted onto a speaker. The results showed that vibration was affected by the different elastomer types and prepreg lay-up, whereas the different metals showed only a small effect.

Rezende et al. (2005) studied the hygrothermal effect on damping behaviour of metal alloy/glass fibre/epoxy hybrid composites. The free vibration damping tests were done by using impact hammer in order to compare the elastic and viscous response of these materials. The study focused on obtaining the viscoelastic properties such as storage modulus (E') and loss modulus (E'') for the glass fibre/epoxy, aluminium 2024-T3 alloy and glass fibre/epoxy/aluminium laminates (GLARE). From this study, the author found that glass fibre/epoxy composites decrease the E' modulus during hygrothermal conditioning up to the saturation point (6 weeks), whereas E' modulus of GLARE laminates remained unchanged (49 GPa).

Sarlin et al. (2012) investigated the damping properties of steel, rubber or epoxy adhesive and glass fibre reinforced epoxy composite. The damping properties of the structures were investigated through the loss factor. The frequency and time domain test methods were used in order to determine the loss factors of hybrid structures and constituent materials. The loss factor of the specimens was estimated by the rule of mixtures. The study has revealed that the use of weight fractions instead of volume

fractions provides a better average estimation of the damping behaviour of the hybrid structure.

Iriondo et al. (2015) fabricated traditional fibre-metal laminate (FML) and fibre-metal laminates (FML) based on self-reinforced polypropylene (SRPP). The author used a base motion produced by an electrodynamic shaker to investigate the characterisation of the complex Young's modulus of traditional FML and FML based on SRPP, as shown in Figure 2.9. The results showed that GLARE and the reference material 2024-T3 gave higher storage modulus than that of FML based on SRPP. Furthermore, FMLs based on SRPP offered higher damping capacity than traditional FMLs which offered better vibrational performance.
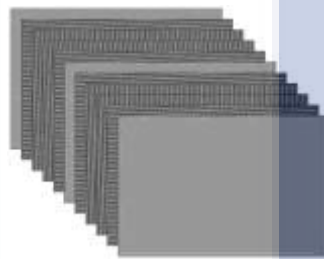
Figure 2.9   The illustration of the stacking configuration

Mathivanan (2016) studied the damping behaviour of aluminium/glass fibre/plastic hybrid laminates at distinct impact velocities by introducing a small percentage of fly ash as micro-filler materials. The damping behaviour was analysed using an instrumented drop weight impact testing machine with low velocity (<11m/s) and an accelerator is fixed onto the specimen while connected to a dynamic signal analyser.

The addition of micro-fillers caused the damping factor to increase as determined by the drop weight method. Samia and Asif (2017) investigated the modal analysis of optimisation techniques for adhesive bonding between carbon fibre reinforced polymer and aluminium. The author only optimised two methods, which are the introduction of fillets and step configuration in standard lap joint configuration. Based on the investigation results, the introduction of fillets and step layout reduced the modal displacement and increased the modal frequencies. A summary of the materials used in FML vibration studies is shown in Table 2.6.

Table 2.6   Summarisation of materials used in FML in vibration studies

Metal alloy	The lay-up scheme of hybrid composite	References
Al 2024-T3	Al/CE/Al/CE/Al (3/2) Al/GE/Al/GE/Al (3/2)	Botelho et al. (2005)
Al 2024-T3	Al/CE 0°/Al/CE 0°/Al (3/2) Al/GE 0°/Al/GE 0°/Al (3/2) Al/KE 0°/Al/KE 0°/Al (3/2)	Malekzadeh et al. (2010)
Al 2024-T3	Al/GE/Al/GE/Al (3/2)	Fu, Yiming, Chen Yang, Zhong Jun (2014)
Al 2024-T3	Al/GE/Al/GE/Al (3/2)	Pardini et al. (2005)
Al 2024-T3	Al/GE/Al/GE/Al (3/2) Al/SRPP/Al/ SRPP /Al (3/2)	Iriondo et al. (2015)

Al: Aluminium, GE: Glass epoxy, CE: Carbon epoxy, SRPP: Self-reinforced polypropylene

2.6.4   Different Boundary Conditions of FMLs

Experimental modal analysis (EMA) is one method to analyse structural vibration behaviour characteristics. Resonance, mode shape, natural frequency and damping can be analysed by using an impact hammer accelerometer, multi-channel data acquisition and analysis software.

Murugan et al. (2016) used the impact hammer test to study the modal response on composite beams. In conducting the vibration test, one end of the specimen was rigidly fixed with a work clamping device while the other end was left free to satisfy the fixed-free boundary condition. The author fabricated a beam with a length of 220 mm. Figure 2.10 shows the arrangement and equipment involved to conduct the vibration test.

Bulut et al. (2016) conducted an impact hammer test to investigate the dynamic characteristics of Kevlar/glass/epoxy resin composite laminates, as shown in Figure 2.11. The vibration test specimens had dimensions of 200 x 12.7 mm, except for the free end beam which was kept at length of 155 mm. The specimens were fixed at the end of one side, while another side was left free. The author used equipment such as National Instrument (NI) with LABVIEW software for output signal acquisition, stimulus force signal and data acquisition. During the dynamic modal analysis tests, the natural frequencies and damping factors were determined.
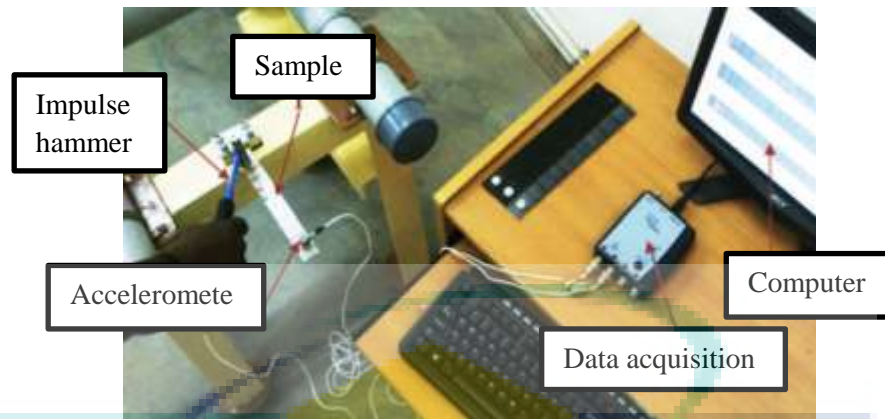
Figure 2.10   The arrangement and equipment during conducting the test
Source: Murugan et al. (2016)
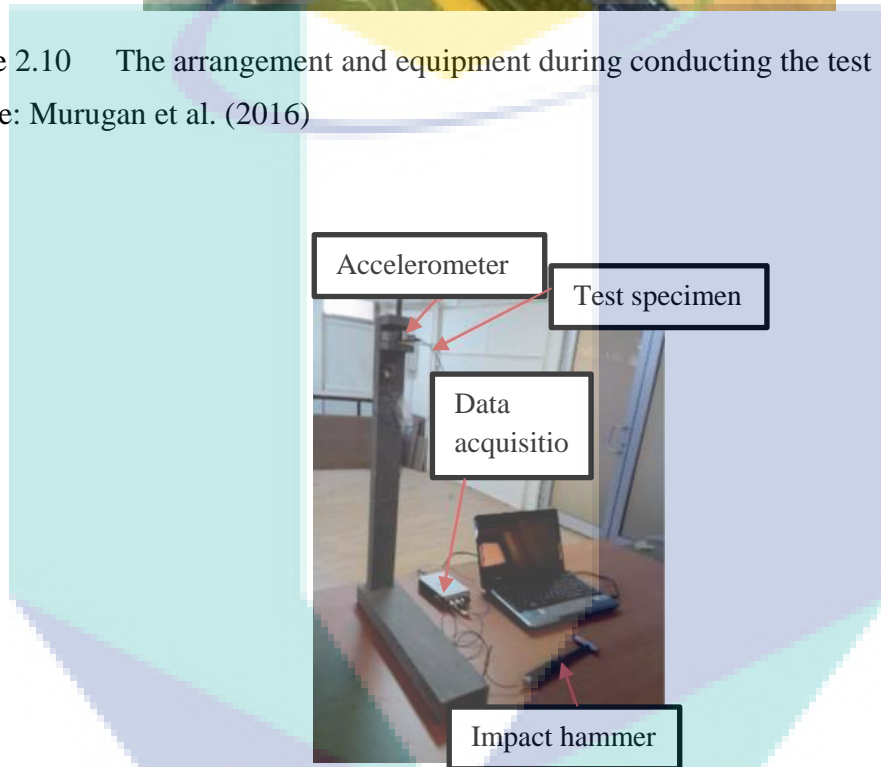
Figure 2.11   Experimental setup for vibration test
Source: Bulut et al. (2016)

In another study Bhudolia et al. (2017), researchers used the impact hammer to conduct forced vibration tests. The structural damping response of the manufactured hybrid composite was investigated by obtaining a frequency response function (FRP). The author fabricated the specimen to 150 mm in length. Senthilkumar et al. (2017) conducted an experiment with a modal analysis setup on sisal fibre polyester composites using an impact hammer, as shown in Figure 2.12. The author has fabricated the laminate composite for the vibration test is 200 mm x 20 mm x 3 mm.
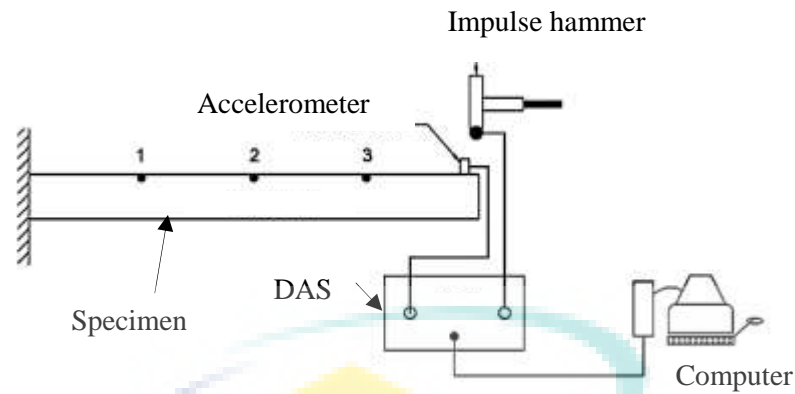
Figure 2.12   The schematic diagram of free vibration test setup
Source: Bhudolia et al. (2017)

Saffr et al. (2013) applied an impact hammer to excite the force each point on the composite plate. The author has fabricated the specimen composed of 3-layer laminated woven Kevlar/carbon fibre composite plate. The dimension of the composite plate was 600 mm x 150 mm. Furthermore, the author also added laser scanning vibrometer to measure the output response.

In another study, Utomo et al. (2017) used an impact hammer to investigate the effect of the number and position of the carbon layer to the dynamic characteristic such as natural frequency and damping ratio. The function of the impact hammer is to excite the specimens. The author fabricated the composite using a combination of glass and carbon fibre. Further, they prepared and cut the specimen into the size of 250 x 10 x 3 mm according to ASTM E756.

Kumar et al. (2014) investigated the free vibration properties of sisal/coconut sheath fibre hybrid-reinforced unsaturated polyester composites. The author used the impulse hammer technique to conduct the modal analysis of hybrid reinforced polyester composites which dimension for specimens 200 x 20 x 3 mm, as shown in Figure 2.13. The author also mentioned the use of sharp hardened tip for the impact hammer to excite the composite laminates.
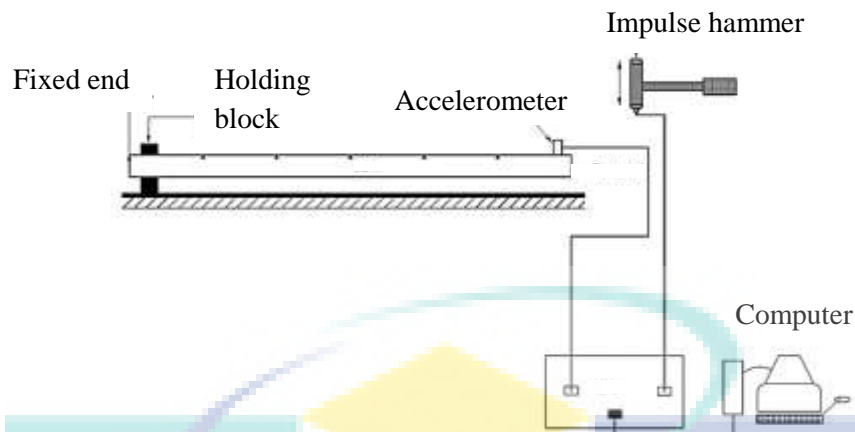
Figure 2.13   Experimental setup for free vibration analysis
Source: Kumar et al. (2014)

Sathishkumar et al. (2017) studied the mechanical behaviour and free vibration of sisal/cotton fabric reinforced polyester hybrid composites. The author conducted an impact test to analyse the natural frequency and modal damping values of the hybrid composites. They also used impact hammer with sharp hardened tip in order to hit the laminates composites with dimensions of 200 mm x 20 mm x 3 mm.

Mansour et al. (2016) conducted a modal testing of aramid/carbon fibre hybrid composites reinforced with silica nanoparticles. The author manufactured the hybrid composite with a dimension of 160 mm x 20 mm x 4 mm for modal testing. Form this research, the specimen was clamped on the rigid support and vibrated by using impact hammer. Rajesh and Pitchaimani (2017) used an impulse hammer method to investigated modal analysis such as natural frequencies and modal damping of woven natural fibre composite.

Susilo et al. (2014) studied the effects of fibre orientation on the dynamic characteristics of carbon/glass fibre hybrid composites and the dimension of the hybrid materials is 250 x 40 x 3 mm. The experiment on dynamic characteristic was done by giving excitation to the hybrid materials specimen using impact hammer and accelerometer attached to the specimen. The author used three different types of supported beam; cantilever beam, simply supported beam and fixed beam. Table 2.7 below summarises the experimental modal analysis of hybrid materials.

40

Table 2.7   Summarises about the experimental modal analysis of hybrid materials

Type of clamping	Plate dimension, mm^2	References
Fixed-free	200 x 20	Senthilkumar et al. (2017)
Fixed-fixed	310 x 25	Rajesh and Pitchaimani (2017)
Fixed-free	220 x 22	Murugan et al. (2016)
Fixed-free	200 x 2	Sathishkumar et al. (2017)
Fixed-free	160 x 20	Mansour et al. (2016)
Fixed-free	200 x 12.7	Bulut et al. (2016)
Fixed-free	250 x 40	Susilo et al. (2014)
Fixed-free	200 x 20	Kumar et al. (2014)
Fixed-free	600 x 150	Saffr et al. (2013)

2.7   Review on Modelling of Composites Materials by Finite Element Analysis

This chapter introduces the finite element method and modelling of hybrid materials. Many researchers nowadays use finite element method to analyse vibrations of hybrid composite structures, which can reduce cost and time for research. FEM is a numerical method for solving engineering problems that cannot be solved by analytical methods. Finite element method has several commercial FE packages available in the current markets such as ANSYS, COMSOL, NASTRAN PATRAN, and ABAQUS.

He et al. (2018) used secondary development interface UMAT subroutine in ABAQUS/Standard to investigate an efficient finite element method for analysing the modal damping of the composite laminates. The author fabricated the carbon/epoxy laminate composites to investigate modal damping and frequency response. The Lanczos method was applied to solve the complex eigenvalues of the composite laminates. Further, the results from ABAQUS are showed in good agreement with test data. Moreover, these numerical methods are very effective for analysis of the dynamic characteristics of various laminates.

Kyriazoglou and Guild (2006) simulated a steady state dynamic response of composite glass fibre reinforced polymer (GFRP) and carbon fibre reinforced polymer (CFRP) laminates using ABAQUS/Standard. All the FE model are developed using 3D-dimensional and in the form of rectangular beams. The FE models also were created using a twenty-node brick element with reduced integration (C3D20R). The material behaviour was modelled as linear elastic and orthotropic. The author concluded that FE is a potentially useful method for simulation damping.

Torabi et al. (2016) used ABAQUS software to simulate the delaminated beams and extraction of the natural frequencies and mode shape. The conventional shell elements are used to model the delaminated beam. Type of meshed that used is S4R elements which refer has used a 4-node doubly curved thin or thick shell, reduced integration, hourglass control and finite membrane strains. In the selection type of materials, they used lamina elastic type and composite continuum shell with Simpson's rule. The author investigated the modal analysis using the step under the procedure type; linear perturbation, frequency. They also used tie constraint in the two faces of delamination. At the same time, they select surface-to-surface contact interaction and tangential behaviour properties.

Furthermore, they concluded that by comparing the constrained and free mode models from both FE and analytical studies, the value of natural frequency obtained from the free mode was lower than the results of the constrained mode model. Jinshui et al. (2013) applied ABAQUS/Standard to analyses the damping loss factor of hybrid carbon composite pyramidal truss sandwich panels with viscoelastic layers. The author used Lanczos eigensolver to determine the frequency. Three-dimensional FE model (3D) was created using eight node and reduced integration (C3D8R). The author stated a good agreement between the results from simulation and experimental results.

Malekzadeh et al. (2010) used finite element method of ABAQUS/Explicit in order to compare the results from the analytical method. The author studied the dynamic response of multilayer circular cylinder shells composed of hybrid composite materials with lateral impulse load. The dynamic explicit analysis was used in ABAQUS software as shown in Figure 2.14. The circular cylinder was modelled using 3040 linear quadrilateral four-noded shell element (S4R). A very good correlation was found between analytical and ABAQUS software analysis results where the overall trends were rather similar.
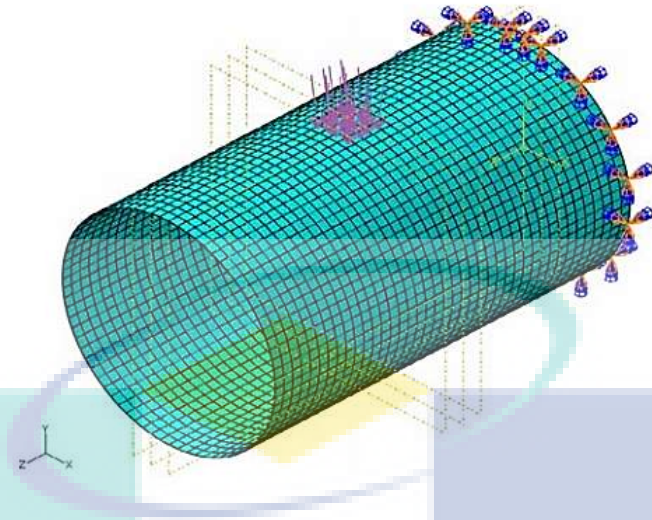
Figure 2.14   The mesh, boundary and loading conditions used for the dynamic explicit in the ABAQUS software.

2.8   Summary

This chapter has reviewed research works on free vibration of composite materials and fibre-metal laminates. A brief overview on the manufacturing of fibre metal laminates, advantages and disadvantages of fibre-metal laminates, theory and formulation, vibration of composite materials in boundary conditions, vibration of FMLs, vibration of FMLs with different boundary conditions and modelling of composite materials. The background of these investigations was related to predict the structural properties of FML materials in a vibration study to avoid typical problems caused by vibration. Several reports and investigations on vibration of FML materials have been reported, which include experimental and numerical studies to determine and predict the natural frequency and mode shapes. Correspondingly, factors that affect the vibration analysis of FMLs were discussed, which are essentially the different boundary conditions. Finally, this chapter also reviewed the modelling of composite materials by finite element analysis.

CHAPTER 3

METHODOLOGY

3.1   Introduction

This chapter presents the details of experimental work on sample preparation, processing equipment used for fabricating the composite FMLs, characterisation of materials properties and test methods. Specimen geometry and configurations are also given here. The characterisation of materials by the tensile test was described. Apart from the mechanical properties of these composites, the free vibration test was also elaborated. The modal analysis test was conducted using FMLs plate with different boundary conditions. The main aim of this experimental work is to investigate the mechanical (Young's modulus, Poisson ratio) and modal properties (frequency and mode shapes) of the FMLs plate.

For a brief review on sample fabrication, mechanical test, experimental modal analysis and finite element analysis, a summary of the entire methodology process is illustrated in Figure 3.1. Materials selection is made according to the literature review. Afterwards, sample fabrication has also proceeded with reference to the literature review. The mechanical test is aimed to obtain the mechanical properties of each material selection. Experimental modal analysis and finite element analysis are used to obtain natural frequency and mode shape. Finally, to verify the results by experimental and simulation analyses. Figure 3.1 shows the flowchart of major methodology process.
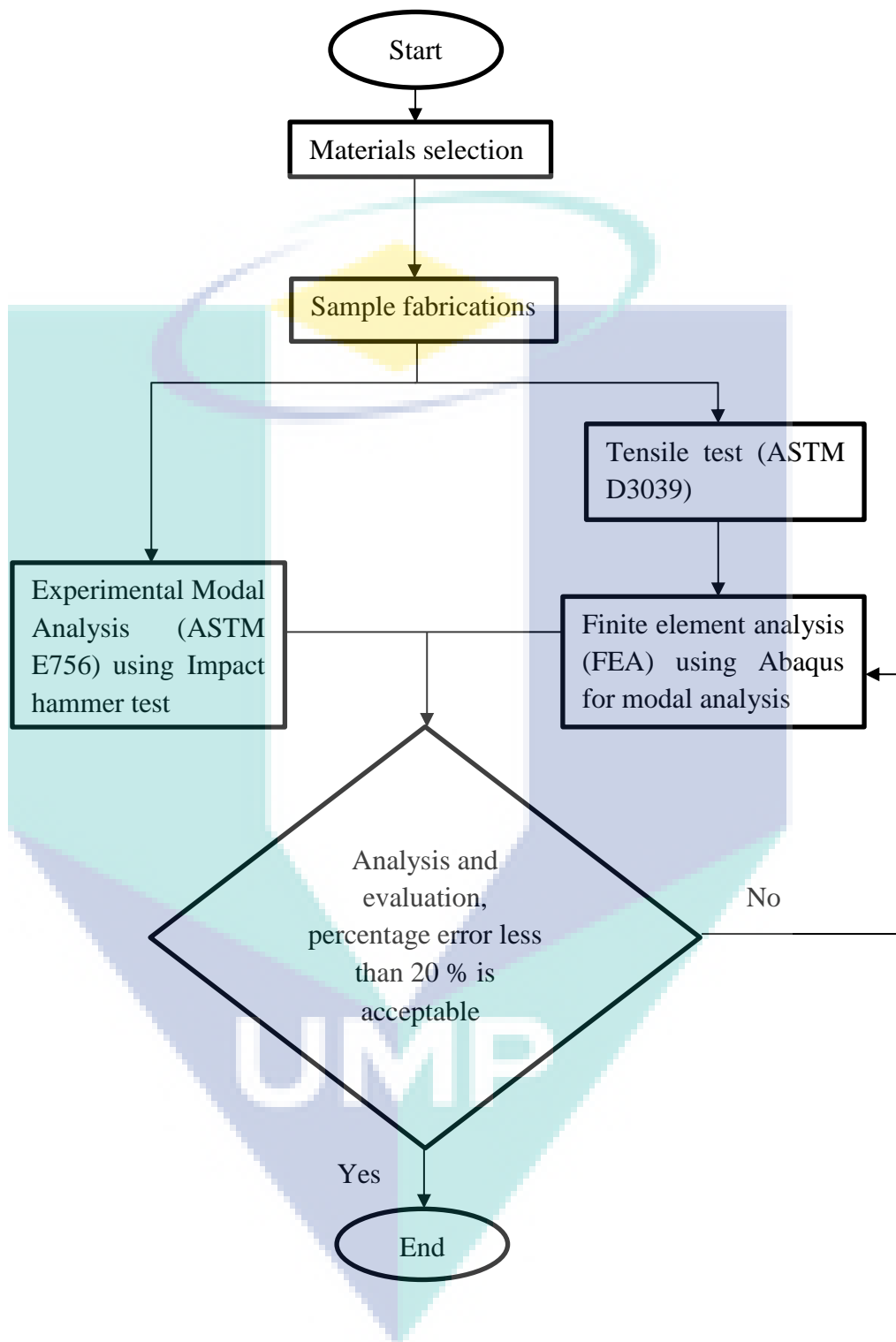
Figure 3.1   Flowchart of methodology process

3.2 Raw Materials

In this present work, glass fibre, carbon fibre, unidirectional prepreg carbon fibre and aluminium 2024-T0 were used to fabricate fibre metal laminates using epoxy resin as the matrix.

3.2.1 Epoxy Resin and Hardener

The D.E.R.^{TM} 331^{TM} Liquid epoxy resin infusion necessitates very low viscosity resin, hardener, which has been usually used in making a boat, aerospace materials bonding and composite structure in automotive body car panel. Table 3.1 showed the properties of the epoxy resin.

Table 3.1   The properties of epoxy resin given by manufacturer

Property	Value
Water Content	700 Max. (ppm)
Density @ 25° C	1.16 (g/ml)
Mix viscosity @ 25° C	11000-14000 (mPa*s)

The JOINTMINE 905-35 are used as hardened for D.E.R.^{TM} 331^{TM} Liquid epoxy resin. The specifications of JOINTMINE 905-35 are shown in Table 3.2.

Table 3.2   The specification of JOINTMINE 905-35 given by manufacturer

Property	Value
Viscosity	200 ~ 400 (BH type @ 25° C. cPs)
Amine value	300 ± 20 (mg KOH/g)

3.2.2 Glass Fibre

Woven glass fibre is used in this study as shown in Figure 3.2. the estimate of the thickness of the woven glass fibre is 0.44 mm and the standing temperature in the range -50 ~ 250 ^{o}C.

Figure 3.2   Photo of woven glass fibre

3.2.3 Carbon Fibre

Carbon fibre mostly used for many applications because of the ability to reduce weights and increase structural stiffness. In this study, woven carbon fibre was used. The carbon fibre is obtained from EasyComposite from United Kingdom (UK).

(a) (b)
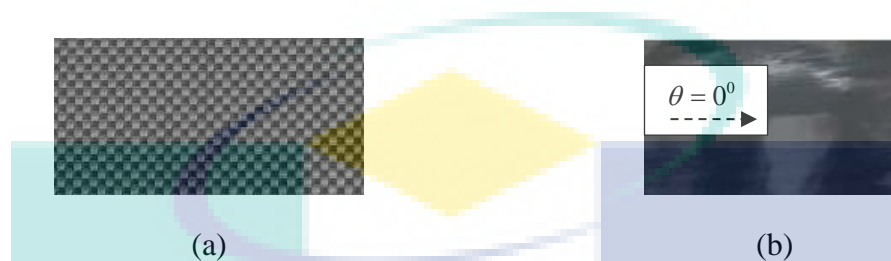
Figure 3.3   Types of carbon fibre (a) Woven, (b) Unidirectional prepreg (0°)

There are two types of carbon fibre which is prepreg and dry fibre. The prepreg fibres will be cured during the hot press process. Meanwhile, the dry fibres will be laminated with thermoset epoxy. The dry fibres will be cured at room temperature for 24 hours. Figure 3.3 showed (a) weave fibre of carbon fibre and (b) showed prepreg unidirectional.

3.2.4 Aluminium Alloy

In the Fibre-metal laminates (FMLs) specimen used aluminium alloy sheet metal then followed by composite materials. The type of aluminium alloy that was used is 2024-T0. Offer a high strength to weight ratio and good fatigue resistance, currently, it has become an aerospace primary structure. A plate of aluminium was taken out from the store and then placed on the clean flat surface as shown in Figure 3.4. The aluminium was cut according to the dimension of 250 mm x 25 mm by using shear cutting machine.

Figure 3.4   A plate of aluminium before cutting to size of 250 mm by 25 mm.

3.3   Aluminium Alloy Surface Treatment

Surface treatment for metal surfaces consisted of five groups which are mechanical, chemical, electrochemical, coupling agent and dry surface treatments. In this experiment, mechanical treatment was used. The surface of the aluminium alloy is treated by using a sandblasting technique. Surface roughness test was done by using MarSurf PS1 machine the as shown in Figure 3.5 shows the reading surface roughness (Ra) process.

| (a) | (b) |
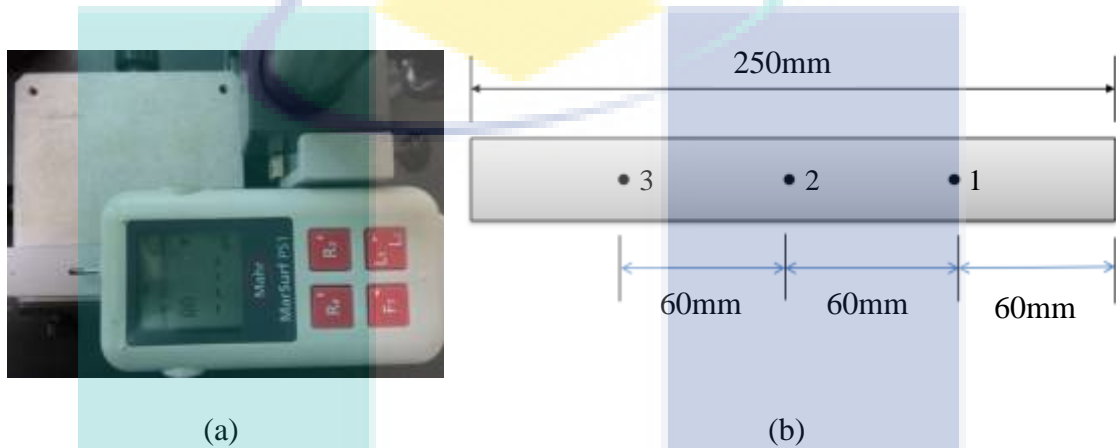
Figure 3.5   Surface roughness from top view (a) MarSurf PS1 machine, (b) schematic diagram of the location reading point on the specimen

Three points and reading were taken. The average value of surface roughness (Ra) for the untreated and treated aluminium alloy are 0.392 µm and 3.149 µm. Based on the results, the reading of surface roughness before and after sandblasting shows an increment. The increase in value meant that there was increased in surface roughness of the aluminium plate surface. This also indicated an improvement of the contact surface and bonding between the composite materials and aluminium surface.

3.4   Preparation of the Specimens

Fibre-metal laminates specimens were manufactured by stacking a series of multilayer configuration, 2/1 lay-up and 3/2 laminate, as shown in Figure 3.6. The FMLs studied in this investigation were based on aluminium 2024-T0, 0.88 mm and fibre/epoxy such as woven glass, woven carbon and unidirectional prepreg carbon fibre supplied by the EasyComposite UK. In Table 3.3 the thickness of the constituent materials and the specific weight of the FMLs materials are shown.

Table 3.3   Thickness of the constituents and the specific weight of the FMLs

Specimens	Configuration	Constituent materials	Thickness (mm)	Mass (g)
C1	2/1	Al/GFRP/Al	2.32	33
C2	2/1	Al/CFRP/Al	2.04	31
C3	2/1	Al/UD-CFP/Al	1.82	29
C4	3/2	Al/GFRP/Al/GFRP/Al	3.50	52
C5	3/2	Al/CFRP/Al/CFRP/Al	3.18	46
C6	3/2	Al/UD-CFP/Al/UD-CFP/Al	2.76	45

Al: Aluminium, **GFRP**; Glass fibre reinforced polymer, **CFRP:** Carbon fibre reinforced polymer, **UD-CFP:** Unidirectional Carbon fibre prepreg
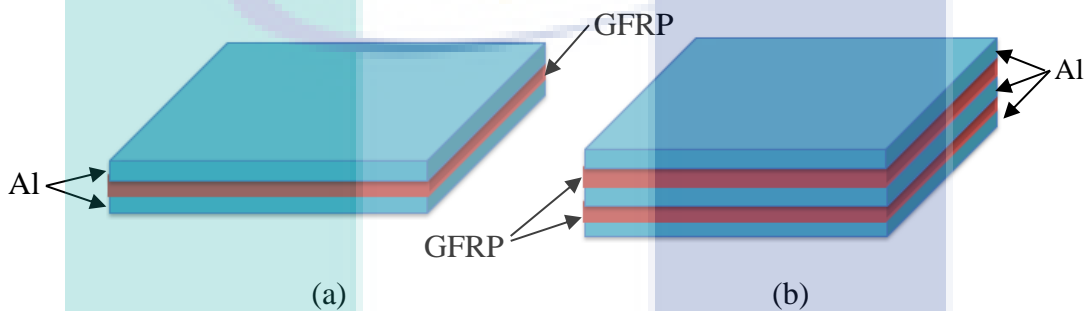
Figure 3.6   The schematic diagram of the stacking arrangement of FML (a) 2/1 and (b) 3/2

The manufacturing of FMLs as shown in Figure 3.7. The laminates were then placed in a hot press machine under a pressure of 0.4 MPa until epoxy resin cured. In addition, for FMLs materials using UD-CFP were heated to a temperature of 125°C.
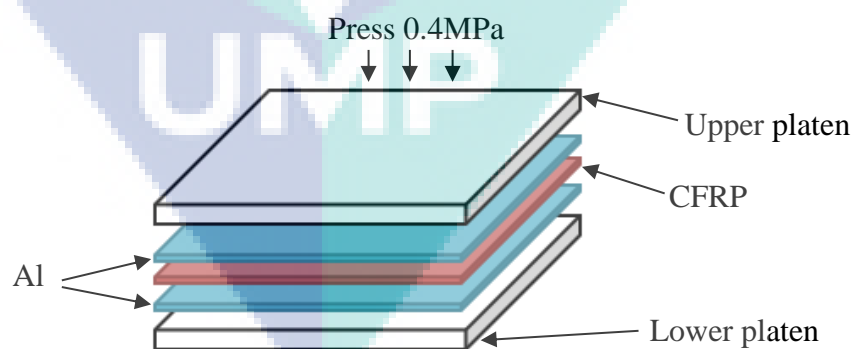
Figure 3.7   The illustration diagram of the manufacturing of a 2/1 FMLs

3.5   Materials Testing and Characterisation

The Instron Universal Testing Machine was used to carry out the tensile testing according to ASTM D3039 for composite and E8/E8M-13a for metallic materials. standard as shown in Figure 3.8. The specification of the UTM Instron machines is shown in Table 3.4. The tensile test was conducted to know the value of elastic modulus, Poisson ratio and tensile strength of the composite materials and aluminium alloys. These mechanical properties will be used in numerical analysis. The specimens with dimensions as depicted in Table 3.5 were tested with the crosshead displacement rate of 2 mm/min. For all mechanical tests, an average of three specimens was prepared.
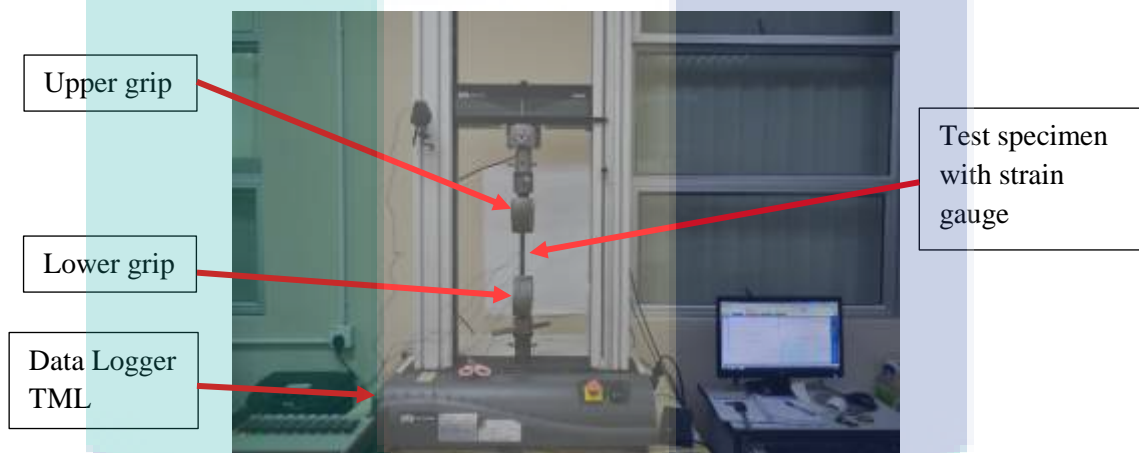
Figure 3.8   Tensile test on composite materials with UTM Instron machines and Data Logger

Table 3.4   Specification of Instron 3360 Series (Type 3369) machine

Load capacity	50 kN
Maximum Speed	500 mm/min
Minimum Speed	0.005 mm/min
Maximum Force at Full Speed	25 kN
Maximum Speed at Full Load	250 mm/min

The mechanical properties such as Elastic modulus, Poisson's ratio and Shear modulus can be calculated after the getting result from the test conducted by using the following equations

$$\text{Stress, } \sigma = \frac{F}{A} \qquad\qquad 3.1$$

Where F and A is force/load and cross-sectional area,

$$\text{Strain, } \varepsilon = \frac{L-l}{L} \qquad\qquad 3.2$$

Where L and l is the initial length and final length

Elastic modulus, $E = \dfrac{\sigma}{\varepsilon}$ 3.3

Where σ and ε is stress and strain

Poisson ratio, $\upsilon = \dfrac{E_T}{E_L}$ 3.4

where E_T and E_L is a transverse strain and longitudinal strain

Shear modulus, $G = \dfrac{E}{2(1+v)}$ 3.5

Table 3.5   Dimension of specimens for tensile test

Materials	Dimension (mm^3)	Mass (g)
Aluminium 2024-T0	250 x 25 x 0.88	14.05
GFRP	250 x 25 x 2.56	27.06
CFRP	250 x 25 x 1.94	10.43
UD-CFP	250 x 15 x 1.08	13.05

In Figure 3.9 the dimension of the specimens were prepared for tensile test (Al 2024-T0, GFRP, CFRP and UD-CFP) are shown.
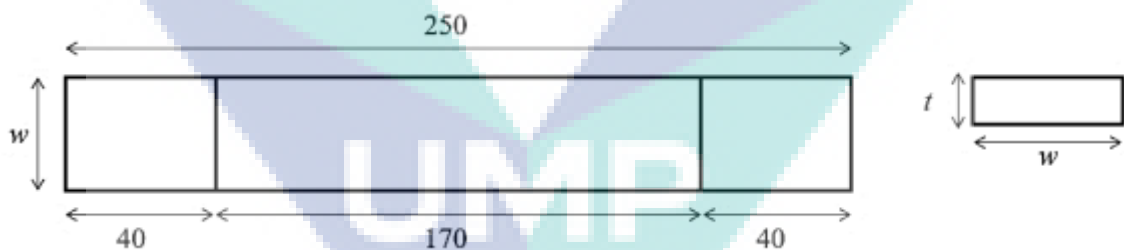
Figure 3.9   The dimension specimen based on ASTM D3039

In order to determine the Poisson's ratio of the materials strain gauges were used during the tensile test. There were two strain gauges placed in the middle of the test specimens, one in the longitudinal direction and another in a transverse orientation as shown in Figure 3.10
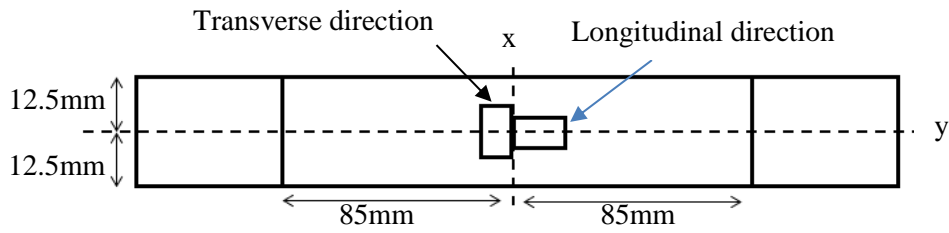
Figure 3.10   The dimension and location of the strain gauges on the specimen
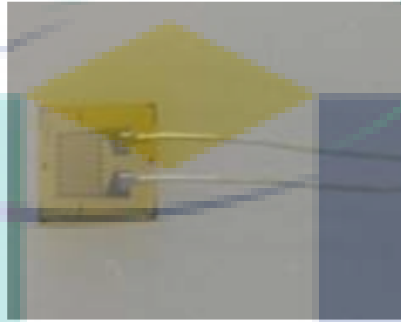
Figure 3.11   The photograph shows TML two pins strain gauge

The specification of the strain gauge as following in Table 3.6. TML Data Logger was used to obtain data from the strain gauge during the experiment. The specification of TML Data Logger is shown in Table 3.7.

Table 3.6   Specification of TML strain gauge

Gauge Length	2 mm
Gauge Resistance	$120 \pm 0.3\ \Omega$
Gauge Factor	$2.10 \pm 1\%$
Transverse Sensivity	0.6%
Test Condition	20ºC

Table 3.7   Specification of the TML Data Logger

Power Supply	AC 250V 50/60 Hz
Weight	9 kg
Dimension	320 mm x 130 mm x 440 mm
Measuring Speed	5 second intervals
Measuring Object	Strain, DC voltage, Thermocouple
Number of Channels	30 internal switching boxes

3.6   Experimental Procedure of Modal Analysis

To ensure that the measurement will be satisfactory as it can, pre-preparation is very important. How well the pre-preparation done will definitely determine the betterment of the expected data in the experiment. Several significant checks that have been done:

52

1.   Excitation method

2.   The marked point on the beam sample

3.   Measuring method

4.   Hammer excitation force transducer

5.   Selection of the excitation signal

3.7   Position of the Accelerometer on the Beam

It is important to know the position at which the accelerometer will be placed. This step was done in order to know the position where to put the reference and moveable accelerometer during the experiment measurement. In this experiment, five different points where accelerometer being positioned during the experiment. The distance between each point is relatively the same.
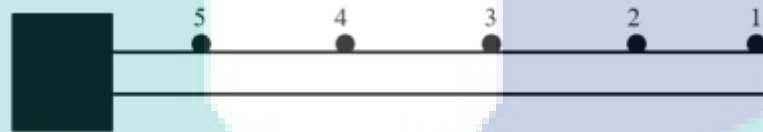
Figure 3.12   Point of the accelerometer

3.8   FMLs Beam Test Description

In this research work, the fibre metal laminates (FMLs) beam were used as the test specimens. The dimensions of the FMLs beam with 250 mm length (l) and width (w) 25 mm. The FMLs beam has the following properties cross-section area of $0.00625\ m^2$. Figure 4 shows the dimension details of the test beams.

Figure 3.13   Details of the dimension of the test beam

In this experiment, there are 5 points for accelerometer are placed. The distance between each point on the beam is equivalent 0.040 m. One accelerometer was used during the experiment. The connection cable pointed toward y, z-direction to the signal analyzer of the accelerometer that response measurement was toward the vertical direction. The impulses are used to excite different point on FMLs beam to get response to different boundary conditions as indicated. For each case, the response was plot in order to see the behaviour i.e modal analysis behaviour of the FMLs beam. All the vibration data acquired are imported to ME'scopVES to process to acquired modal parameters are frequencies and mode shapes. In this case, the peak-picking technique is used. This method is being used to process the acquired data, the sampling frequency, 2000 Hz. The modal parameter (eigenfrequencies and mode shapes) are extracted first using frequency-domain in order to extract the dynamic performance of the beam. The experiment set-up is illustrated in Figure 3.14.
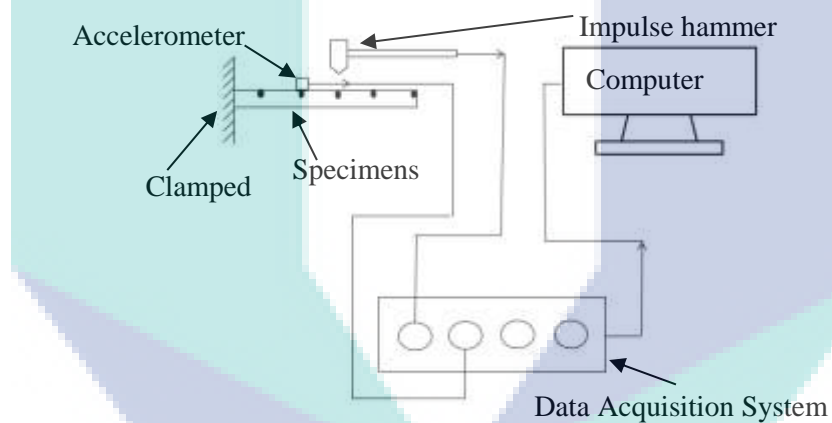
Figure 3.14   The experimental set-up

3.9   Measuring Equipment

Several equipments were used in this experiment.

1.   Data Acquisition System

2.   Accelerometer

3.   Impact Hammer

4.   ME'scopeVES software

3.9.2 Data Acquisition System

National instruments show in Figure 3.15 was used as data acquisition system and has 4 input channels and need to connect to the impact hammer and accelerometer to get the data analysis.
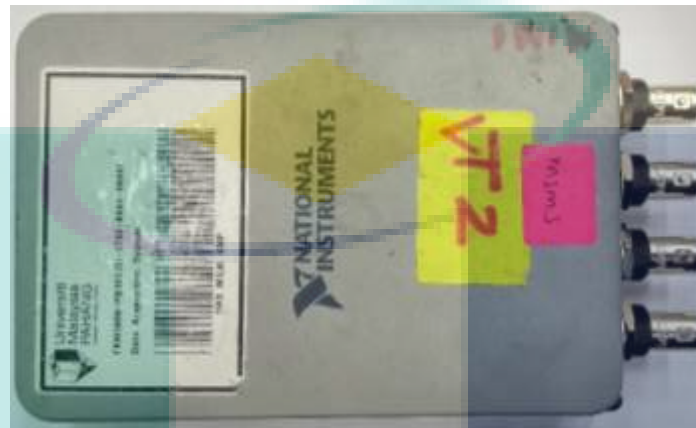
Figure 3.15   The NI acoustic and vibration data logger

3.9.3 Accelerometer

The accelerometer (ICP® accelerometer) is of type PCB Piezotronics Accelerometer,(see Figure 3.16) and measures the accelerometer of the vibrations. This accelerometer ICP uni-axial accelerometer with the following calibration values for reference accelerometer at *z-axis* with sensitivity 2.25 mV(m/s^2).

Figure 3.16   PCB Piezotronics accelerometer

3.9.4 Impact Hammer

The impact hammer is of type Figure 3.17 and used to determine component or system response to impacts of varying amplitude and duration. The impact has sensivity 101 mV(m/s^2).

Figure 3.17   Impact hammer

3.10 Experiment Specifications

The FMLs specimen is based combination between composite materials (glass fibre, carbon fibre and unidirectional carbon fibre prepreg) and aluminium alloys. The dimension of the FMLs is 250 mm length, however, once it been clamped one side, the length becomes 213 mm. as depicted in Figure 3.18 (a) and (b). Another experimental were done with different boundary conditions known as fixed-fixed boundary conditions as shown in Figure 3.19.

(a)   (b)
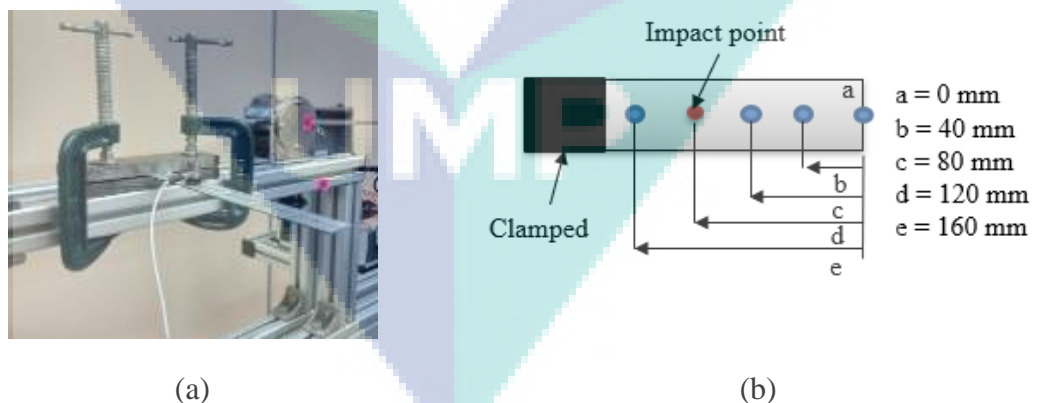
Figure 3.18   (a) A photo of fixed-free clamped (b) a schematic diagram of the point of the accelerometer.
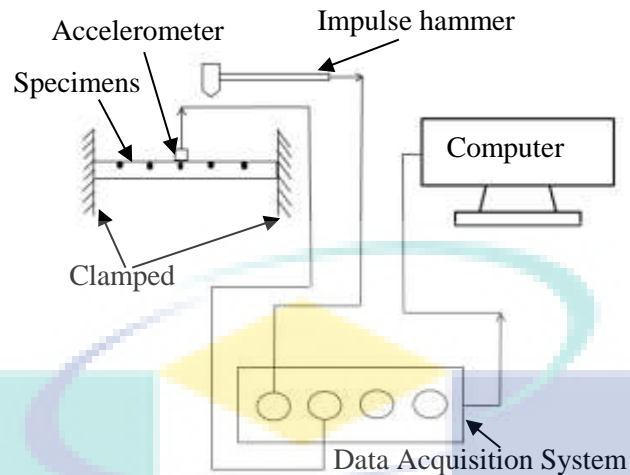
Figure 3.19   A details schematic diagram of the experimental setup for fixed-fixed clamped

By considering a number of boundary conditions, it can to observe how the beam behaves when excited and how the vertical displacement was affected. The natural frequency was monitored and the manner in which they differ between boundary condition needs to be considered

3.11   Modelling the Finite Element Analysis on FML materials

This section introduces finite element models for composite structures. The finite element models of FMLs have been developed using commercial finite element analysis (FEA) software, ABAQUS/CAE. The functions were compared with the corresponding experimental results. ABAQUS/CAE was used for creating, submitting, monitoring and visualising the results for dynamic models. The model of the test was created with the same dimension as the experiment. The simulation parameter and boundary conditions were set to be similar to the experiment. The materials properties were taken from the experiment tensile test.

3.11.1 Geometry, Mesh and Boundary Condition of FML Materials

Pre-processor is basically used to input the entire requirement for creating a model, defining materials properties, assembly of the model, specifying boundary conditions and external load and meshing. During creation, define base feature is where shape parameters are defined, for example solid, shell, wire and point and modelling space. The specimen for finite element analysis is created in ABAQUS simulation

57

software as a 3D deformable part. In this analysis, the selected part is a solid with dimension of 250 mm in length and 25 mm in width.

The next step is to define material properties, from the edit material menu in the ABAQUS. The material properties are defined as engineering constant for elastic under mechanical properties for composite materials while isotropic for aluminium. The Young's modulus of composite materials in engineering constant is E_1, E_2, and E_3 and Poisson's ratio v_1, v_2, and v_3 were defined based on results from the tensile test. After the material section was assigned to the part, its materials orientation was defined.

The geometric, mesh generation, boundary conditions are shown in Figure 3.20 and Figure 3.21. The composite materials and aluminium layers were meshed with C3D8R elements, which are eight-node, linear hexahedral elements with reduced integration and hourglass control. Meshing is assigned to each part with mesh/seed of 0.003 mm amounting to 3344 elements. The cantilever plate size was 250 mm x 25 mm. The boundary conditions of the clamping area are U1=U2=U3=UR1=UR2=UR3=0 with the dimension of about 37 mm. A tie constraint ties two separate surfaces to ensure no relative motion between aluminium and composite materials layers.

The solution stage is where the analysis type is introduced, for example, buckle, frequency, static or linear perturbation and steady-state dynamics. This simulation selected frequency as the analysis. Linear perturbation and Lanczos method were used to extract eigenvalues of the modes. In this stage, the number of eigenvalues requested or maximum frequency of interest need to be defined. In the case of fixed-free boundary condition, the maximum frequency interest is 1000 Hz, while 2000 Hz is the frequency for fixed-fixed boundary condition.

Post-processing is helpful to find the output of the simulation such as result summary and list results. In this simulation, the first three output of natural frequency and mode shape were investigated. The simulation was repeated with different material properties. Figure 3.21 shows the fixed-fixed boundary condition. In this case, both sides of the specimen are clamped with 37 mm.

Mesh sensitivity analysis was carried out by varying the mesh density within the plane and thickness. The mesh was improved until further refinements did not change the prediction appreciably. The results of the natural frequency of Mode 1 were then

compared between the variation meshing sizes, as shown in Figure 3.22. the accuracy of the model can be improved with the increasing of mesh density. However the computation time increased. Therefore, it's recommended to find the balance between element size and natural frequency values. The figure shows the different of meshing size shows the natural frequency give accuracy value at element size 0.005 until 0.0006. Therefore, the element size between 0.005 and 0.0006 was used in order to get accurate prediction.
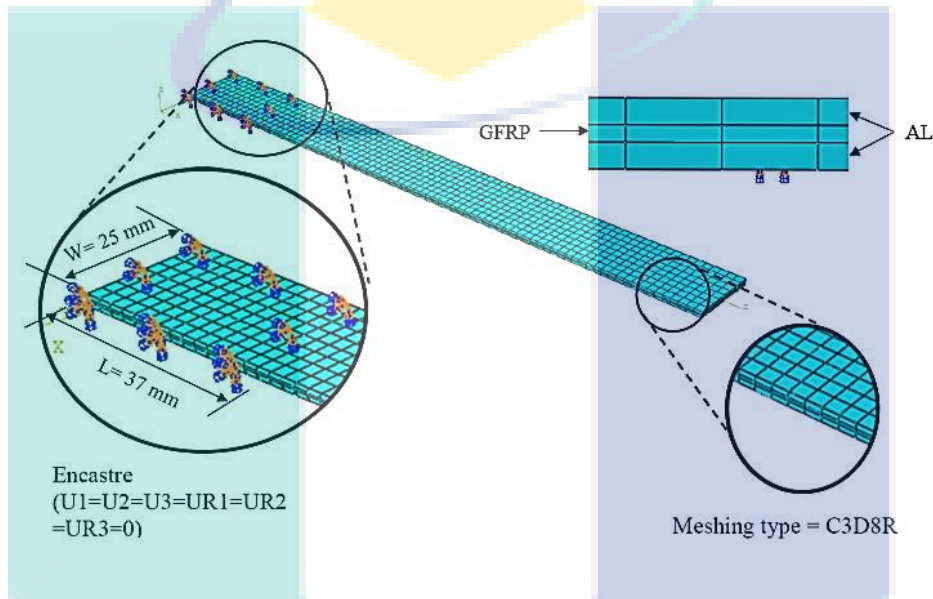
Figure 3.20   The geometry, mesh and boundary conditions (fixed-free) of the model for 2/1 FMLs
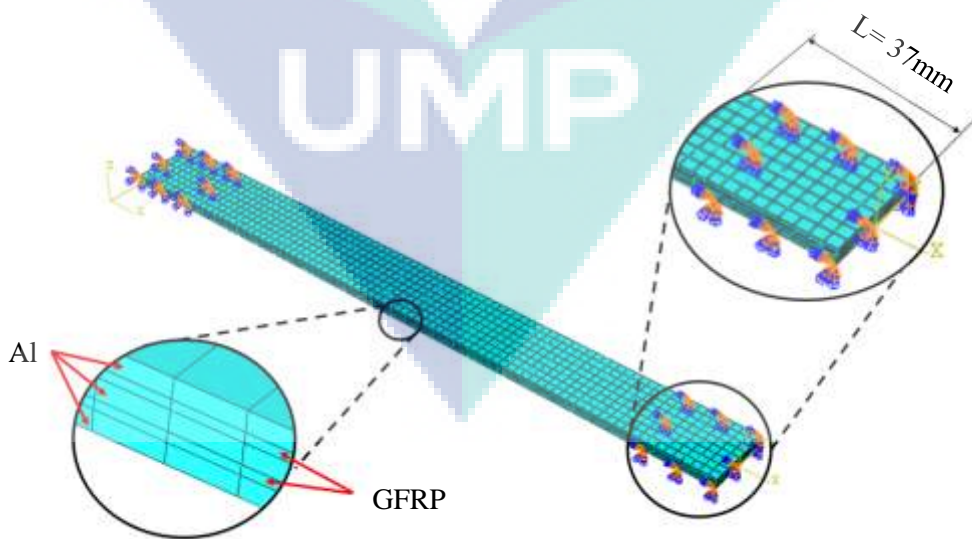
Figure 3.21   Boundary condition of model 3/2 FMLs for fixed-fixed
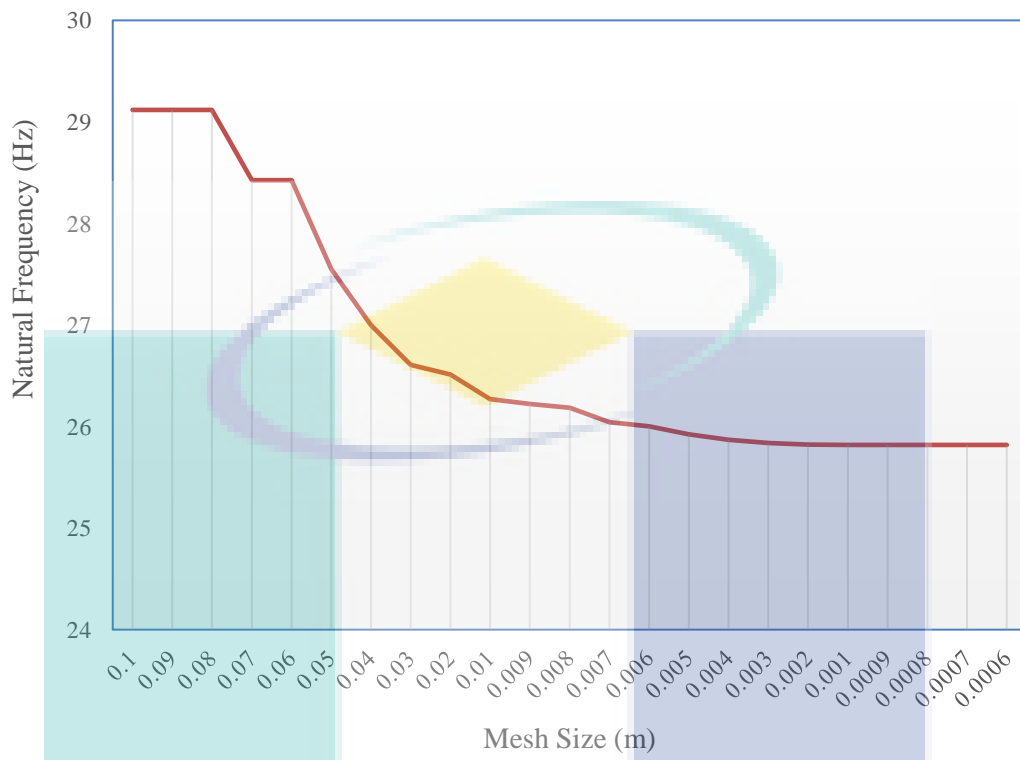
Figure 3.22   Sensitivity of natural frequency versus mesh size

CHAPTER 4

RESULTS AND DISCUSSION

4.1   Introduction

This chapter explains the results of the mechanical properties of materials obtained from the series of tensile tests. Furthermore, the dynamic test with different boundary conditions was carried out. However, only output data from modal testing namely the mode shape and frequencies were used to compare the numerical results

4.2   Tensile Test on the Materials

The tensile test was conducted for Al, CFRP, GFRP and UD-CFP materials. Three samples for each type of materials were tested. From these results, the mechanical properties of the materials can be determined. Typical tensile stress-strain curves for the Al, CFRP, GFRP and UD-CFP materials are given in Figure 4.1, shows the tensile stress-tensile strain curves an aluminium alloy specimen. Based on the graph, Al specimen shows a high degree of ductility. The ultimate tensile strength of an aluminium alloy was recorded at 151 MPa, where yield strength was at 76 MPa.
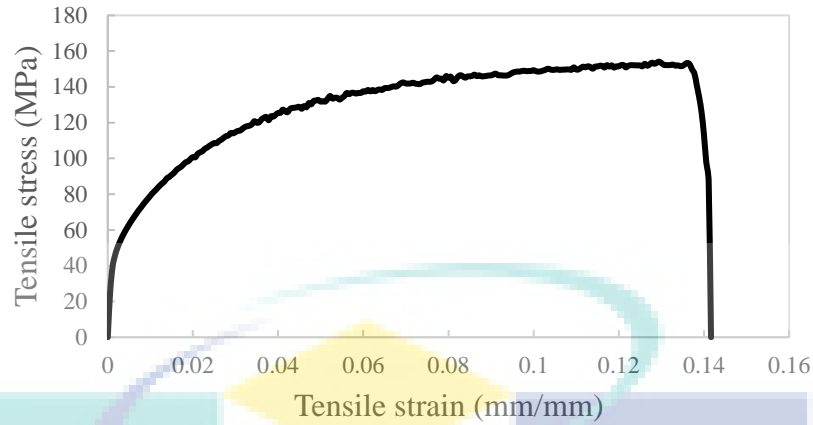
Figure 4.1 Tensile stress-strain curves for the aluminium alloy (Type 2024-T0)

GFRP test result showed that the longitudinal tensile strength and elastic modulus were recorded at 135.16 MPa and 7 GPa, respectively, as seen in Figure 4.2. Furthermore, transverse elastic modulus, E_2 was assumed the same as E_1 because of woven glass also has an orientation of $0°$ and $90°$ The Poisson's ratio was calculated from the strain gauge result with an obtained value of 0.22.
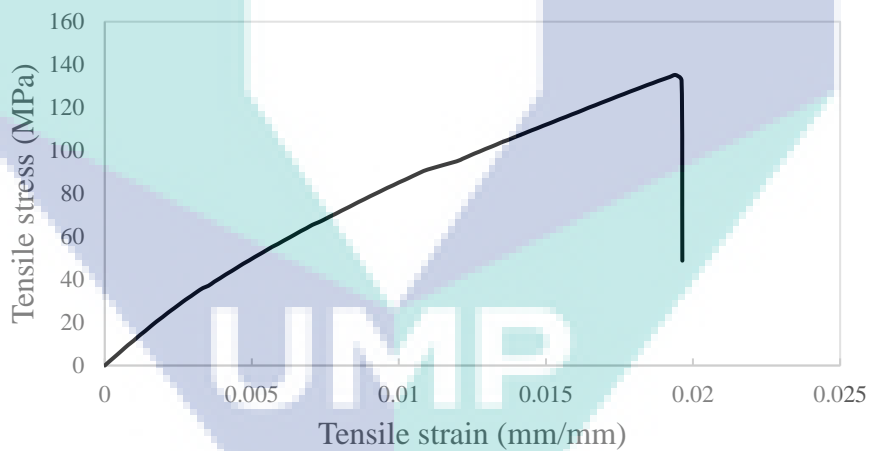
Figure 4.2 Tensile stress versus tensile strain graph on GFRP

Localised fracture

Figure 4.3 Tensile tested for GFRP specimen

The tensile test of CFRP showed the longitudinal tensile strength and elastic modulus were recorded at 335.96 MPa and 17.5 GPa, respectively, as shown in Figure 4.4. Furthermore, transverse elastic modulus, E_2 was assumed the same as E_1 because the woven glass consists of orientation $0°$ and $90°$. The Poisson's ratio was calculated from the strain gauge result with an obtained value of 0.22.
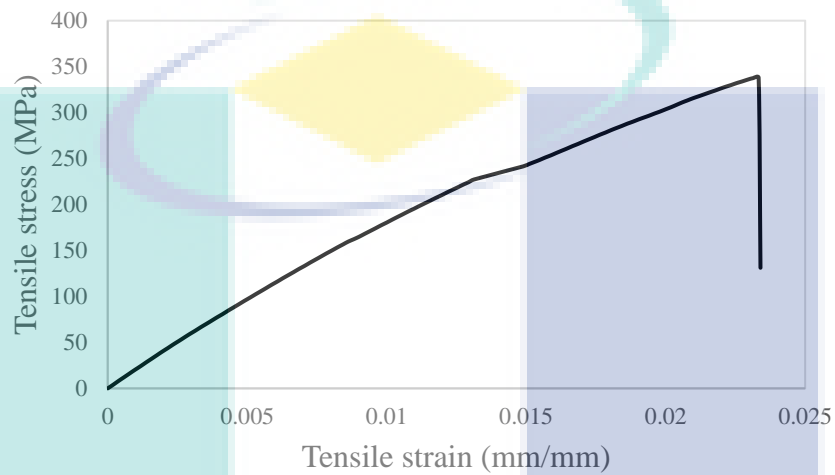
Figure 4.4   Tensile stress versus tensile strain graph on CFRP
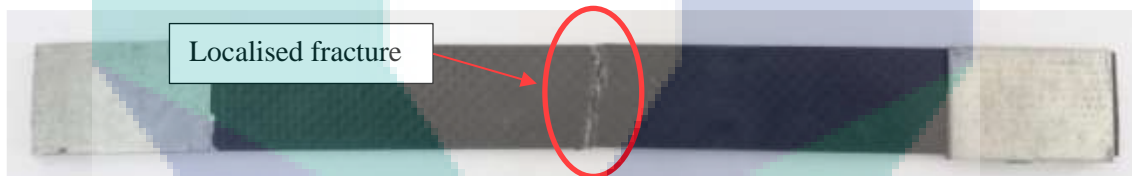
Figure 4.5   Tensile tested for CFRP specimen

For the UD-CFP tensile test, it was showing longitudinal tensile strength and elastic modulus of 869.27 MPa and 107 GPa, respectively, as shown in Figure 4.6. The Poisson's ratio was calculated from the strain gauge result with an obtained value of 0.27. Based on the graph, it clearly shows the zig-zag pattern. Cracking and explosive sound were heard when some of the unidirectional carbon prepreg fibres started to fail before resulting in a more rapid total failure, as shown in Figure 4.7.
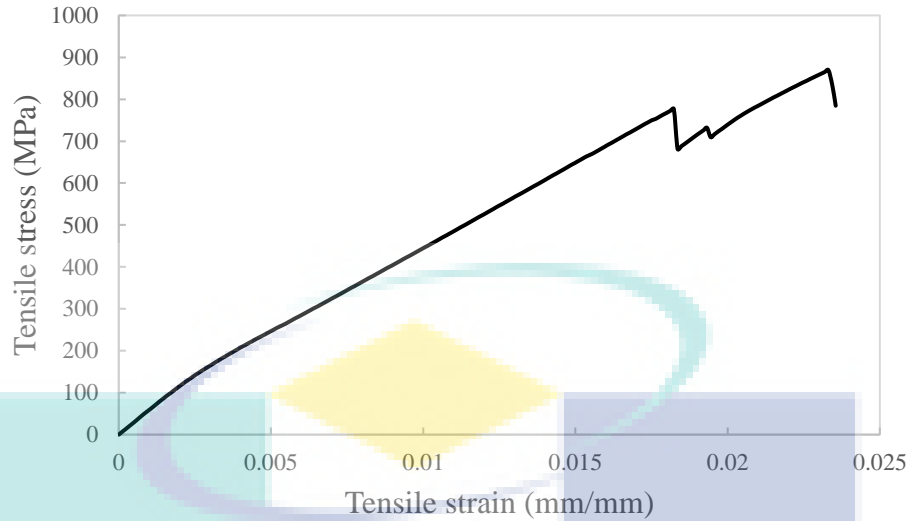
Figure 4.6   Tensile stress versus tensile strain graph on UD-CFP

Figure 4.7   Tensile tested for specimen UD-CFP specimen

Table 4.1   Mechanical properties of composite materials and aluminium

Materials	E_1(GPa)	E_2(GPa)	ν	G_{12}(GPa)	G_{13}(GPa)	ρ(kg/m³)
GFRP	7.00	7.00	0.22	1.00	2.50	1720.00
CFRP	17.50	17.50	0.24	2.00	10.50	1430.00
UD-CFP	107.00	10.00	0.27	4.00	4.00	1384.00
Al	70.60	70.60	0.30	28.00	28.00	2780.00

4.3   Results of Modal Testing

EMA is one of the techniques used to investigate the modal properties of the structures. Accelerometer and impact hammer is required to perform the modal testing. In this work, a roving accelerometer was considered. The results of dynamic tests were obtained from the investigation using different configuration lay-ups and boundary conditions. However, only output data from modal testing, which are frequency and mode shapes, were used to compare the numerical results.

4.3.1 Experimental Modal Analysis

The curve fitting method was applied to the graph of FRF are presented in Figure 4.8. Table 4.2 shows the values of the natural frequency obtained by using ME'scopeVES software. The range of frequency was taken between 0 and 1000 Hz for the fixed-free boundary condition.
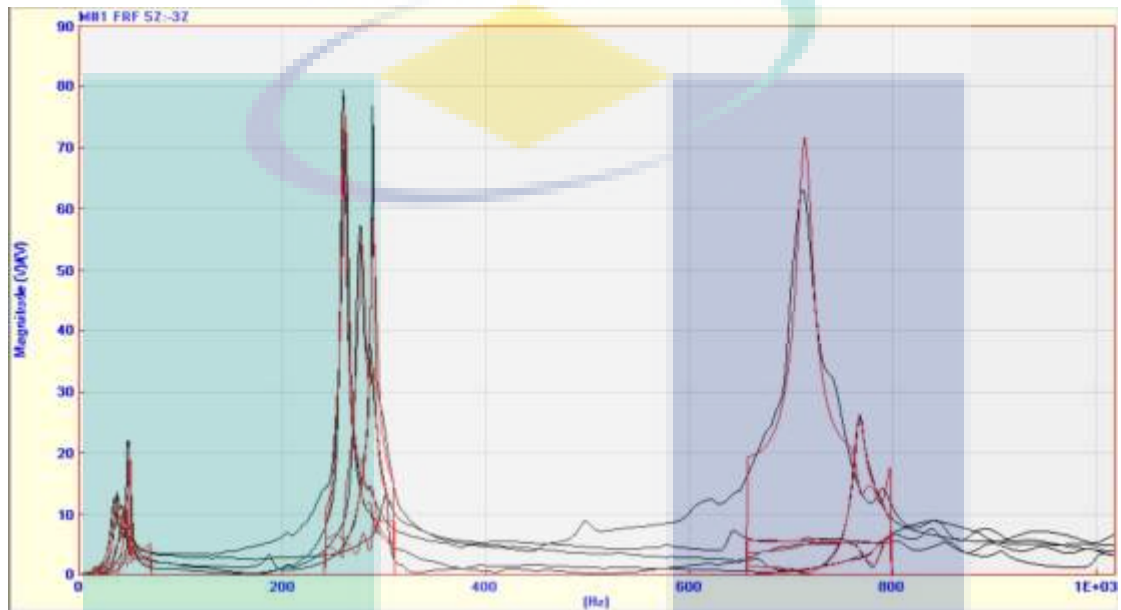
Figure 4.8   Curve fitting method for FRP graph from ME'scopeVES for specimen C5

Table 4.2   Results of natural frequencies for fixed-free (a), (b), and (c)

(a)

Specimens	Mode 1 (Hz)	Mode 2 (Hz)	Mode 3 (Hz)
GFRP	20.20	132	382
CFRP	11.70	105	309
Al	13.40	95	249
UD-CFP	65.10	437	825

(b)

Specimens	Mode 1 (Hz)	Mode 2 (Hz)	Mode 3 (Hz)
C1	29.03	187	525
C2	21.50	159	458
C3	23.20	175	468

(c)

Specimens	Mode 1 (Hz)	Mode 2 (Hz)	Mode 3 (Hz)
C4	50.78	298	871
C5	41.77	266	716
C6	40.17	296	763

Table 4.2 (b) notable differences in natural frequency observed from the different types of composite layers in FMLs which is C1, C2 and C3. The first three modes of natural frequency C1, C2, and C3 were 29.03 Hz, 187 Hz, 525 Hz and 21.50 Hz, 159 Hz, 458 Hz, and 23.20 Hz, 175 Hz, 468 Hz, accordingly. The higher of first natural frequency value was C1 due to the GFRP having more thickness than the others. It was observed that dissimilar thickness significantly influences the natural frequency of the FMLs.

The effect from the number of Al layers in the composite material plate (CFRP, GFRP, and UD-CFP) shows that natural frequency increases as more Al plate were embedded in the composite material plates. Table 4.2 (c) shows the first mode of the natural frequency of C4, C5, and C6 of 50.78 Hz, 41.77 Hz and 40.17 Hz.

Figure 4.9 shows the effect of Al plates embedded in the composite materials on the natural frequency. Figure 4.9 (a) shows that when the number of Al plate combined with GFRP materials increase, the value of natural frequency also increases. In Mode 1, natural frequency did not increase much, but Mode 2 and Mode 3 shows significant differences. The percentage increase in the frequency of GFRP to C1 at Mode 1 was found to be 30.41% and GFRP to C4 was 60.22%, at Mode 2 for GFRP to C1 was found to be 29.41% and GFRP to C4 was 55.70% and at Mode 3 for GFRP to C1 was found to be 27.23% and GFRP to C4 was 56.14%. For CFRP in Figure 4.9 (b), the percentage increase in the frequency of CFRP to C2 at Mode 1 was 45.58% and CFRP to C5 was 71.98%, at Mode 2 for CFRP to C2 was 33.96% and CFRP to C5 was 60.52% and at Mode 3 for CFRP to C2 was 32.53% and CFRP to C5 was 56.84%.

This happened due to the lateral stiffness of Al plates was more than that of FRP. Furthermore, the different densities of each material also affect natural frequency. In this case, Al layers contain high density with respect to that of FRPs, which can increase the moment of inertia of the plate. The strength and stiffness of the plate and also natural frequency of the plate increased in the case of Al plates being placed in the middle layer of the composite materials.
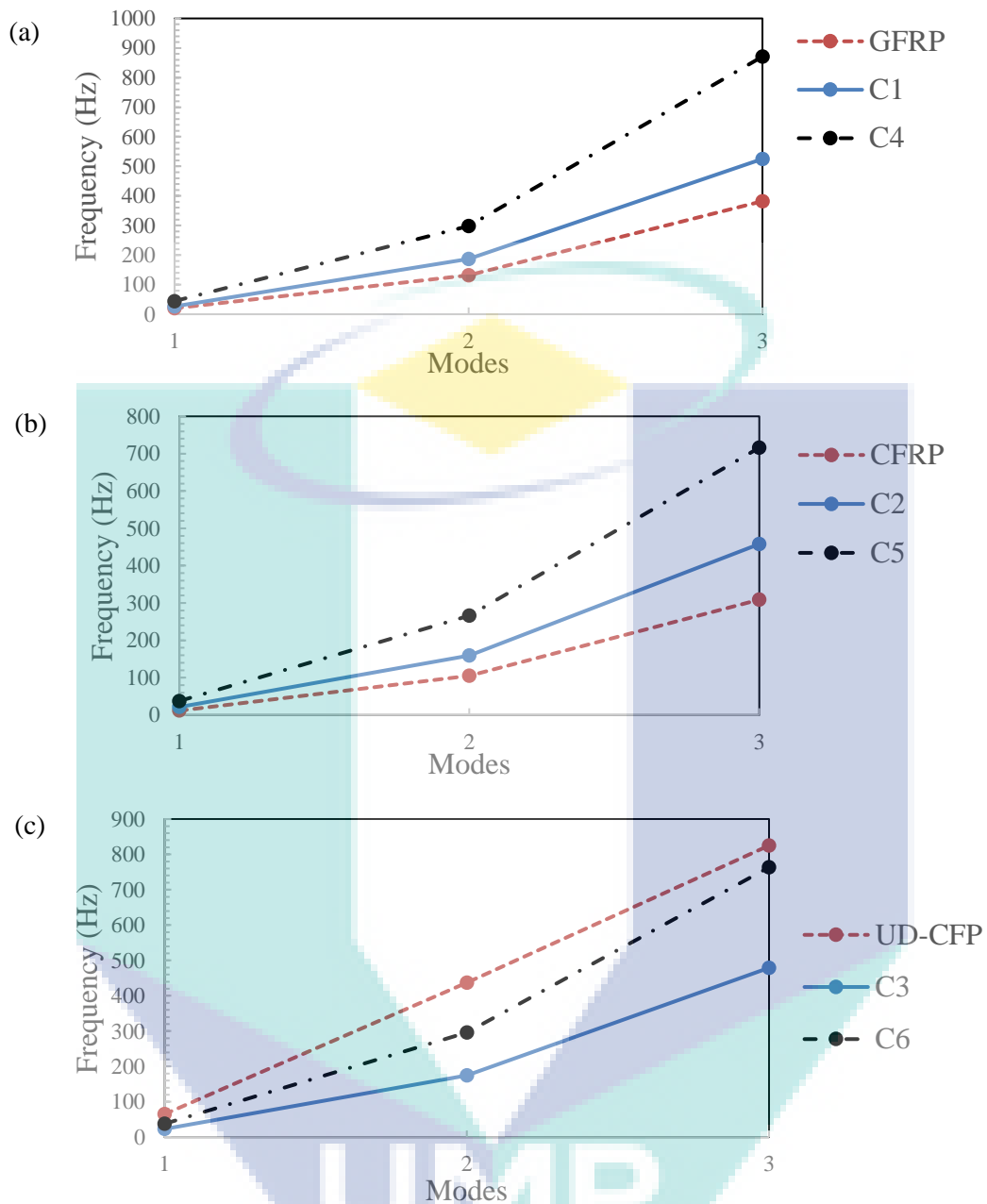
Figure 4.9   Effect of the number of Al plate in FMLs for different composite materials: (a) GFRP, (b) CFRP, and (c) UD-CFP.

Mode shapes of the specimens obtained from the EMA by using ME'scopeVES software are shown in Table 4.3. The mode shapes indicated a deformed pattern and corresponding modal frequency. The observed modal shape was transverse bending.

Table 4.3   Modes shapes for C1 for fixed-free boundary condition

(a)

Mode	Mode shape
1	
2	
3	
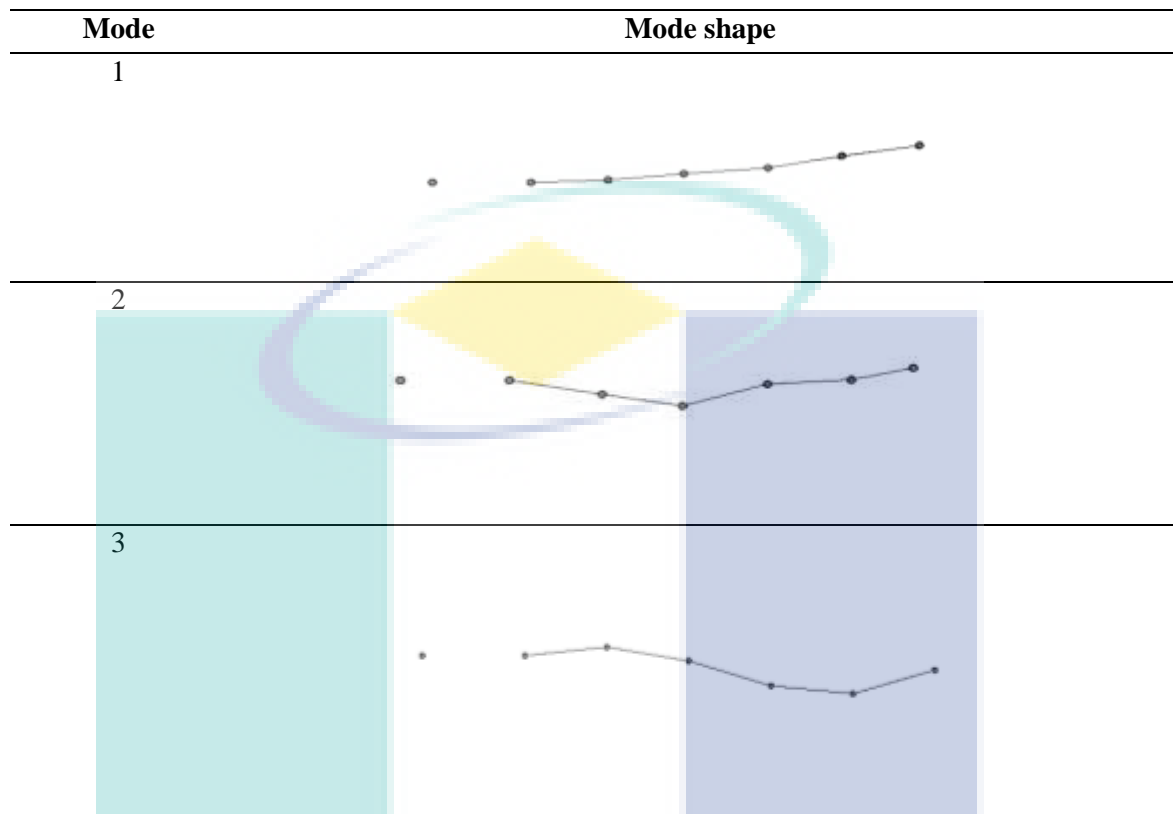
The fixed-fixed condition is another boundary condition to examine the natural frequency of FML plates. The first three natural frequencies of the FML plates with different composite lay-up area are introduced in Table 4.4. The range of interest for the frequency of fixed-fixed boundary condition was up to 2000 Hz.

Table 4.4   Results of natural frequencies for fixed-fixed; (a), and (b)

(a)
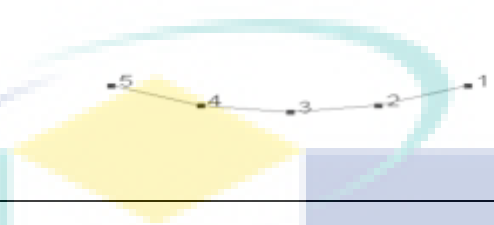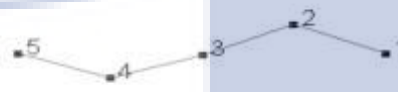
Specimens	Mode 1 (Hz)	Mode 2 (Hz)	Mode 3 (Hz)
C1	255.01	605.90	1219.52
C2	187.47	512.67	1077.60
C3	182.70	476.30	1027.58

(b)

Specimens	Mode 1 (Hz)	Mode 2 (Hz)	Mode 3 (Hz)
C4	347.04	1007.63	1677.20
C5	302.36	829.20	1632.93
C6	292.69	787.34	1672

The first three mode shape of C1 specimen is drawn by ME'ScopeVES which is shown in Table 4.5.

Table 4.5   First three mode shapes for C1 plate

Mode	Mode shape
1	
2	
3	

4.3.2   Effect of Boundary Conditions on Natural Frequency

Based on Figure 4.10 it is noticed that the EMA results are in good relation for all boundary. In Figure 4.10 (a), the 1st, 2nd, and 3rd natural frequencies from EMA were observed as the minimum of (29.03, 187, 525) for C1 fixed-free boundary condition and a maximum of (225.01, 605.90, 1219.52) for C1 fixed-fixed boundary condition. The natural frequencies of the FML plates for fixed-free and fixed-fixed were increased by 87.09 % in the 1st Mode, 69.13 % in the 2nd Mode and 56.95 % in the 3rd Mode. In the case of C2 in Figure 4.10 (b), the 1st, 2nd, and 3rd natural frequencies from EMA were observed as minimum of (21.50, 159, 458) for C1 fixed-free boundary condition and as maximum of (187.47, 512.67, 1077.60) for C1 fixed-fixed boundary condition.

The natural frequencies of FML plates for fixed-free and fixed-fixed were increased by 88.53 % in the 1st Mode, 68.98 % in the 2nd Mode and 57.48 % in the 3rd Mode. In the case of C3 in Figure 4.10 (c), the 1st, 2nd, and 3rd natural frequencies from

EMA were observed as minimum of (23.20, 175, 468.89) for C1 fixed-free boundary condition and as maximum of (182.70, 476.30, 1027.58) for C1 fixed-fixed boundary condition. The natural frequencies of the FML plates for fixed-free and fixed-fixed were increased by 87.30 % in the 1st Mode, 63.25 % in the 2nd Mode and 54.36 % in the 3rd Mode.
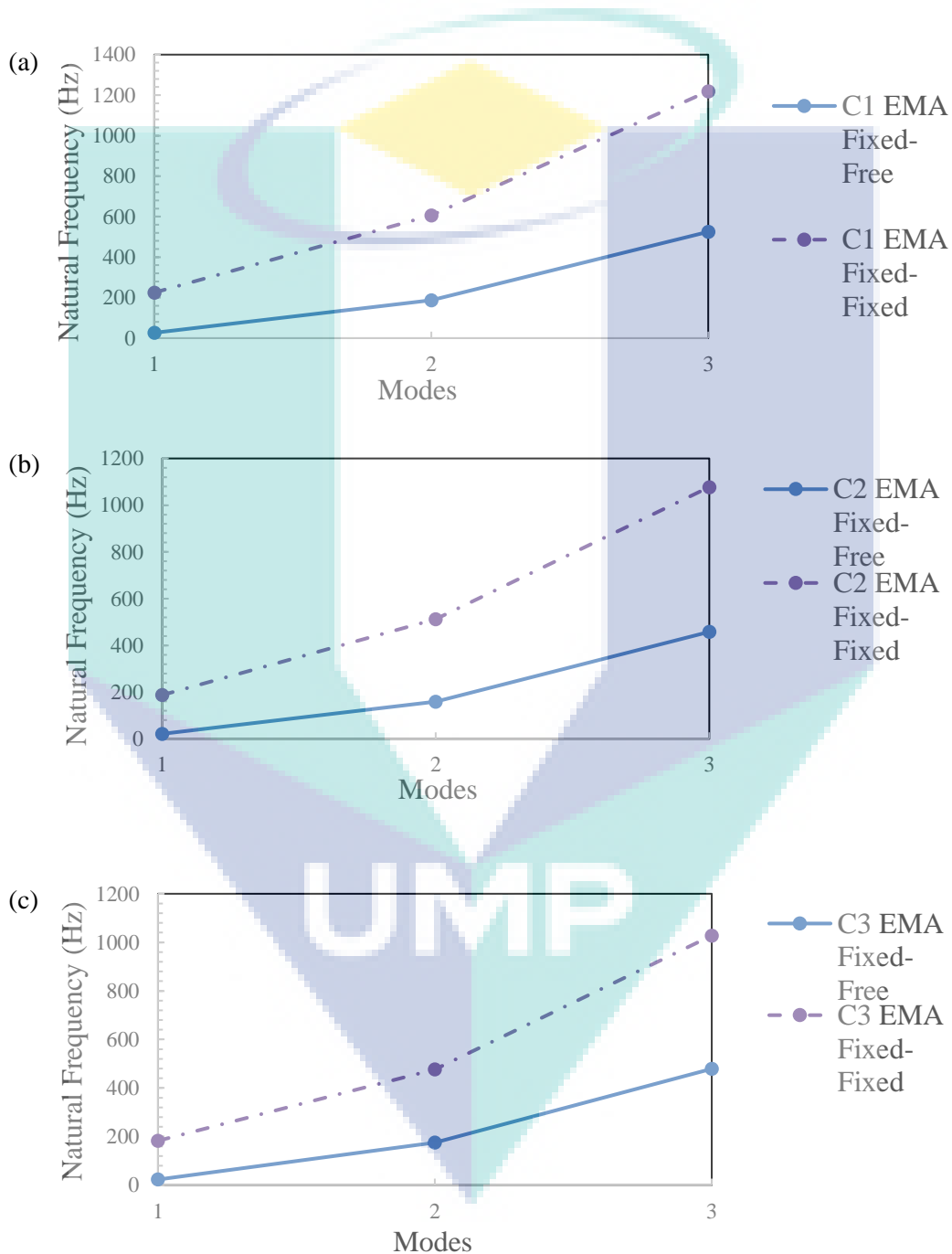
Figure 4.10   Effect of boundary condition on natural frequency on FML plate (a) C1, (b) C2, and (c) C3

As seen in Table 4.6 all the results obtained from experimental studies show that the natural frequency is higher in fixed-fixed boundary condition than in fixed-free boundary condition. This is due to the below equation:

$$\omega_n = \sqrt{\frac{k}{m}} \qquad\qquad 4.1$$

The FML plates are significantly reliant on the boundary conditions. The fixed-fixed condition will generate greater stiffness than fixed-free since the mass remains constant in the situation. The overall natural frequency is reduced under fixed-free due to reduced stiffness. The results from (Dhanduvari et al., 2015) found that natural frequency of fixed-fixed boundary condition is high followed by cantilever and simply support.

Table 4.6   Summary of the effect on the natural frequency with different boundary condition

Specimens	Fixed-Free			Fixed-Fixed		
	Mode 1 (Hz)	Mode 2 (Hz)	Mode 3 (Hz)	Mode 1 (Hz)	Mode 2 (Hz)	Mode 3 (Hz)
C1	29.03	187.00	525.00	255.01	605.90	1219.52
C2	21.50	159.00	458.00	187.47	512.67	1077.60
C3	23.20	175.00	468.89	182.70	476.30	1027.58
C4	50.78	298.00	871.00	347.04	1007.63	1677.20
C5	41.77	266.00	716.00	302.36	829.20	1632.93
C6	40.17	296.00	763.45	292.69	787.34	1672.00

4.4   ABAQUS Graphical Results

These are following dynamic analysis for different boundary conditions. The result obtained is generated in the form of graphical view which shows the modal concept and influence of each boundary conditions for the vertical frequency of the FE solid model of the beam.

4.4.1   Fixed-Free Boundary Condition

The results shown below are the graphical solution of the deformed shape of C1 at first 3 modes.
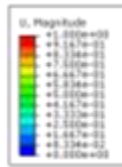
Figure 4.11   Mode 1 under fixed-free boundary conditions

Figure 4.12   Mode 2 under fixed-free boundary conditions

Figure 4.13   Mode 3 under fixed-free boundary conditions

Table 4.7   The table has shown the mode frequencies in Hz experiment and ABAQUS

Mode	Experiments	ABAQUS	Error (%)
1	29.03	30.42	4.78
2	187.00	190.28	1.75
3	525.00	532.25	1.38

4.4.2 Fixed-Fixed Boundary conditions

The results shown below are the graphical solution of deformed shape for C1 at first 3 modes.
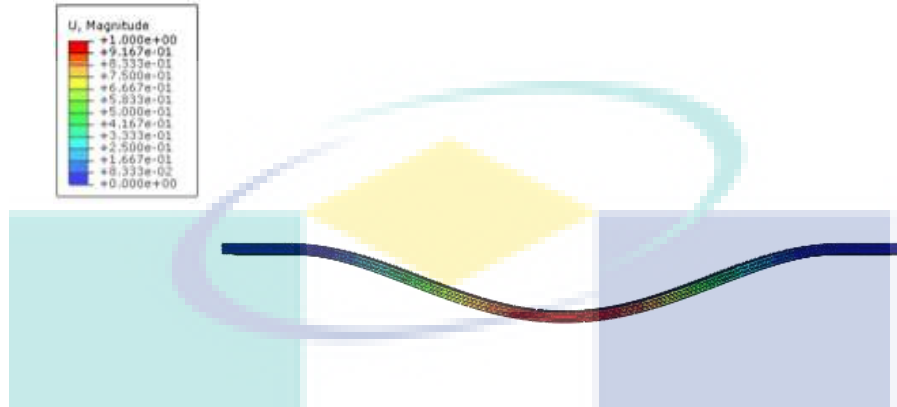
Figure 4.14   Mode 1 under fixed-fixed boundary conditions
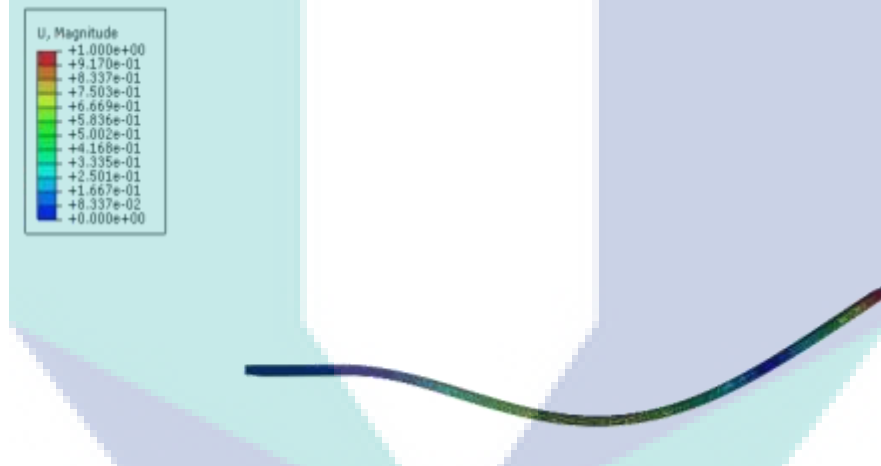
Figure 4.15   Mode 2 under fixed-fixed boundary conditions
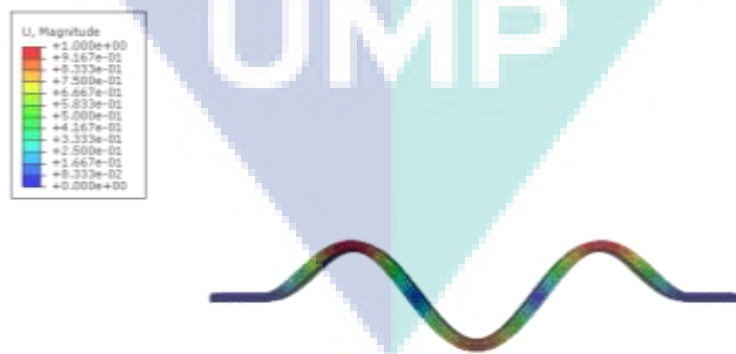
Figure 4.16   Mode 3 under fixed-fixed boundary conditions

Table 4.8   The percentages error in the natural frequencies experiment and ABAQUS

Modes	Experiments (Hz)	ABAQUS (Hz)	Error (%)
1	225.01	222.57	1.03
2	605.52	611.52	0.94
3	1219.52	1204.30	1.24

The ABAQUS results show small relative errors compared with the experiment as shown in Table 4.7 and Table 4.8.

4.5   Comparison Between EMA and FEA Results

For FEM, the mechanical properties of each material need to be obtained before performing the numerical simulation as shown in Table 4.1. Two sets of results can be obtained from modal properties which are natural frequencies and mode shapes. Table 4.9 shows a comparison of natural frequency (Hz) of EMA and FEA software for fixed-free boundary conditions according to each mode. Three modes were compared and the percentage errors between EMA and FEA values were calculated.

Table 4.9   Comparison between FEA and EMA for fixed-free (a), and (b)

(a)

Modes	Natural Frequency (Hz)								
	C1			C2			C3		
	FEA	EMA	Error %	FEA	EMA	Error %	FEA	EMA	Error %
1	30.42	29.03	4.78	25.64	21.50	16.17	29.49	23.20	12.43
2	190.28	187.00	1.75	160.63	159.00	1.02	182.83	175.00	4.79
3	532.25	525.00	1.38	450.01	458.00	1.29	453.39	468.89	3.30

(b)

Modes	Natural Frequency (Hz)								
	C4			C5			C6		
	FEA	EMA	Error %	FEA	EMA	Error %	FEA	EMA	Error %
1	48.64	50.78	4.21	41.59	41.77	0.40	47.82	40.17	15.94
2	303.66	298.00	1.86	260.35	266.00	2.12	298.84	296.00	0.95
3	845.58	871.00	2.91	722.84	716.00	0.95	834.92	763.45	9.36

Based on Table 4.9 (a) and (b) above, when comparing the numerical method to the finite element, it can be seen that the result show small relative errors with experiment data. The highest percentage error obtained for the cantilever plate was about 16.17%, occurring in Mode 1 of C2, whereas the lowest was about 0.40%, occurring in Mode 1 of C5.

There are many factors contributing to the error such as imperfect experiment setup while performing EMA. Imperfect experiment setup also affects the results of mode shapes and natural frequency of the fibre-metal laminated cantilever plates. A more likely cause of these discrepancies could be due to that the boundary conditions are applied to the beam during the experiment. In the numerical analysis, all boundary conditions are considered to be ideal, i.e perfectly for a fixed end and perfectly fixed-fixed.

When moving the accelerometer, one has to unmount and remount the accelerometer at the different measurement points. The effects of moving the accelerometer also change the mass distribution of the structure, and the value of natural frequency also effected.

Furthermore, when considering natural frequency, the further observation about the error between numerical and ABAQUS may be made. The increase in the number of elements reduces errors. By referring to the mode shapes provided from ABAQUS in Figure 4.11 until 4.14 of this work, it can be seen that relatively smooth

Table 4.10 shows the comparison of FEA and EMA for fixed-fixed boundary condition.

Table 4.10   Comparison between EMA and FEA for fixed-fixed (a), and (b)

(a)

| Modes | Natural Frequency (Hz) | | | | | | | | |
| | C1 | | | C2 | | | C3 | | |
	FEA	EMA	Error %	FEA	EMA	Error %	FEA	EMA	Error %
1	222.67	225.01	1.03	190.20	187.47	1.46	175.04	182.70	4.19
2	611.62	605.90	0.94	524.10	512.67	2.23	482.46	476.30	0.29
3	1204.30	1219.52	1.24	1028.10	1077.64	4.59	946.99	1027.58	7.84

(b)

Modes	Natural Frequency (Hz)								
	C4			C5			C6		
	FEA	EMA	Error %	FEA	EMA	Error %	FEA	EMA	Error %
1	347.04	339.05	2.35	302.36	298.00	1.46	292.12	292.69	0.19
2	950.65	1007.63	5.65	838.82	829.20	1.16	804.50	787.34	2.18
3	1812.70	1677.20	8.08	1634.20	1632.93	0.08	1572.80	1672.00	5.93

4.6   Summary of Results

Given the various effect of design parameter on the natural frequency on FMLs, then now in position to point out the best material's configuration for the natural frequency. Table 4.9 and 4.10 is a summary of experimental work and numerical analysis regarding the FMLs configurations and different boundary conditions for each vibration mode. As far as natural frequency is concerned, combination glass fibre reinforced epoxy with aluminium alloys is the best for vibration design, presenting high value of natural frequency compared with other materials. In case of fixed-free boundary condition, the best materials configuration is C4 (Al/GFRP/Al/GFRP/Al), presenting high value of natural frequency from mode 1 until mode 3 is 50.78 Hz, 298.00 Hz and 871.00 Hz. In case fixed-fixed boundary condition, the best materials configuration is C4 (Al/GFRP/Al/GFRP/Al), presenting high value of natural frequency from mode 1 until mode 3 is 339.05 Hz, 1007.63 Hz and 1677.20 Hz.

CHAPTER 5

CONCLUSION

5.1   Introduction

This chapter summarises the results and findings of this research.

1.   To investigate the mechanical properties of aluminium alloys and composite materials

In this experiment, the mechanical behaviour of Aluminium (Al), glass fibre reinforced polymer (GFRP), carbon fibre reinforced polymer (CFRP) and unidirectional carbon fibre prepreg (UD-CFP) have been investigated. Composite materials are brittle materials and aluminium is ductile materials. The results obtained from the experiment showed that Young's modulus of UD-CFP has the best performance compared to GFRP and CFRP. The results show the tensile strength value of 0° orientation UD-CFP is 869.27 MPa is higher than those of woven orientation fibre GFRP is 135.16 MPa and CFRP is 335.96 MPa.

2.   To evaluate the dynamic behaviour of combination between aluminium alloys and three different composite materials by free vibration test:

The natural frequencies and mode shapes of the fibre metal laminates plates consisting of different types of laminates composite layer (glass fibre/epoxy, carbon fibre/epoxy and unidirectional carbon prepreg) have been reported. In this present work, the natural frequencies and mode shapes were obtained using free vibration analysis excited via impact hammer. The dimensions of specimen followed ASTM E756 standards. The fixed-free and fixed-fixed experiment setup were performed.

The mode shapes and natural frequency of aluminium 2024-TO (Al), glass fibre/epoxy (GF-E), carbon fibre/epoxy (CF-E), unidirectional carbon fibre prepreg (UD-CFP) have been investigated. Vibration characteristics of all samples were determined by free vibration analysis. Two parameters were tested which are the effect of the layer sequence of the metal layer and different boundary conditions. Based on the conducted experiments and numerical analysis, the following conclusions were made.

The different materials (glass fibre, carbon fibre ply and unidirectional carbon fibre prepreg) used in this experiment showed significant influence on the natural frequency. After tensile test, higher Elastic modulus is found in UD-CFP materials. Among the composite materials, the one with higher density of GFRP of 1720 kg/m^3, has higher natural frequency when combining with aluminium alloy. The natural frequency of the FML plates increased when more Al layers were embedded in the composite layer, improved by almost 27.23 % and 71.98 %. The value of lateral stiffness of Al plates is more than that of FRP.

For the case of different boundary conditions, the natural frequency of FML plates is clearly reliant on the boundary conditions due to the restraint effect at the edges. The fixed-fixed condition has generated greater stiffness than fixed-free since the mass remains constant in the situation, approximately 54.36 % and 88.53%. The overall natural frequency is reduced under fixed-free due to reduced stiffness.

3.   To verify dynamic behaviour results obtained from the experiment works and finite element analysis

The model validation provides useful information concerning the results' accuracy and validity. The vibration analysis of FML plates was done via ABAQUS and ME'scopeVES to attain the natural frequency whereby the results are in very good agreement. The percentage error between numerical analysis and experiment are observed in between 0.08 % and 16.17 %.

There are many factors contributing to the error such as imperfect experimental setup while performing EMA. Imperfect experiment setup also affects the results of mode shapes and natural frequency of the fibre-metal laminated cantilever plates. In the numerical analysis, all boundary conditions are considered to be ideal, i.e perfectly for a

fixed end and perfectly fixed-fixed. When moving the accelerometer, one has to unmount and remount the accelerometer at the different measurement points. The effects of moving the accelerometer also change the mass distribution of the structure, which could alter the natural frequencies. Furthermore, when considering natural frequency, the further observation about the error between numerical and ABAQUS may be made. The increase in the number of elements reduces errors.

These conclusions are unquestionable about the feasibility of using composite materials with aluminium in many application where vibration is required. In any structural applications required materials that having a high value of natural frequency, thus making structure suitable for the task design for. The value of natural frequency is important to point out as the structure will tend to vibrate when subjected to certain external forces. Materials that possess high value of natural frequency are tendency to withstand resonance or external force and which may endanger its strength. These frequencies are dependent on the way mass and stiffness are distributed with the structure. Consequently, the engineer has to persistently continue the development of more accurate models to characterize the impact of vibrations on the integrity of the structural applications.

5.2   Recommendation for Future Work

There are several recommendations that can be considered in the future:

1.   Investigate the dynamic behaviour of FMLs with different oriented lamina composite materials

2.   The other boundary conditions such as fixed-support and all edge clamped can also be studied

3.   Perform modal updating to diminish the percentage error

4.   Perform test using the different dimension of specimens

REFERENCES

Abdullah, Secgin, Cesim, Atas, Saide, & Sarigul, A. (2009). The Effects of Composite Plate Design Parameters on Linear Vibrations by Discrete Singular Convolution Method. *Journal of Composite Materials, 43*(24), 2963-2986

Abdullah, M. R., & Cantwell, W. J. (2006). The impact resistance of polypropylene-based fibre–metal laminates. *Composites Science and Technology, 66*(11-12), 1682-1693.

Abraham, D., Matthews, S., McIlhagger, & R. (1998). A comparison of physical properties of glass fibre epoxy composites produced by wet lay-up with autoclave consolidation and resin transfer moulding. *Composites Part A: Applied Science and Manufacturing, 29*(7), 795-801.

Adediran, O. (2007). *Analytical and Experimental Vibration Analysis of Glass Fibre Reinforced Polymer Composite Beam.* (Master's Degree), Blekinge Institute of Technology, Karlskrona, Sweden.

Alderliesten, R. C. (2005). Fatigue crack propagation and delamination growth in Glare. *TU Delft, Delft University of Technology*.

Alderliesten, R. C. (2009). On the development of hybrid material concepts for aircraft structure. *Recent Patents Eng, 3*, 25-38.

Alderliesten, R. C., & Benedictus, R. (2007). Fiber/metal composite technology for future primary aircraft structures. *In: 48th Aiaa/Asme/Asce/Ahs/Asc structures, structural dynamics, and materials conference 15th, Honolulu, Hawaii, pp 1–12, April 23–26, 2007*.

Anand, Venkatachari, Sundararajan, Natarajan, Manickam, & Ganapathi. (2018). Variable stiffness laminated composite shells – Free vibration characteristics based on higher-order structural theory. *Composite Structures, 188*(15), 407-414.

Aniket, Salve, Ratnakar, Kulkarni, Ashok, & Mache. (2016). A Review: Fiber Metal Laminates (FML's) - Manufacturing, Test methods and Numerical modeling. *INTERNATIONAL JOURNAL OF ENGINEERING TECHNOLOGY AND SCIENCES (IJETS), 6*(1).

Arafa, E.-H. (2016). Free Vibration Analysis of Stiffened Laminated Composite Plates. *International Journal of Computer Applications, 156*(1).

Baumert, E.K., Johnson, W. S., Cano, R. J., Jensen, B. J., & Weiser, E. S. (2009). *Mechanical evaluation of new fiber metal laminates made by the VARTM process.* Paper presented at the Proceedings of the International Conference on Composite Materials, Edinburgh, UK.

Bellini, C., Di Cocco, V., Iacoviello, F., & Sorrentino, L. (2019). Performance evaluation of CFRP/Al fibre metal laminates with different structural characteristics. *Composite Structures*, 111117.

Benedict, A. V. (2012). An Experimental Investigation of GLARE and Restructured Fiber Metal Laminates.

Beumler, T., Pellenkoft F., Tillich A., Wohlers W., Smart C. (2006). Airbus costumer benefit from fiber metal laminates. *Airbus Deutschland GmbH; Ref. no: L53pr0605135-Issue 1, pp. 1–18, 2006 May*.

Bhudolia, S.K., Kam, K.K., Joshi, & S.C. (2017). Mechanical and vibration response of insulated hybrid composites. *Journal of Industrial Textiles*, 1528083717714481.

Bieniaś, Jarosław, Jakubczak Patryk. (2017). Impact damage growth in carbon fibre aluminium laminates. *Composite Structures, 172*, 147-154.

Botelho, E C, Campos, A. N., Barros, d. E., Pardini, L. C., & Rezende, M. C. (2005). Damping behavior of continuous fiber/metal composite materials by the free vibration method. *Composites Part B: Engineering, 37*(2-3), 255-263. doi:10.1016/j.compositesb.2005.04.003

Bulut, Mehmet, Erkliğ, Ahmet, Yeter, & Eyüp. (2016). Experimental investigation on influence of Kevlar fiber hybridization on tensile and damping response of Kevlar/glass/epoxy resin composite laminates. *Journal of Composite Materials, 50*(14), 1875-1886.

Burdzik, R. (2013). Identification of Vibration Transfer to Car-Body from Road Roughness by Driving Car. *Vibroengineering PROCEDIA, 1*, 27-30.

Carrillo, J. G., & Cantwell, W. J. (2009). Mechanical properties of a novel fiber–metal laminate based on a polypropylene composite. *Mechanics of Materials, 41*(7), 828-838.

Chang, Po-Yu, Yeh, Ching, P., Yang, & Ming, J. (2008). Fatigue crack initiation in hybrid boron/glass/aluminum fiber metal laminates. *Materials Science and Engineering: A, 496*(1-2), 273-280.

Chun, S. C., Wei, R. C., & Rean, D. C. (2009). Stability of parametric vibrations of hybrid composite plates. *European Journal of Mechanics A/Solids, 28*, 329–337.

Cortes , P., Cantwell WJ. (2006). The prediction of tensile failure in titanium-based thermoplastic fibre–metal laminates. *Compos Sci Technol, 66*, 2306-2316.

Cortes, P., & Cantwell, W. J. (2004). Fracture properties of a fiber–metal laminates based on magnesium alloy. *Journal Materials Sciences, 39*, 1081-1083.

Deepesh, B. (2015). Free Vibration Analysis of Composite Laminate for Different Simply Supported Boundary Condition. *International Journal for Scientific Research & Development, 3*(1).

Dhanduvari, Dinesh, K., Gundala, S., Sri, H. M., Vinay, K., & Reddy, V. (2015). An Experimental and Numerical Approach to Free Vibration Analysis of Glass/Epoxy Laminated Composite Plates. *International Journal of Engineering Research & Technology, 4*(6).

Fu, Yiming, Yang, Chen, Jun, & Zhong. (2014). Analysis of nonlinear dynamic response for delaminated fiber–metal laminated beam under unsteady temperature field. *Journal of Sound and Vibration, 333*(22), 5803-5816.

Fu, Yiming, Chen Yang, Zhong Jun. (2014). Analysis of nonlinear dynamic response for delaminated fiber–metal laminated beam under unsteady temperature field. *Journal of Sound and Vibration, 333*(22), 5803-5816.

Ghasemi, Faramarz, Ashenai, Reza, Paknejad, & Malekzadeh, F. K. (2013). Effects of geometrical and material parameters on free vibration analysis of fiber metal laminated plates. *Mechanics & Industry, 14*(4), 229-238.

Ghasemi, & Mohandes, M. (2017). Free vibration analysis of rotating fiber–metal laminate circular cylindrical shells. *Sandwich Structures and Materials*, 1-3.

Ghasemi, & Mohandes, M. (2018). Free vibration analysis of micro and nano fibermetal laminates circular cylindrical shells based on modified couple stress theory. *Mechanics of Advanced Materials and Structures*, 1-12.

Ghashochi, B. H., & Sadr, M. H. (2013). PSO algorithm for fundamental frequency optimization of fiber metal laminated panels. *Structural Engineering and Mechanics, 47*(5), 713-727.

Gonzalez, Canche, N. G., Flores, Johnson, E. A., Carrill, & J.G. (2017). Mechanical characterization of fiber metal laminate based on aramid fiber reinforced polypropylene. *Composite Structures, 172*, 259-266.

Gutowski, T. G. (1997). Advanced Composites Manufacturing, First edition, John Wiley & Sons, New York, USA.

Hammond, M. W. (2005). Evaluation of the crack initiation and crack growth characteristics in hybrid titanium composite laminates via in situ radiography.

Hariharan, E., & Santhana, K. R. (2016). Experimental analysis of fiber metal laminates with aluminium alloy for aircraft structures. *JESRT*, 2277-9655.

Harshan, Ravishankar, Revathi, Rengarajan, Kaliyannan, D., & Bharath, K. (2016). Free Vibration Bahaviour of Fiber Metal Laminates, Hybrid Composites, and Functionally Graded Beams using Finite Element Analysis. *International Journal of Acoustics and Vibration, 21*(4).

He, Yi, Xiao, Yi, Liu, Y., & Zhang, Z. (2018). An efficient finite element method for computing modal damping of laminated composites: Theory and experiment. *Composite Structures, 184*, 728-741.

Houmat, A. (2018). Three-dimensional free vibration analysis of variable stiffness laminated composite rectangular plates. *Composite Structures, 194*(15), 398-412.

Iriondo, J., Aretxabaleta, L., Aizpuru, & A. (2015). Characterisation of the elastic and damping properties of traditional FML and FML based on a self-reinforced polypropylene. *Composite Structures, 131*, 47-54.

Jinshui, Y., Xiong, J., Ma, L., Wang, B., Zhang, G., & Wu, L. (2013). Vibration and damping characteristics of hybrid carbon fiber composite pyramidal truss sandwich panels with viscoelastic layers. *Composite Structures, 106*, 570-580.

Kahya, V., & Turan, M. (2017). Bending of laminated composite beams by a multi-layer finite element based on a higher-order theory. *Acta Physica Polonica A, 132*(3), 473-475.

Kaw, A. (2006). *Mechanics of composite material, second edition.*: CRC Press, Taylor & Francis Group.

Khalili, S.M.R., Malekzadeh, Keramat, Davar, A., & Mahajan, P. (2010). Dynamic response of pre-stressed fibre metal laminate (FML) circular cylindrical shells subjected to lateral pressure pulse loads. *Composite Structures, 92*, 1308–1317.

Khan, S., Alderliesten, R., & Benedictus, R. (2009). Post-stretching induced stress redistribution in fibre metal laminates for increased fatigue crack growth resistance. *Composites Science and Technology, 69*(3), 396-405.

Krimbalis, P. P. (2009). On the development of a strength prediction methodology for fibre metal laminates in pin bearing.

Kumar, Senthil, K., Siva, I., Rajini, N., Jeyaraj, P., & Winowlin, J. T. (2014). Tensile, impact, and vibration properties of coconut sheath/sisal hybrid composites: Effect of stacking sequence. *Journal of Reinforced Plastics and Composites, 33*(19), 1802-1812.

Kyriazoglou, C., & Guild, F. J. (2006). Finite element prediction of damping of composite GFRP and CFRP laminates–a hybrid formulation–vibration damping experiments and Rayleigh damping. *Composites Science and Technology, 66*(3-4), 487-498.

Laliberte, J. (2000). Applications of fiber-metal laminates. *Polymer composites, 21*(4), 558-567.

Lawcock, G. D. (1998). Effects of fibre/matrix adhesion on carbon-fibre-reinforced metal laminates-I: Residual strength. *Composites Science and Technology, 57*(12), 1609-1619.

Liaw, B.M., Liu, Y.X., & Villars, E.A. (2001). *Impact damage mechanisms in fiber-metal laminates.* Paper presented at the Proceedings of the SEM Annual Conference on Experimental and Applied Mechanics.

Lin, C., Kao, P., & Yang, F. (1991). Fatigue behaviour of carbon fibre-reinforced aluminium laminates. *Composites, 22*(2), 135-141.

Liu, J., & Liaw, B. (2002). Vibration and impulse responses of fiber metal laminated beam. 1411-1416.

Malekzadeh, Keramat, Khalili, S., Mohammad, R., Davar, A., & Mahajan, P. (2010). Transient dynamic response of clamped-free hybrid composite circular cylindrical shells. *Applied Composite Materials, 17*(2), 243-257.

Mallick, P. K. (2007). *Fiber-reinforced composites: materials, manufacturing, and design*: CRC press.

Mansour, G., Tsongas, K., Tzetzis, & D. (2016). Modal testing of epoxy carbon–aramid fiber hybrid composites reinforced with silica nanoparticles. *Journal of Reinforced Plastics and Composites, 35*(19), 1401-1410.

Marissen, R., Vogelesang, L.B. (1981). *Development of a new hybrid material: ARALL.* Paper presented at the Proceedings of the Second International SAMPE European Conference, Cannes, Frances.

Mathivanan, P. (2016). Damping behaviour of Hybrid Aluminium-Glass Fiber Reinforced Microfiller Plastic Laminates. *International Journal of Innovative Research in Science, Engineering and Technology, 5*(12).

Mohamad, S. Q. (1991). Free vibration of laminated composite rectangular plates. *International Journal of Solids and Structures, 28*(8), 941-954.

Mohamed, G, . (2012). Dynamic Deformation And Fracture Of Aerospace Structural Materials.

Morinière, F.D., Alderliesten, R.C., Benedictus, & R. (2014). Modelling of impact damage and dynamics in fibre-metal laminates–a review. *International Journal of Impact Engineering, 67*, 27-38.

Müller, Bernhard, Palardy Genevieve, Teixeira De Freitas Sofia, Sinke Jos. (2017). Out-of-autoclave manufacturing of GLARE panels using resistance heating. *Journal of Composite Materials*, 0021998317727592.

Murugan, R., Ramesh, R., Padmanabhan, & K. (2016). Investigation of the mechanical behavior and vibration characteristics of thin walled glass/carbon hybrid composite beams under a fixed-free boundary condition. *Mechanics of Advanced Materials and Structures, 23*(8), 909-916.

Ozsoy, N., Ozsoy, M., Mimaroglu, A. (2016). Mechanical properties of chopped carbon fiber reinforced epoxy composites. *Acta Physica Polonica A, 130*(1), 297-299.

Pardini, L.C, Botelho, E.C, Rezende, & M.C. (2005). Comparison between the elastic modulus obtained by tensile and free vibration experiments for glare material.

Patil, D. R., Damle, P. G., Deshmukh, & S., D. (2014). Vibration Analysis of Composite Plate at Different Boundary Conditions. *International Journal of Innovative Research in Science, Engineering and Technology, 2*(12).

Pho, J. (1992). Fracture Mechanics of Glare and Quantitative Prediction of Residual Strength. *Delft University of Technology, The Netherlands*.

Poodts, E., Ghelli, D., Brugo, T., Panciroli, R., & Minak, G. (2015). Experimental characterization of a fiber metal laminate for underwater applications. *Composite Structures, 129*, 36-46.

Rajesh, M., & Pitchaimani, J. (2017). Experimental investigation on buckling and free vibration behavior of woven natural fiber fabric composite under axial compression. *Composite Structures, 163*, 302-311.

Rath, MK, Sahu SK. (2012). Vibration of woven fiber laminated composite plates in hygrothermal environment. *Journal of vibration and control, 18*(13), 1957-1970.

Rattan, R., & Bijwe, J. (2006). Carbon fabric reinforced polyetherimide composites: Influence of weave of fabric and processing parameters on performance properties and erosive wear. *Materials Science and Engineering: A, 420*(1–2), 342-350.

Reyes, G., & Kang, H. (2007). Mechanical behavior of lightweight thermoplastic fiber–metal laminates. *Journal of materials processing technology, 186*(1-3), 284-290.

Rezende, MC, Botelho, EC, Pardini, & LC. (2005). Hygrothermal effects on damping behavior of metal/glass fiber/epoxy hybrid composites. *Materials Science and Engineering, 399*(1-2), 190-198.

Saffr, Z.A.C., Majid, D.L., Haidzir, & N.H.M. (2013). *Operational Modal Analysis Implementation on a Hybrid Composite Plate*. Paper presented at the Proceedings of World Academy of Science, Engineering and Technology.

Samia, F., & Asif, I. (2017). Modal analysis of optimization techniques of adhesively bonded Aluminum and CFRP Composites. *International Journal of Scientific & Engineering Research,, 8*(1).

Santiago, Rafael, Cantwell, Wesley, Alves, & Marcílio. (2017). Impact on thermoplastic fibre-metal laminates: Experimental observations. *Composite Structures, 159*, 800-817.

Sara, Black. (2017). Fiber-metal laminates in the spotlight. Retrieved from https://www.compositesworld.com/articles/fiber-metal-laminates-in-the-spotlight

Sarlin, E., Liu, Y., Vippola, M., Zogg, M., Ermanni, P., & Vuorinen, J., Lepistö, T. (2012). Vibration damping properties of steel/rubber/composite hybrid structures. *Composite Structures, 94*(11), 3327-3335.

Sathishkumar, T.P., Naveen J., Navaneethakrishnan, P., Satheeshkumar, S., & Rajini, N. (2017). Characterization of sisal/cotton fibre woven mat reinforced polymer hybrid composites. *Journal of Industrial Textiles, 47*(4), 429-452.

Senthilkumar, Krishnasamy, Siva Irulappasamy, Mohamed, S., Thariq Hameed, Rajini Nagarajan, . . . Ahmad, H. (2017). Static and Dynamic Properties of Sisal Fiber Polyester Composites–Effect of Interlaminar Fiber Orientation. *BioResources, 12*(4), 7819-7833.

Seo, H. (2010). Numerical simulation of glass-fiber-reinforced aluminum laminates with diverse impact damage. *AIAA, 48*(3), 676-687.

Sessner, V., Stoll, M, Feuvrier, A., Weidenmann, & A, K. (2017). *Determination of the Damping Characteristics of Fiber-Metal-Elastomer Laminates Using Piezo-Indicated-Loss-Factor Experiments.* Paper presented at the Key Engineering Materials.

Sexton, Anthony, Cantwell, Wesley, Kalyanasundaram, & Shankar. (2012). Stretch forming studies on a fibre metal laminate based on a self-reinforcing polypropylene composite. *Composite Structures, 94*(2), 431-437.

Shooshtari, A., & Razavi, S. (2010). A closed form solution for linear and nonlinear free vibrations of composite and fiber metal laminated rectangular plates. *Composite Structures, 92*(11), 2663-2675.

Sinmazçelik, Tamer, Egemen Avcu, Özgür, M., Bora, & Çoban, O. (2011). A review: Fibre metal laminates, background, bonding types and applied test methods. *Materials & Design, 32*(7), 3671-3685.

Sinmazçelik, Tamer, Avcu Egemen, Bora Mustafa Özgür, Çoban Onur. (2011). A review: Fibre metal laminates, background, bonding types and applied test methods. *Materials & Design, 32*(7), 3671-3685.

Sugiman, S., & Crocombe, A. D. (2012). The static and fatigue response of metal laminate and hybrid fibre-metal laminate doublers joints under tension loading. *Composite Structures, 94*(9), 2937-2951.

Sun, C.T., Dicken,, A., Wu,, H.F. (1993). Characterization of impact damage in ARALL laminates. *Composites Science and Technology, 49*(2), 139-144.

Susilo, Didik, D., Hafid, Nur, Raharjo, & Wijang, W. (2014). *The Effect of Fiber Orientation on the Dynamic Characteristic of the Carbon–Glass Fiber Hybrid Composite.* Paper presented at the Proceeding of 1 st International Conference on Engineering Technology and Industrial Application.

Thomas, P, Jenarthanan, M.P., Sreehari, & V.M. (2018). Free vibration analysis of a composite reinforced with natural fibers employing finite element and experimental techniques. *Journal of Natural Fibers*, 1-12.

Torabi, K., Shariati-Nia, M., Heidari-Rarani, & M. (2016). Experimental and theoretical investigation on transverse vibration of delaminated cross-ply composite beams. *International Journal of Mechanical Sciences, 115*, 1-11.

Upadhya, A. R., Dayananda, G. N., Kamalakannan, G. M., Ramaswamy, S. J., Christopher, & J, D. (2011). Autoclaves for Aerospace Applications: Issues and Challenges. *International Journal of Aerospace Engineering, 2011*, 11.

Utomo, Julian, T., Susilo, Didik, D., Raharja, & Wijang, W. (2017). *The influence of the number and position of the carbon fiber lamina on the natural frequency and damping ratio of the carbon-glass hybrid composite.* Paper presented at the AIP Conference Proceedings.

Vermeeren, C. A. J. R. (2003). An historic overview of the development of fibre metal laminates. *Applied Composite Materials, 10*(4-5), 189-205.

Vlot, A. (1993). Impact properties of fibre metal laminates. *Composites Engineering, 3*(10), 911-927.

Vlot, A. (1996). Impact loading on fibre metal laminates. *International Journal Impact Engineering, 18*(3), 291–307.

Vlot, A. (2001). Glare: history of the development of a new aircraft material. *Springer Science & Business Media*.

Vlot, A., & Gunnink, J. W. (2001). Fibre Metal Laminates. *Kluwer Academic Publishers, Dordrecht, The Netherlands*.

Vogelesang, L. B., & Gunnink, J. (1983). ARALL, a material for the next generation of aircraft. A state of the art. *Delft University of Technology*.

Vogelesang, L. B., & Vlot, A. (2000). Development of fibre metal laminates for advanced. *Journal Materials Process Technology, 103*, 1-5.

Wambua, Paul, Vangrimde, Bart, Lomov, S., & Verpoest, I. (2007). The response of natural fibre composites to ballistic impact by fragment simulating projectiles. *Composite Structures, 77*(2), 232-240.

Yang, Chen, Yiming, Fu Jun, Zhong, & Chang , T. (2017). Nonlinear dynamic responses of fiber-metal laminated beam subjected to moving harmonic loads resting on tensionless elastic foundation. *Composites Part B: Engineering, 131*, 253-259.

Yuan, Du, Haichao, L., Qingtao, G., Fuzhen, P., & Liping, S. (2019). Dynamic and Sound Radiation Characteristics of Rectangular Thin Plates with General Boundary Conditions. *Curved and Layered Structures, 6*(1), 117–131.

APPENDIX

RESEARCH PUBLICATIONS

1. **Merzuki**, **M. N. M.,** Rejab, M. R. M., Sani, M. S. M., Zhang B., Quanjin, M., & Rafizi, W. (2019, January). Investigation of Modal Analysis on Glass Fiber Laminate Aluminium Reinforced Polymer: An Experiment Study. In *IOP Conference Series: Materials Science and Engineering* (Vol. 469, No. 1, p. 012065). IOP Publishing.
2. **Merzuki**, **M. N. M.,** Rejab, M. R. M., Romli, N. K., Bachtiar, D., Siregar, J., Rani, M. F., Salleh, S. M. (2017). Finite Element Simulation of Aluminium/GFRP Fiber Metal Laminate under Tensile Loading. In *IOP Conference Series: Materials Science and Engineering* (Vol. 318, No. 1, p. 012072). IOP Publishing.
3. **Merzuki, M. N. M.,** Rejab, M. R. M., Sani, M. S. M., Zhang B., Quangjin M (2019). Experimental Investigation of Free Vibration Analysis on Fiber Metal Composite Laminates. *Journal of Mechanical Engineering and Sciences,13*(4), 5753-5763: http://doi.org/10.15282/jmes.13.4.2019.03.0459
4. Romli, N. K., Rejab, M. R. M., Bachtiar, D., Siregar, J., Rani, M. F., Salleh, S. M. **Merzuki, M. N. M.,** (2018, March). Failure Behaviour of Aluminium/CFRP Laminates with Varying Fibre Orientation in Quasi-Static Indentation Test. In *IOP Conference Series: Materials Science and Engineering* (Vol. 319, No. 1, p. 012029). IOP Publishing.
5. Romli, N. K., Rejab, M. R. M., Bachtiar, D., Siregar, J., Rani, M. F., Harun, W. S. W., Salleh, S. M. & **Merzuki, M. N. M.** (2017, October) The Behaviour of Aluminium Carbon/Epoxy/Fiber Metal Laminate under Quasi-Static Loading, In *IOP Conference Series: Materials Science and Engineering* (Vol. 257, No. 1, p. 012046). IOP Publishing.

RESEARCH COMPETITIONS

1. A New Investigation Technique for Dynamic Behaviour of Aluminium/GFRP Hybrid Laminated Plate by The Free Vibration Method. Creation, Innovation, Technology & Research Exposition (CITREX) 2019. Silver Medal
2. Fibre Metal Laminate for Quasi-Static Damage Resistance. Creation, Innovation, Technology & Research Exposition (CITREX) 2018. Silver Medal